Spatial Statistical Data Fusion on Java-enabled Machines in Ubiquitous Sensor Networks

Javier Palafox-Albarrán

Universität Bremen 2014

Spatial Statistical Data Fusion on Java-enabled Machines in Ubiquitous Sensor Networks

Vom Fachbereich für Physik und Elektrotechnik

der Universität Bremen

zur Erlangung des akademischen Grades eines

Doktor-Ingenieur (Dr.-Ing.)

genehmigte Dissertation

von

M.Sc. Javier Palafox-Albarrán

wohnhaft in Bremen

Referent	Prof. Dr.-Ing. Walter Lang
Korreferent	Prof. Dr.-Ing. Hans-Jörg Kreowski
Eingereicht am:	3.Dezember 2013
Tag des Promotionskolloquiums:	16. April 2014

Aknowledgments

It is with pleasure that I express my gratitude to all those who offered this opportunity to me: Institute for Microsensors, -actuators and –systems (IMSAS), Institute for Production and Logistic (BIBA) in the University of Bremen. I thank Prof. Walter Lang and Prof. Hans-Jörg Kreowski, my thesis supervisors, for their guidance patronage. I highly appreciate the support and guidance of Reiner Jedermann throughout the thesis. Additionally, I wish to thank Ingrid Rügge and the graduates at the International Graduate School for Dynamics in Logistics (IGS) for all their help and support. Also, I would like to thank Professors Bonghee Hong and Dr Sang-Hwa Chung at Pusan National University (PNU) for their support during my research internship in Korea.

I especially thank my family in Mexico for their support and encouragement throughout my thesis. My loving family have also made sacrifices during my long stay in Germany, without their unconditional care I would not made it this far.

Bremen, December. 2013

Javier Palafox

Abstract

Wireless Sensor Networks (WSN) are the cornerstone of Ubiquitous Sensor Networks (USN). They consist of small, cheap devices that have a powerful combination of sensing, computing and communication capabilities. The first technical challenge in USN is in fact due to energy constraints of WSN nodes. They must be able to communicate and process data efficiently using minimum amount of energy and cover an area of interest with the minimum possible number of sensors. The second technical challenge is to establish the communication to the external networks such as the Internet or Cellular and to react to unexpected events; the reaction to dynamic changes in the environment sometimes requires the deployment of new software features into the sensor nodes.

To solve the first technical challenge, this thesis proposes the use of Information Fusion (IF) techniques in WSN. The basic problems of data fusion are to determine the best procedure to combine the available data and the way to describe the relationship between different sources. It proposes the use of techniques that were designed for Geostatistics and applies them to WSN field. Kriging and Cokriging interpolation that can be considered as Information Fusion algorithms were tested to prove the feasibility of the methods to increase coverage with theoretical guarantees through the use of the so called Kriging variances. To reduce energy consumption, an innovative distributed compression method that surpasses the existing ones was developed. The method is “a real-valued” version of Distributed Source Coding (DSC). The modeling of correlations is based on using the so-called variogram, and uses data fusion techniques to recover the compressed data at the sink.

The second challenge is approached through the use of existing technologies. The time required for commercial Java-enabled sensor nodes and gateways to run IF algorithms and selected benchmarks were tested. The Java programming language, developed by Sun Microsystems, was selected because it was designed to offer a programming language, able to support flexible solutions to address diverse hardware devices, and because features such as over the air (OTA) programming in resource-constrained devices are already standardized. The connection to the external world is demonstrated through an exemplary implementation that can perform remote monitoring, send SMS alarms and deploy remote updates. It uses JavaME for sensor nodes and Java/OSGi in the gateway.

Zusammenfassung

Drahtlose Sensornetze (engl. Wireless Sensor Networks (WSN)) sind der Grundstein von allgegenwertigen Sensornetzen (engl. Ubiquitous Sensor Networks (USN)). Sie bestehen aus kleinen, kostengünstigen Geräten, welche eine leistungsstarke Kombination aus Mess-, Rechen- und Kommunikationsfähigkeiten besitzen. Die erste technische Herausforderung in USN entsteht durch Energie-Einschränkungen der WSN Knoten, denn sie müssen in der Lage sein, auf effiziente Weise Daten zu verarbeiten und zu kommunizieren, und dabei geringe Energiemengen verbrauchen und eine möglichst große Fläche mit minimaler Anzahl an Sensoren abdecken. Die zweite technische Herausforderung besteht darin, die Kommunikation zu externen Netzwerken wie etwa das Internet oder mobilen Netzwerken zu etablieren und auf unerwartete Ereignise zu reagieren: die Reaktion zu dynamischen Veränderungen in der Umgebung braucht ein Vielfaches der Zeit, die dafür benötigt wird, neue Software-Funktionen für die Sensorknoten bereitzustellen.

Um die erste Herausforderung zu meistern, wird in der vorliegenden Doktorarbeit die Benutzung von Informationsfusions (IF) Techniken in WSN vorgeschlagen. Das Hauptproblem bei Datenfusion ist die korrekte Wahl des Verfahrens, um die Daten zu kombinieren und die Beziehung zwischen verschiedenen Quellen zu beschreiben. Die vorgeschlagenen Techniken wurden ursprünglich für die Geostatistik entwickelt und wurden im Rahmen dieser Arbeit im Bereich der WSN angewandt. Kriging und Cokriging Interpolation, welche als Informationsfusion Algorithmen zählen, wurden getestet, um die Realisierbarkeit der Methoden zur Vergrößerung der Abdeckung mit theoretischen Garantien durch Anwendung sogennanter Kriging Varianzen zu untersuchen. Um der Energieverbrauch zu reduzieren, wurde eine innovative Methode zur verteilten Kompression entwickelt, welche bereits vorhandene Methoden übertrifft. Diese entwickelte Methode ist eine reellwertige Version von Distributed Source Coding (DSC). Das Modellieren von Korrelationen basiert auf der Benutzung eines sog. Variogramms und benutzt Datenfusions-Techniken um komprimierte Daten zurück zu gewinnen.

Der zweiten Herausforderung wird durch die Benutzung bereits vorhandenen Technologien begegnet. Die von kommerzielle Java Sensorknoten und Gateways benötigte Zeit um IF Algorithmen durchzuführen und ausgewählte Benchmarken wurden getestet. Die Java Programmiersprache, entwickelt von Sun Microsystems, wurde ausgewählt, denn es ist genau dafür gedacht, flexible Lösungen und diverse Hardware-Geräte zu unterstützen, und weil Funktionalitäten wie over-the-air (OTA) Programmierung in ressourcenbeschränkten Geräten standard sind. Die Verbindung zur externen Welt wird mittels eine Beispielsimplementierung demonstriert, welche eine Fern-Überwachung, das Senden von SMS Alarmen und das Bereitstellen von Fern- Aktualisierungen durchführt. Diese benutzt JavaME für die Sensorknoten und Java / OSGi beim Gateway.

Table of Contents

1 Introduction

1.1 General Context

In the so called cold-chain, perishable goods are transported using reefer container or trucks. Pervasive and real time monitoring of the cargo is required, both in storage and in transit. Management of the effect of different temperature ranges on the price depreciation due to irreversibility of quality degradation and easy installation and operation without the necessity of manual activities to collect temperature data are only some of the challenges [1]. Typical industries demanding it are: pharmaceutical, fruits & vegetables, seafood, dairy products, meet & poultry, processed food, floral, biological samples, blood units and beverages [2].

For the logistic companies, an inadequate management of the quality degradations lead to profit reductions. According to the Food and Drug Association (FDA) 20% of all perishable food is wasted during transportation[3].

The quality of the fresh goods is mostly determined by maintaining environmental parameters of interest within tolerable limits. Blocked airflows or defective seals can lead to temperature differences; such local variations are found in almost any transport and the hot spots patterns are not repeatable from transport to transport even when the same packing and loading schemes were used. Temperature differences up to 12 Kelvin can result in the reduction of local quality and shelf-life [4]. Temperature is of greatest influence on the ripening state; however, low humidity levels might lead to quality degradation by decreasing weight. The deteriorations can lead to a decrease in the aesthetic appeal, as well as a reduction in nutritional value.

1.2 Cold-chain monitoring

Traditionally, only temperature at the reefer unit were recorded during transportation and the data was analyzed at the destination point. With the advancements in technology, digital, portable data-loggers were being used to monitor the temperature inside several positions in the cargo itself. The data was retrieved at the unloading facilities. The unpredictability of the quality inside the cargo often led to decreased profitability for the food transport companies. The importance of an instant identification of the quality of the assets was recognized. A new technology was required that was able to monitor the ambient conditions, to communicate wirelessly, be cost-efficient, small, easy to deploy, and have some smart features to detect unwanted events such as sudden increase of temperature.

During the last decade a new promising technology has been emerging; it consists of small, cheap devices that have a powerful combination of sensing, computing and communication capabilities. In 2003, MIT's magazine of innovation for technology review in [5] cited Wireless Sensor Networks (WSN) as one of the top 10 emerging technologies that will have an influence in the future.

The use of WSN in cold-chain monitoring offers additional technical challenges, such as the restriction in mobility of the nodes once the sensors are placed into the boxes containing the goods. Another challenge is to enable the gathered data to be transmitted using existing internet or cellular network infrastructure [6] and to act to according to the actual quality state of the cargo. The information about the status of the product must be available at any time and *everywhere* in order to have valuable information that allows taking proper logistic actions. This leads to further advantages such as reduction of transport volume and greenhouse gas emissions. Actions against faulty cooling conditions can be taken as soon as a problem arises. Goods can be sorted in the warehouse by their actual quality condition.

The deployment of WSN on refrigerated containers and trucks has, however, some advantages that are not found on other applications: the spatial positions of the sensors can be estimated and controlled during loading of the cargo and the environmental parameters inside the refrigerated containers are correlated; the trucks are normally equipped with communication gateway which have long range communication capabilities with no energy constraints and superior computing capabilities.

1.3 Outline of the thesis

The thesis consists of two main sections: the first one focuses on exploiting the spatial correlations between measurement points, and on the use of information fusion (IF) techniques to improve two important figures of merit in a wireless sensor deployment: high energy efficiency and large area coverage. The second part studies the feasibility of the integration of existing technologies to be used in WSN. These include the execution time of selected benchmarks on Java-enabled devices; and the efficient transmission of the gathered information over external communication networks using off-the shelf hardware.

The first chapter introduces to the research problem and objectives. The second chapter describes the concept of ubiquity, the technological requirements for ubiquitous computing, and the relation with the existing technologies nowadays such as WSN, Internet and Cellular;

special focus is made on the existing solutions to manage coverage, energy and maintainability in WSN. Their relationship with IF techniques is addressed and summarized.

Third chapter presents a novel method to compress data in correlated environments. The method uses variography and IF techniques for compression, rate assignment and data recovery. Simulation results with real world acquired datasets demonstrate their simplicity, accuracy, and robustness. The method is suitable for data recovery at the sensor level due to the absence of binary codes; the method can be seen as a real-valued version of Distributed Source Coding (DSC).

Fourth chapter makes use of existing Geostatistic methods such as Kriging and Cokriging methods and explain why these belong to the Best Linear Unbiased Estimators (BLUE) described as an IF method. Through simulations it is shown that the methods are also suitable to be used in WSN. They provide a measure of the accuracy of the estimates and do not require node mobility.

Fifth chapter presents the benefits of using Java technologies in WSN. Java editions suitable for different types of devices are described; the selected sensor nodes and gateways are presented. Selected IF methods and performance benchmarks are tested in diverse hardware platforms to determine their feasibility of deployment in terms of their running time.

Chapter six presents a demonstrator using only off-the shelf components. The overlap of WSN with Machine-to-Machine (M2M) and other technologies are mentioned and the concept is introduced. The demonstrator shows how gathered and processed data can be visualized in a web page, how SMS alerts might be sent and remote software deployments are possible with existing technology.

Finally, general conclusions are summarized and suggestions for future research work are given.

2 State of the art

2.1 Ubiquitous technologies

The ubiquity or omnipresence of the information was first conceived by Mark Weiser in 1991 [7]. He termed it ubiquitous computing, where the machines fit the human environment so that no one notice their presence. He also described the technology required to achieve it, he wrote:

„ The technology required for ubiquitous computing comes in three parts: cheap, low-power computers that include equally convenient displays, software for ubiquitous applications and a network that ties them all together"

Today, Weisers' predictions for the computer of the 21st century cannot be more accurate. The internet is connecting everybody everywhere; mobile devices are getting smarter and cheaper and WSN technology, despite the remaining technological challenges, is promising to get smaller and ubiquitous. An ubiquitous application consists of three categories [8]:

Sensor Level: consists of sensor nodes that measure environmental parameters such as humidity or temperature; convert it to a binary representation to be read by digital devices. Each node has energy, communication and processing constraints. They are relatively cheap, small and independently energy supplied.

Server Level: It is the intermediary sink node. Commonly named gateways they are capable of collecting data from the sensor nodes and to communicate with external networks. They are commonly expensive, with no severe energy or computational constraints.

Client Level: Unlike sensor and server levels which are hardware-related solutions, client level is software-related and consists of the visualization of the data and the maintainability and management of the network.

Sensor networks are recognized to be a key technology for building an ubiquitous system [9], they work at the sensor level, and because they have short range communication capabilities, WSN must rely on communication with specialized gateways, which work at the server level, to communicate with fixed Ethernet LAN, WLAN, UMTS/GPRS, etc up to the end user at client level.

2.2 Wireless Sensor Networks

The research directions in WSN can be summarized in:

Increase the area of coverage: Usually, a region of interest (ROI) is covered by the use of several nodes. Normally some regions can be more properly monitored than others and individual sensor nodes might have either complementary or redundant information about a specific region. An efficient WSN deployment must be the one that -differentiate the regions that can be properly monitored from those that cannot. It must be also be able to monitor making use only of the necessary sensors and avoid using redundant information Nevertheless; it has to be smart enough to make use of redundant information to make the WSN less vulnerable to failures of a single node.

Increase energy efficiency: The most challenging issue is to improve the energy efficiency. The energy can be consumed basically by radio communication and hardware operation. Research work has been focused on developing energy-efficient processing techniques to reduce radio communication and complicated computations. Distributed approaches where the processing is made inside each node to reduce inter-node communication and avoid central coordination are top research topics.

Improve the flexibility and maintainability: A desirable feature in a WSN is its ability to react to environment changes and failures that were unknown at the time of their initial deployment. Therefore, it should be able to provide dynamic features to allow complete or partially update of the code in the sensor nodes over the air (OTA) during runtime.

An ideal WSN deployment is the one that has all desired figures of merit: broad sensing coverage, low energy consumption, low deployment costs, and high flexibility and maintenance. Unfortunately, several trade-offs exist between them.

The trade-offs are summarized In Table 2.1. If big batteries are used, the deployment costs are increased but allows the use of hardware devices that are less-prone to failures and easy to maintain. The use of powerful processors allow the programming of smarter algorithms that might increase flexibility and maintenance but would increase costs and energy consumption. Finally, deployment of large number of nodes increases the sensing coverage but increases significantly the deployment costs and make them difficult to maintain.

Table 2.1 Trade-offs between figures of merit in WSN

	Sensing Coverage	Energy consumption	Deployment costs	Flexibility and maintenance
Big batteries	No trade-off	"Do not worry about it"	⇧	⇧
Powerful Hardware	No-trade-off	⇧	⇧	⇧
Dense Deployment	⇧	No trade-off	⇧	⇩

2.2.1 Methods to reduce energy consumption

Advancements in wireless telecommunications and electronics have been more than evident over the last few years. Hardware devices have become smarter, smaller, multi-functional and cheaper. These developments are in part due to Moore's law, that states that the computing processing is doubling approximately every 2 years, such trend has been happening for at least three decades.

WSN however is a technology that does not benefit from this trend; the sensor nodes are designed to be small and cheap but they have inherent memory, computing power and energy constraints. As Schlachter mentioned in [10]:

"There is no Moore's Law for batteries. The reason there is a Moore's Law for computer processors is that electrons are small and they do not take up space on a chip. Chip performance is limited by the lithography technology used to fabricate the chips; as lithography improves ever smaller features can be made on processors. Batteries are not like this. Ions, which transfer charge in batteries are large, and they take up space, as do anodes, cathodes, and electrolytes. A D-cell battery stores more energy than an AA-cell. Potentials in a battery are dictated by the relevant chemical reactions, thus limiting eventual battery performance. Significant improvement in battery capacity can only be made by changing to a different chemistry"

Limitations in energy storage in WSN nodes lead to the necessity to use hardware devices with low current-draw. Typical sensor nodes make use of energy-efficient microcontrollers and radio transceivers. Because the radio transmission is the most expensive functionality, short-range transmission and limited communication are basic features.

Anastasi [11] identified three main enabling techniques to reduce energy consumption in wireless sensor networks: duty cycling, data-driven approaches and mobility.

As the name suggests, in *duty cycling* the nodes are sleeping part of their lifetime. When the nodes are sleeping, the radio-transceiver is a low-power mode whenever communication is not required. As soon as a new data packet arrives the radio should be switched on. A distributed sleep/wakeup algorithm is required to decide which sensors should remain active and which inactive.

Data-driven approaches exploit spatial and temporal correlations to avoid communication of redundant data. Data processing and fusion techniques are applied in the context of wireless sensor networks. This is a hot research field because algorithms in digital signal processing and information fusion are normally energy-demanding itself to be applied in WSN.

In some cases, if the sensors are mobile, *mobility* can be used to reduce communication. Nodes closer to the sink, have to relay more packets and therefore they are more prone to suffer from premature depletion [12]. If some nodes are mobile, the traffic flow can be altered to distribute more efficiently the relay of packets.

Heterogeneity can be also used to prolong the network lifetime in two ways. All normal nodes can send data report to the sink via the nearest heterogeneous node, which possess high-speed microprocessors, bigger batteries, and high-bandwidth, long-distance network transceivers.And the nodes near the sink do not need forward vast packets from other nodes [13]. Device heterogeneity may also be exploited by shifting resource intensive processing tasks to other nodes within the network [14].

2.2.1.1 ***Data-driven approaches***

According to [11], data-driven approaches can be divided into data-reduction schemes that address the problem of sending unnecessary data and energy-efficient data acquisition that aims to reduce the energy spent by the sensing subsystem. This thesis focus only in data-reduction schemes; they can be divided into: *in-network processing, data compression and data prediction.*

2.2.1.2 ***In-network processing***

In-network aggregation is the global process of gathering and routing information through a multihop network, processing data at intermediate nodes with the objective of reducing resource consumption (in particular energy), thereby increasing network lifetime [15].

As the previous definition explains, in-network data aggregation involves many layers of the protocol stack. The most important focus is on the design of an efficient routing protocol [16]. The application, routing and data aggregation layers are closely interrelated.

According to [15], we can distinguish them into two approaches:

In-network aggregation with size reduction refers combines and compress data from different sources in order to reduce the amount of information propagating over the network. This approach may reduce accuracy; after the information is received at the sink is usually not possible to recover it; i.e. lossy aggregation.

In-network aggregation without size reduction merges incoming packets coming from different sources and merges it without signal processing. This is done for example when two attributes, for example temperature and humidity, are sent because they cannot be aggregated together. This approach preserves the original information and can be considered lossless.

2.2.1.3 ***Data compression***

Radio communication is the most power consuming task in wireless sensor networks. Minimizing the data size before transmission is an effective way to reduce total power consumption. One obstruction is that most data compression algorithms are not feasible for WSN's [17]. Kimura [17] mentioned two reason for that: the size of the algorithms exceeds the memory size and the processing speed is too low in comparison to other wireless technologies. He also mentioned the necessity to design a low-complexity and small size data compression algorithm for sensor networks. He enlisted some of the data compression schemes suitable for WSN, namely, coding by ordering, pipelined in-network compression, low-complexity video compression and distributed compression.

Coding by ordering was introduced in [18], as in the case of in-network compression, is closely related to routing protocols, in this case it is part of data funneling routing. The algorithm combines different packets into a single one with a single header; it can be combined with signal processing and source coding techniques. The method presents good compressing ratio and in simple enough to be applied in WSN.

Pipelined in-network compression is present in [19]; in contrast to in-network aggregation it is applicable to any kind of query; several queries and statistical measure cannot be supported by aggregation. The basic idea is to collect sensor data in aggregation node's buffers for some time and combined the data into one single packet without redundancy.

Distributed Source Coding (DSC) was pioneered four decades ago by Slepian and Wolf 1973 [20]. They studied joint decoding of two the independently encoded correlated sources. Their results became famous; surprisingly, if two random variables are correlated, they can be compressed and decompressed *lossless* without necessity of communication between the encoders. This is possible as long as the source rates satisfy conditional entropies constraints. The correlation between the sources is known as *a-priori*; the sink may have to collect information over the network, calculate the correlations between the sensors and send it before each sensor starts compressing its reading.

DSC is protocol agnostic, it operates with any MAC protocol, network protocol and application layer protocol [21].

2.2.1.4 ***Data prediction***

Data prediction techniques build a model describing the sensed phenomena [11, 22]. They can be classified into three main classes: *stochastic approaches, time series forecasting and algorithmic approaches.*

Stochastic methods map data into terms of probabilities and statistics. Chu's approach [23] is a good example. As the authors said, the idea is to maintain dynamic probabilistic model, one is distributed in the sensor network while the other is in the base station. The model in the base station requires a training phase to build up a probability density function. They also investigate how temporal and spatial correlations interact with the network topology and evaluate the performance in real-world sensor networks.

In *time series forecasting* a set of historical values is used to predict future values of the same time series. The time series is modeled for example by a Moving Average(MA), Auto-Regressive (AR) or Auto-Regressive of a Moving Average processes. A good example is PAQ and [24] SAF [25] that use an AR model. Their model does not include sensor readings and is associated with an error-bound that is used to determine the validity of the model.

A method that does take into account sensor readings is the one developed by the author of this thesis which is described in [26]. The system is based on parametric system identification and a parameter adaptation algorithm described in [27]. It was specifically adapted for the identification of a system which contains non-linear feedback and makes use of an intermediary variable to transform the system into a pseudo linear one. The method is accurate, energy-efficient and easy to implement on sensor nodes.

2.2.2 Methods to increase coverage

The coverage problem in sensor networks has been defined in the literature in a variety of ways Most literature defines coverage in sensor networks for tracking applications. An interesting definition is the one from Djidjev and Potkonjak [28]. They define the goal of static coverage as to cover a specific area of interest using the smallest number of sensors, however they focus on dynamic coverage in which the sensor are allow to move in the area of interest.

Coverage holes are defined in [29] as the degree of tolerance/redundancy of a given target area for accurate localization. Huang and Tseng [30] discus the problem of discovering insufficiently covered regions, where the sensing ranges are modeled as unit disk or spheres.

The authors in [31] introduce the concept of deterministic and stochastic coverage. In deterministic coverage, a static network is deployed according to a predefined shape, this can be for example a regular grid, whereas stochastic coverage deals with the situation where the deployment is random for example if the sensor are dropped off from a plane.

Only little research has been done on coverage for environmental monitoring. Lazos and Poovendran [32-33] are the exception. They define coverage as the way to quantify how well is the field of interest sensed by the deployment of the sensor network and raise a question: "*How many sensors are needed to achieve the desired coverage with a probability higher than a threshold value?* "They focus in stochastic (probabilistic) deployments for heterogeneous sensor network and make use of integral geometry to tackle the problem.

A really interesting approach is the one proposed by [34]. The authors follow information driven approach for sensing optimization; they find the optimal positions of the sensor in order to extract the maximum information. They use Kriging interpolation which was developed to mining and geology to determine the best position of the new measurement locations, the sensors are allowed to move until convergence is achieved. Umer [35] proposed a distributed algorithm for Kriging interpolation in resource constrained sensor nodes.

Krause and Guestrin's [36-37] solution is similar. They introduce an algorithm with strong theoretical guarantees for cases when the functions present *submodularity,* which means that addition of new measuring points, is more useful if few observations are available and less helpful if there are already enough observations. Their goal is to minimize the Kriging variance in unobserved locations.

Sensing optimization using Kriging can be found in geostatistics literature. For example, in Szidarovszky [38], it is proposed a Branch-and-Bound algorithm to find the optimal sites of drillholes; for the estimation of the minimum number of sensors, a method that takes advantage of interesting feature of Kriging interpolation was selected. The Kriging-Variance (KV), that measures the uncertainty of the estimation before actual measurements are available. KV is monotonic, that means that increasing the number of measuring points will not increase the KV. The method minimizes the number of required additional points subject to upper bounds of the Kriging-Variance. The method, that is an unconstrained Branch-and-Bound (BnB) algorithm, adds a measuring point if it improves the variance, or removes it, if it does not bring any accuracy improvement. To avoid, calculation of matrix inverses each time a point is added or removed, calculations of the inverse of a partitioned matrices are done.

2.3 Requirements for flexibility and maintenance

Traditionally, sensor network algorithms are hard-coded. Typical sensor nodes as TelosB [39] are programmed using a C-type language called NesC that is specially designed for highly resource constrained devices and can only run on TinyOS [40]. As mentioned by Mahgoub [41], an ability to program sensors dynamically is important according to the user needs. The use of a programming language able to support flexible solutions to address diverse hardware devices and sensor nodes and gateways able to be reprogrammed on the demand over-the-air is required. The main issues to consider are [8]:

- Checking the downloaded software for integrity, version mismatch, platform mismatch, etc.
- Version control, that is, prevention of version mismatch
- Heterogeneity of sensor nodes. There may be a mix of platforms.
- How software would be activated. It may be automatically or manually activated.
- Problems related to very resource-constrained nodes, such as limited code memory
- Performance. The time required to update nodes as wells as tradeoffs between time and energy.

2.4 Sensor data fusion in WSN

According to Iyengar [8], the development of applications in WSN requires interdisciplinary collaboration in computer science and engineering disciplines. He mentioned the necessity of advancements in data fusion to combine data from multiple sources to create more complete

representation of the world. Data fusion is *per se* interdisciplinary; it is defined as set of theories techniques and tools that are used to combine sensor data to improve the performance of the system in some way. Being more specific, classified according the relation among the sources, the ways the fusion can improve the system is in its completeness, accuracy and certainty [42]. Incomplete information might be found, for instance, when two sources posses information about different portions of the same environment at different positions. Inaccurate information might be the result of environmental noise or error models, if two or more sensors posses information about the same source, the redundant information can be used to fuse them into a single filtered estimation that is more accurate. Certainty might be, for instance, improved by fusing several estimations of a point of interest each one of them with high uncertainties into a new estimation with low, acceptable variance.

The fusion type might be performed across sensors, attributes or time [43]. Fusion across sensors is the most common one and is made through measurements of the same variable of attribute. Fusion across attributes is made over a number of measurements that are associated with the same situation, for example temperature and humidity in a room. Fusion across time current measurements are fused with historical information, with this type of fusion is possible for example predict future values with the learned information.

2.4.1 Methods and techniques in Information Fusion

As mentioned before, sensor fusion is interdisciplinary; it involves disciplines like communication engineering, geostatistics and process automation and artificial intelligence. The methods and techniques, however can be summarized into inference, estimation, aggregation and compression [44].

2.4.1.1 *Inference*

Inference is the act of deriving conclusions based on evidence. The classical inference method is Bayesian inference used extensively in communication engineering, mathematically speaking an uncertainty is represented in terms of conditional probabilities describing an *a-priori* beliefs. The posterior probability represents the belief of hypothesis V given the information U. The probability is calculated by:

$$\mathbf{Pr}(V|U) = \frac{\mathbf{Pr}(U|V)\mathbf{Pr}\,(\mathbf{V})}{\mathbf{Pr}\,(\mathbf{U})} \qquad \textbf{(2.1)}$$

Where $\Pr(V|U)$ is the belief of hypothesis V given the information U. Pr (V) is the prior probability of V and $\Pr(U|V)$ is the probability of receiving U if V is true. The main design issue is the setting of the probabilities that have to be guessed beforehand.

2.4.1.2 *Estimation*

Estimation methods were developed in the control engineering field and make extensive use of state vectors. The most common estimation methods are the Kalman Filter and Best Linear Unbiased Estimator (BLUE)

The Kalman filter is over 50 years old but still one of the most important data fusion algorithms [45]. The typical uses is to smooth (filter) noisy data to provide estimates of the state vectors of the model of a dynamic system. Its mathematical derivation uses linear matrix algebra as a minimum mean squared estimator [46]. Two pieces of information are available, estimations and measurements, they are fused to provide the best possible estimate. The Gaussian probability density functions of both pieces of information are multiplied together, giving as a result another Gaussian function , that is a key point to perform the filtering in recursive way.

Best Linear Unbiased Estimator (BLUE) has application where the Kalman Filter does not. For example when no complete prior information is available [47], or when different attributes must be fused, or where the dynamic model is too complex to be modeled.

A Best Linear Unbiased Estimator has the following properties:

*Is Linear in data***:** The estimate is calculated by the sum of all the resulting multiplications of assigned weights and available data

$$\widehat{\mathbf{U}}_0 = \sum_{i=1}^{n} a_i U_i \qquad (2.2)$$

Is unbiased **:** The expectation of the prediction is equal to the "real value" of the attribute**.**

$$E(\widehat{\mathbf{U}}_0) = \sum_{i=1}^{n} a_i E(U_i) = U_0 \qquad (2.3)$$

*Possesses theoretical Guarantees***:** A variance of the estimation is provided as a measure of accuracy.

$$Var(\widehat{\mathbf{U}}_0) = E\left[\left(\sum_{i=1}^{n} a_i U_i - \sum_{i=1}^{n} a_i E(U_i)\right)^2\right] = a^T C a \qquad (2.4)$$

Where $\boldsymbol{a}$ is a vector containing n weights and $\boldsymbol{C}$ is the covariance Matrix.

2.4.1.3 *Aggregation*

Aggregation techniques are extensively used by database systems, developed to be used in query languages as SQL, they summarize data. They are feasible to implement in sensor nodes, it processess the incoming data with the local measurement by performing aggregation operations, such as average, sum, minimum or maximum. This approach may reduce

accuracy; after the information is received at the sink is usually not possible to recover it. In this thesis we are mostly interested in the average operation, that according to the law of large numbers, the average of the results obtained from a large number of trials should be close to the expected value.

$$\boldsymbol{E(\mathrm{U}) \approx avg(U) = \frac{1}{n}\sum_{i=1}^{n} U_i} \quad \textbf{(2.5)}$$

2.4.1.4 *Data compression*

Data compression is not information fusion method, however they are mentioned here because they use Bayesian inference to decompress the received measurement. They are based on information theory concepts. If two measurements are spatially correlated, they can be compressed and decompressed without loss. The correlation between the sources has to be known a-priori; the sink may have to collect information over the network, calculate the correlations between the sensors and inform the sources how many bits are required to send in order to be able to achieve lossless compression. The method is known as Distributed Source Coding (DSC)

Table 2.2 summarizes some of the most important Information Fusion techniques used in WSN

Table 2.2 Information Fusion in WSN

	What Improves?	Fusion Types	Methods
In-network aggregation with size reduction	Energy consumption	Across sensors	Aggregation
In-network aggregation without size reduction	Energy consumption	• Across attributes • Across sensors	Aggregation
Coding by ordering	Energy consumption	Across sensors	Compression
Pipelined in-network compression	Energy consumption	Across sensors	Compression
Distributed Source Coding	Energy consumption	• Across sensors r • Redundant • Complementary	• Inference • Compression • Estimation
Stochastic approaches	Energy consumption	Across time	• Inference • Data prediction
Time series forecasting	Energy consumption	• Across time • Across sensors	• Data prediction • Estimation
Kriging	• Coverage • Certainty	Across sensors	• Estimation • Inference

3 Distributed Compression at the Sensor Level

Low energy consumption is one of the most important figures of merit in sensor networks. Exploiting the spatial correlation between the sensed points to reduce radio communication data rates is a really good approach that can help achieve this objective. The methods used to compress the data must be simple, accurate, and robust. Modelling the spatial correlations using variography that is the traditional method to measure spatial correlations between variables using two-point approaches seem to be the obvious start point.

Geostatistics is a theory of regionalized variables [48] in which variables or attributes of interest are spatially distributed. It already has mature methods developed and tested in the field. However their applicability to sensor networks has been limited; exceptions are for example, [49] and [50], where kriging interpolation is performed with the aim of reducing the number of sensors deployed.

Only a few research works have considered the links between geostatistics, data compression, and transmission of correlated observations. Research made in [51] considered it to guide the optimization of source-channel coding schemes, while Oldewurtel [21] applied spatial statistics only for data modelling and simulation. DSC approach fails to make a correct link with statistics and random fields; as a matter of fact, research work on Distributed Source Coding (DSC) has focused mainly on finding the more robust codes and the most efficient decoders.

In the present chapter, a method that combines geostatistical and information fusion methods for data compression in sensor networks is presented. The reconstruction of the measurement data can be largely simplified if the global mean of the probe points is available; the mean is approximated by the strong law of large numbers, and by combining it with an estimation of the variogram and with continuous-valued source space partitions, it is proved that it is possible to perform energy-efficient, robust, and consistent data compression in sensor networks.

3.1 Experimental Data

The procedures were tested on two datasets recorded in a refrigerated container of dimensions $2.2 \times 2.2 \times 5.4$ m as part of a collaborative internship with the Research Centre for Logistics Information Technology (LIT) at the Pusan National University in Korea in 2012.

In order to increase spatial variability, the container was first cooled from ambient temperature (15 °C) to a set point of 0 °C for 3 hours and then warmed to a set point of 25 °C for about 2 hours, prior to performing the actual experiment, that comprised cooling the container to 5 °C for 80 minutes. As the most significant influence on the cargo container is the loading state, two configurations were tested: one with an empty container and the other with pallets covering the floor to deflect the air flow.

In total, 60 ASN 405T [52] wireless sensor nodes were placed in the walls, doors, ceiling, and floor, forming a grid of 55 cm lag distance. Each node contains a SHT20 [53] sensor capable of measuring humidity and temperature with accuracies of ± 3% RH and ± 3 °C, respectively, and sending the data to a gateway.

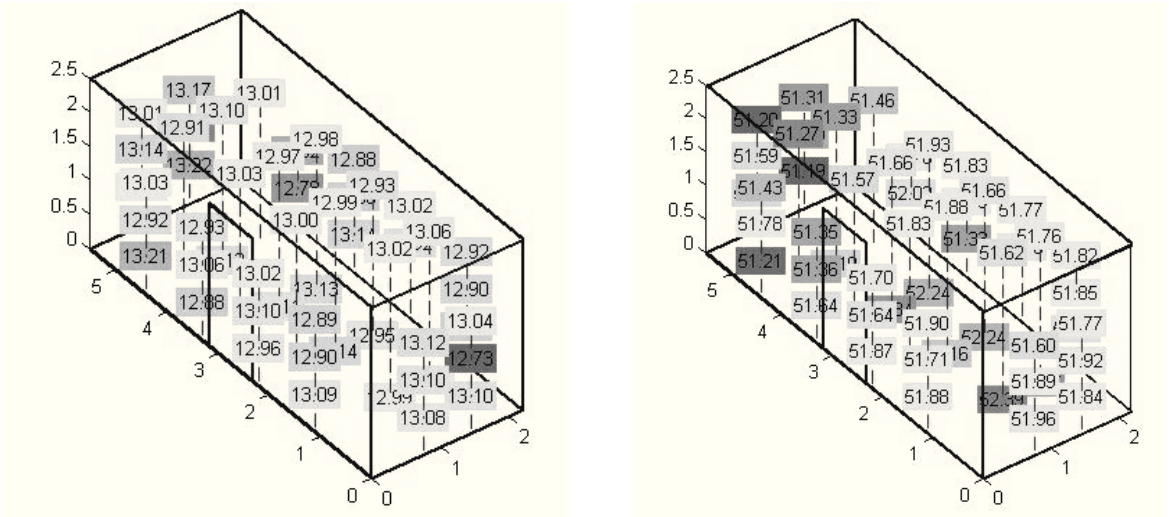

(a) **(b)**

Figure 3.1 Spatial distribution of the measurement points at the walls of the container: (a) temperature, (b) humidity

Figure 3.2 shows the measurements of the same experiment over time; it can be seen that the variations are high at the beginning and low at the end of the experiment.

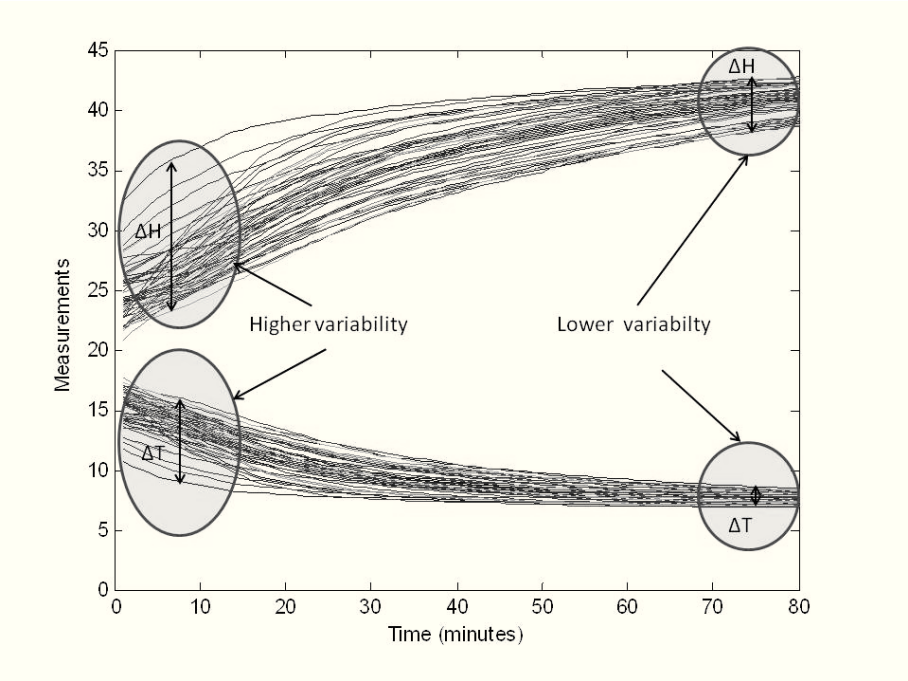

Figure 3.2 Temperature and humidity variability over time at the measurement points on the walls of the container

3.2 Distributed Source Coding

Distributed Source Coding (DSC) was pioneered four decades ago, in 1973, in a famous paper [20] by Slepian and Wolf. They studied joint decoding of two independently encoded correlated sources. Surprisingly, if two random variables U and V are correlated, they can undergo *lossless* compression and decompression without the need for communication between the sources.

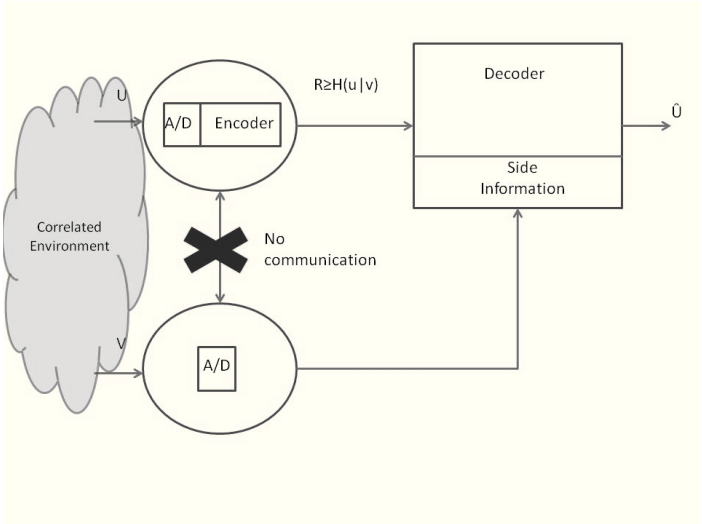

Figure 3.3 Distributed Source Coding concept: only the decoder has access to Side Information V

The correlated environment is modelled by a Binary Source Channel (BSC). Usually, if U is the binary source and V is the sink, the correlation between them is modelled by an additive noise η with variance σ_e^2 and mean zero.

$$\boldsymbol{V = U + \eta(0, \sigma_e)} \tag{3.1}$$

Given a quantization step Δ, the Chebyshev's inequality can be used to bound the probability of bit flipping to be less than a value p if the source is compressed to n bits by [54-55]

$$\boldsymbol{n = \frac{1}{2} log_2 \left(\frac{\sigma_e^2}{\Delta^2 p}\right) + 1} \tag{3.2}$$

$$\boldsymbol{p = \Pr(u \neq i \,|s = i)} \tag{3.3}$$

When dealing with continuous-valued values, such a model becomes more complex due to the fact that the least significant bits will have more probability of flipping than the most significant ones, as shown in Figure 3.4. In order to increase the probability of correct decoding, the decoder must have been set properly with different bit-flipping probabilities for each bit, resulting in a complex correlation model and decoding methods; for example, the authors of [56] proposed hybrid decoding for such a purpose

$$\boldsymbol{p_1 \geq p_2 \geq \cdots \geq p_m} \tag{3.4}$$

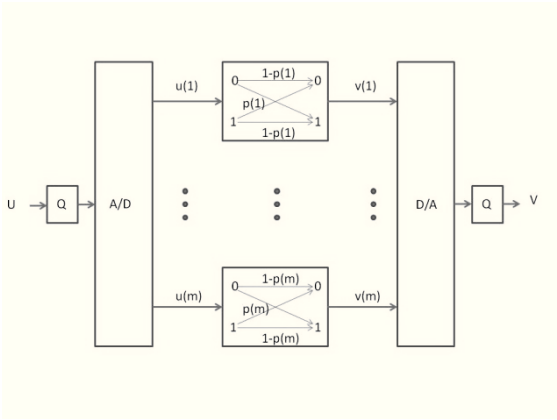

Figure 3.4 Probabilities of bit-flipping of continuous-valued sources

If the decoder receives incomplete but sufficient information about a source it can be recovered perfectly by using the so-called mutual information (MI), that is a measure of the amount of information a random variable contains about another variable from a second source v. Source coding theorems are used to determine the necessary number of bits to be transmitted in order to achieve lossless communication.

$$\boldsymbol{MI(u, v) = H(u) + H(v) - H(u, v)} \tag{3.5}$$

$H(u)$ and $H(v)$ are the so-called marginal entropies and $H(u,v)$ is their joint entropy. Mitchel [42] rewrites the last equation in a more useful representation. $H(v|u)$ is the conditional entropy.

$$\boldsymbol{MI(u,v) = H(u) - H(u|v) = H(v) - H(v|u)} \quad \textbf{(3.6)}$$

$$\textbf{or} \qquad \boldsymbol{H(u) = MI(u,v) + H(u|v)} \quad \textbf{(3.7)}$$

In bit terms, if M is the number of bits of the uncompressed word and N is the number of bits of the compressed word, the compression rate is defined as

$$\boldsymbol{R = \frac{M}{N}} \quad \textbf{(3.8)}$$

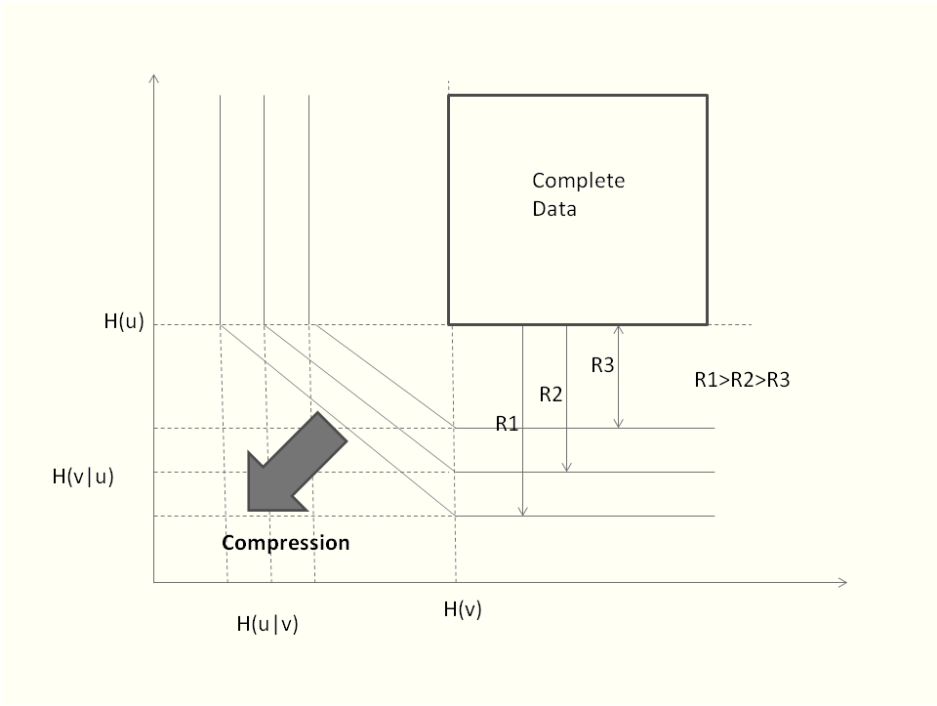

Figure 3.5 Achievable rate regions for Slepian-Wolf coding of two sources

The theorem has applicability as a data compression technique in the sense that redundant information should be transmitted only once and used in the decoder to complement the conditional entropy to recover the joint entropy. Because it is based on binary codes and information theory concepts, the research focus was on channel modelling and code design.

3.2.1 DSC in wireless sensor networks

The most referenced implementation of DSC in WSNs is DISCUS (Distributed Source Coding Using Syndromes) [57]. It uses the concept of "binning" to partition the source space into bins that will be treated as smaller channel codes, each one indexed by the so-called syndrome. The syndrome is sent to the decoder, where the source is estimated using the side information as support. The rate of transmission R must be bigger than the conditional entropy to achieve lossless decoding.

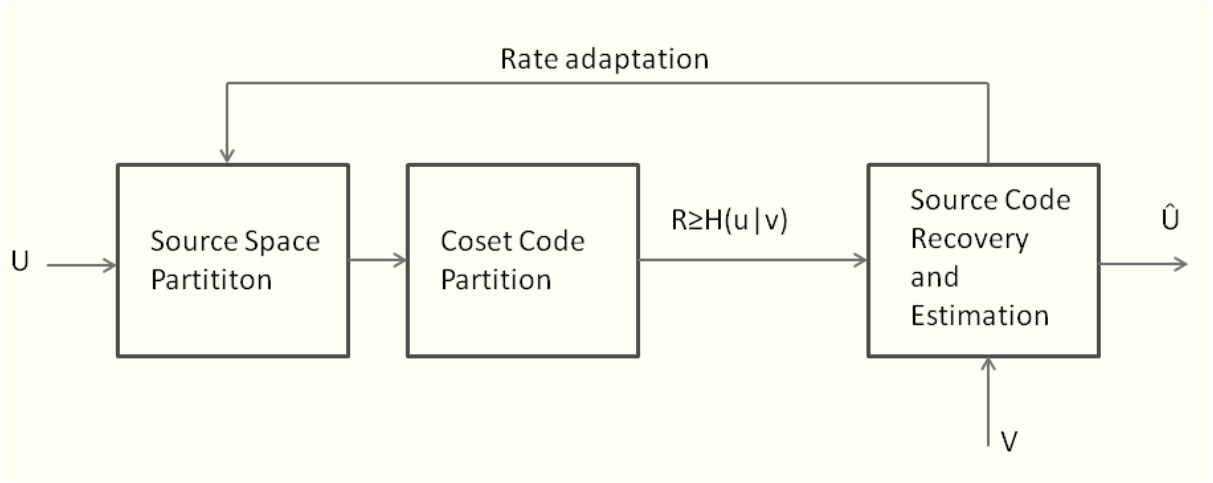

Figure 3.6 Diagram of DISCUS

3.2.2 Source space partition

In the source partition process, a linear block code family is selected. A good linear code is the one that exhibits a large Hamming distance d, that is, the number of positions at which each pair of binary words inside every coset or bin is different. There are several code types to be selected such as LDPC, turbo codes, projective geometry codes, and so on. For example, Figure 3.7 shows the Hamming distances for different compression rates of a family of geometric codes used in [21] when M is equal to 11 bits and the compressed words are of 2, 3, 5, and 8 bits correspondingly. The more compressed a binary word is, the more difficult it is to recover it, because each coset has more binary words in it and that are more similar to one another.

A mathematical representation of a linear block code is a parity matrix H consisting of N rows and M columns, where M is the number of bits of the binary word. By using H, the source space will be partitioned into 2^N bins or cosets, each consisting of 2^{M-N} binary words.

For example, the parity matrix shown Figure 3.8 is an 11 × 8 (M × N) geometry code used in [21].

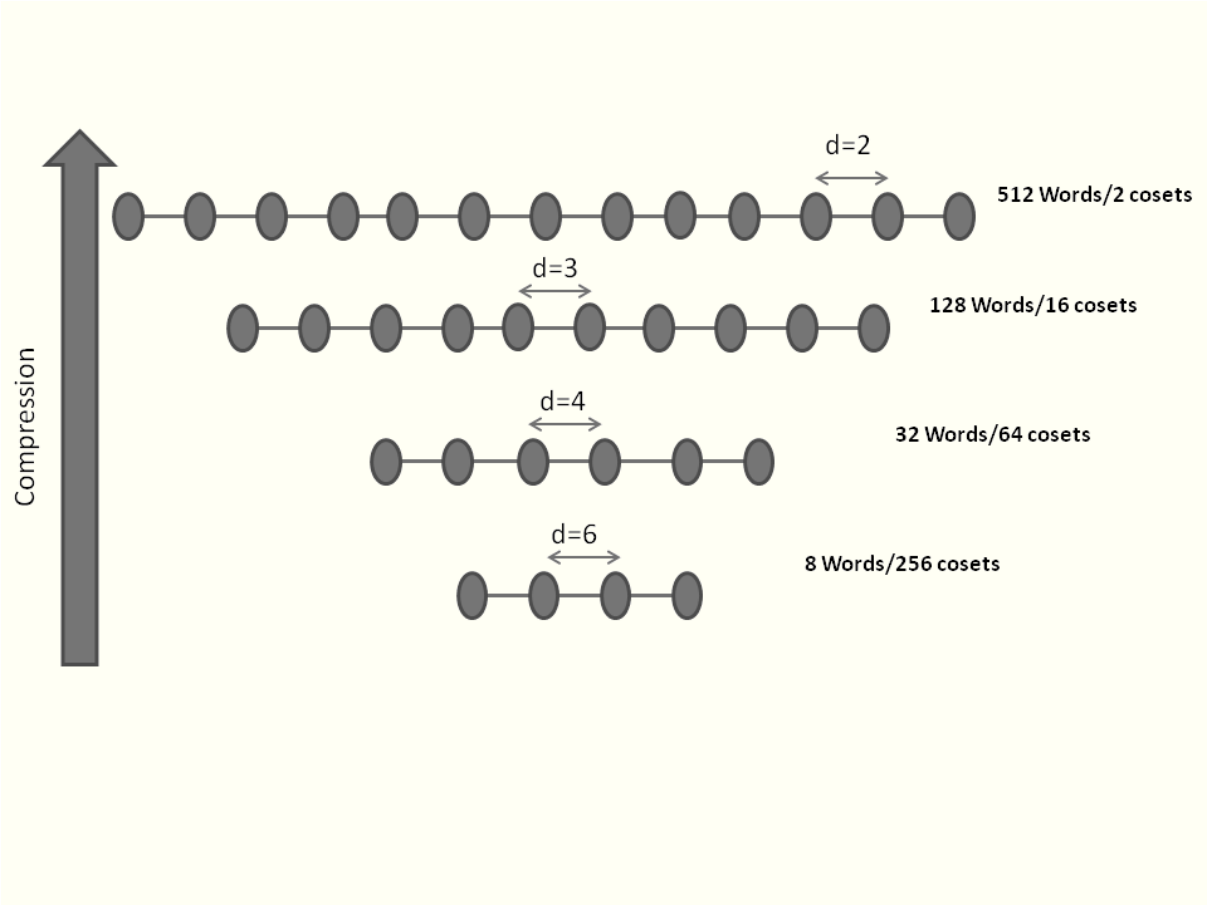

Figure 3.7 Source Space partition. The Source is divided into cosset, the bigger the compression, the lower the number of the hamming distance

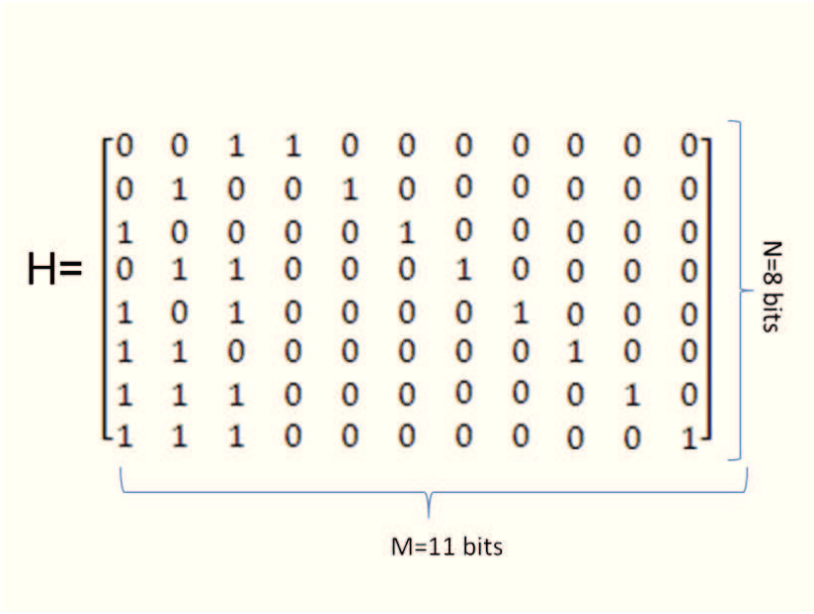

Figure 3.8 Parity matrix H of an 11 × 8 geometry code

3.2.3 Coset code partition

Once the parity matrix is selected for a desired compression rate R, the process of coset code partition is performed by a simple matrix multiplication as follows:

$$\mathbf{s=H\,u} \qquad \textbf{(3.9)}$$

The resulting value s is the index of the coset containing the active word u. It is not unique; there are 2^{M-N} representations of u that result in the same syndrome. For example, the eight binary words of u indexed by coset number five for the previous parity matrix are shown in Figure 3.9(b).

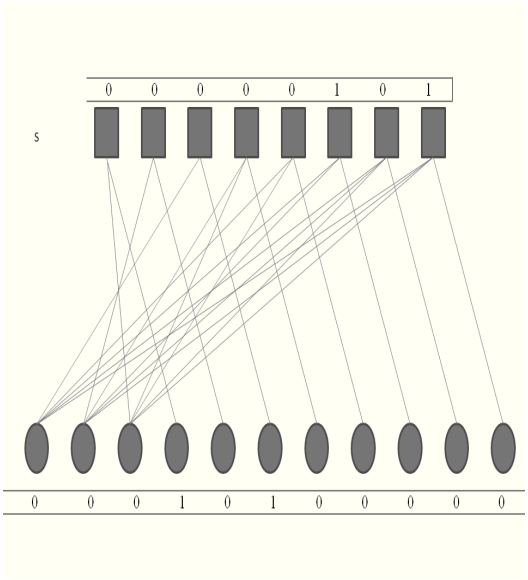

(a)

	Binary Words in coset number 5										
1	0	0	0	1	0	1	0	0	0	0	0
2	1	1	0	1	1	0	1	1	0	0	0
3	1	0	1	0	0	0	1	0	1	0	0
4	0	1	1	0	1	1	0	1	1	0	0
5	1	1	1	0	1	0	0	0	0	1	1
6	0	0	1	0	0	1	1	1	0	1	1
7	0	1	0	1	1	1	1	0	1	1	1
8	1	0	0	1	0	0	0	1	1	1	1

(b)

Figure 3.9 Code partition in coset number 5 (a) Graphical representation (b) Possible binary words

3.2.4 Source code recovery and estimation

The estimation will be a channel decoding process. A traditional decoding algorithm can be used with the exception that the decoder aims to find the most probably coded word with the received syndrome instead of trying to correct the error (with the all-zero syndrome).

A decoding algorithm, that uses Bayesian inference, is the so-called Maximum-Likelihood (ML)algorithm, in which, the inference process is as follows: The most likely sent codeword is found by calculating all conditional probabilities for all possible individual codeword and choose the one with maximum probability. The process is time-consuming and might lead to inaccurate estimations, it depends on setting the right probabilistic of bit-shift, the robustness

of the used code and the number of iterations. The maximum likelihood decoding for the Binary Symmetric Channel is NP-complete [58].

Another common decoding algorithm is the belief propagation algorithm [59] that is a message passing one. These are iterative algorithms, and their name implies that at each iteration the algorithm passes messages from message nodes to check nodes, and vice versa. The messages that are passed are probabilities or *beliefs*. One very important figure of merit of the algorithm is its sunning time, in general, is faster than the ML algorithm, but is less powerful [60].

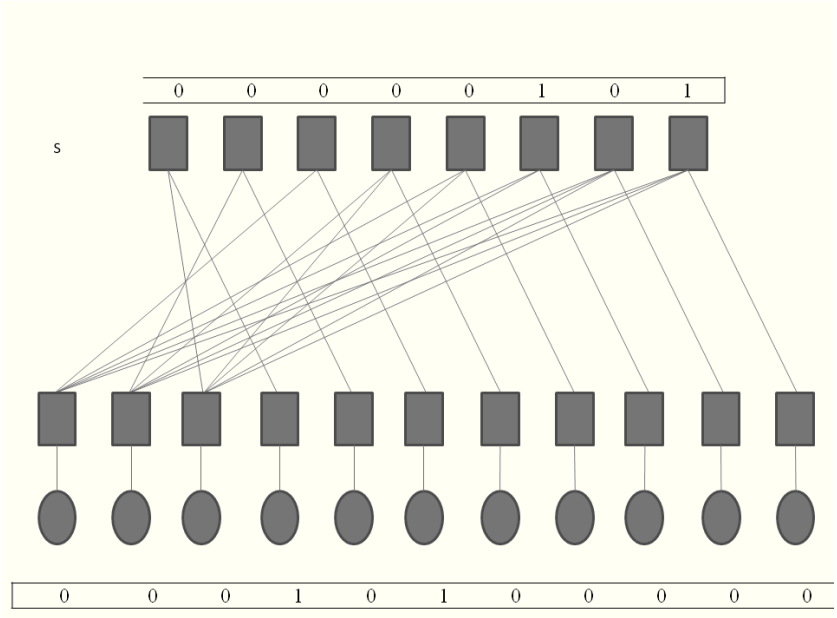

Figure 3.10 Graphical representation of the estimation process.

DSC has been extended in several research works for multiple sources and non-asymmetric cases [61]. In non-asymmetric DSC decoding, multiple sources are compressed and decoded jointly; the sum of the rates of the individual sources must be larger than H(u,v). In such cases, all code words can be recovered by a normal channel decoder (with syndrome equal to zero) without the need for modification of the code.

3.3 Continuous-valued versus binary sources

3.3.1 The need for signal quantization and A/D conversion

Figure 3.11 shows the architecture of a sensor node. As can be seen, the output of the sensor is real valued and converted to a binary word so that it can be processed.

Due to the fact that environmental data have a continuous range of values, the measurements have to be converted into a binary representation in order to be interpreted by a digital system

such as a microprocessor. Such a process has two main steps: quantization and analogue-to-digital conversion.

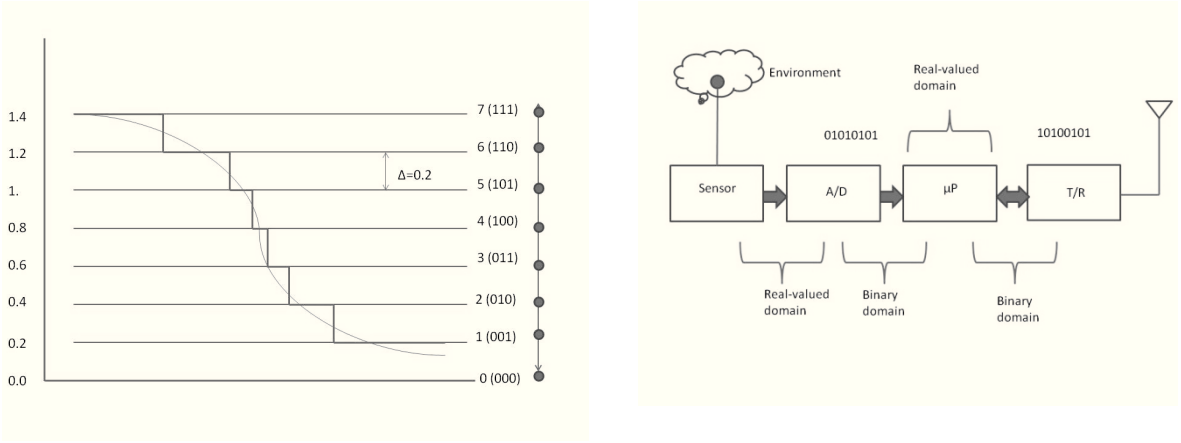

(a) **(b)**

Figure 3.11 Conversion from real-valued to binary domain: (a) Linear quantization. (b) Block Diagram illustrating the working domains

Linear quantization replaces the range of continuous values with a set of discrete ones by dividing the data range into a number of uniform intervals of a power of two. The quantized value is the one that is closest to the actual measurement. The decimal value resulting from the quantization process is then converted to a binary representation.

$$\boldsymbol{\Delta = \frac{higher_{limit} - lower_{limit}}{2^M - 1}} \quad \textbf{(3.10)}$$

$$\boldsymbol{Decimal = round\left(\frac{U - lower_{limit}}{\Delta}\right)} \quad \textbf{(3.11)}$$

3.4 Shifting Distributed Compression into the Continuous-Valued Domain

In the Slepian-Wolf approach, compression is done via channel coding; that is, the acquired signal is processed digitally in the microprocessor. However, quantization of a measured environmental variable is required only to be interfaced to an embedded system that works in a binary domain and to be communicated via radio in the form of a bit stream. Additional features such as data compression and recovery can be performed in a continuous-valued domain.

3.4.1 Variography

The approach adopted in this research work is to use a real-valued statistical domain to model the correlation between any pair of sensing points of the environment, and geostatistical methods are selected. The experimental variograms (EVs) from the acquired datasets need to be calculated.

The variogram $\gamma(h)$ describes the statistical dependency across sensors by the expected value *E* for the square of the difference in value of two points as a function of the distance *h*.

$$\boldsymbol{\gamma_U(h) = \frac{1}{2} E\left\{\left(U(k+h) - U(k)\right)^2\right\}} \quad \textbf{(3.12)}$$

These experimental curves must be approximated by theoretical variograms conforming to the limitations of being conditionally negative semi-definite functions. Only a limited set of functions can be applied as theoretical variograms, for example, Gaussian, Exponential and Spherical. They are usually described with three parameters: range, nugget and sill. The range gives the maximum distance up to which the mutual influence of two probe points has to be considered. Nugget and sill give the expected squared temperature deviation for very small and very large distances.

According to Kanevski [48], Spherical, Exponential and Gaussian variogram models are the most commonly used. The behaviour of them near the origin is of most importance in spatial predictions: Spherical model has a linear behaviour near the origin; the Gaussian variogram presents a very smooth behaviour at short distances, whereas an Exponential model reaches 95% of sill at the radius r. Other models include Power, Gamma, Stable and Bessel.

Spherical model:

$$\boldsymbol{\gamma(\mathbf{h})} = \begin{cases} \boldsymbol{\gamma_0 + (\gamma_\infty - \gamma_0)\left(\frac{3h}{2r} - \frac{1}{2}\left(\frac{h}{r}\right)^3\right)}, & \textbf{if } \mathbf{h} \leq \mathbf{r} \\ \boldsymbol{\gamma_0 + (\gamma_\infty - \gamma_0)}, & \textbf{if } \mathbf{h} > r \end{cases} \quad \textbf{(3.13)}$$

Exponential model:

$$\boldsymbol{\gamma(h) = \gamma_0 + (\gamma_\infty - \gamma_0)(1 - e^{\frac{3h}{r}})} \quad \textbf{(3.14)}$$

Gaussian model:

$$\boldsymbol{\gamma(h) = (\gamma_\infty - \gamma_0)\left(1 - e^{3\left(\frac{h}{r}\right)^2}\right)} \quad \textbf{(3.15)}$$

3.4.1.1 *Automatic curve fitting for the variogram*

An efficient variogram-fitting algorithm was found in [62], that provides a Matlab script to minimize the fitting error for an experimental, isotropic variogram. the minimum is found by using the Nelder and Mead algorithm [63], that is a heuristic, well-known method that is effective and computationally compact as it does not need any matrix inversion.

Furthermore, the algorithm provides additional advantages that may improve the good fitting of the function: it allows the least squares to be weighted if the number of observations per experimental lag is provided. Two weighting schemes are selected from the geostatistics literature. The first one is based on Cressie [64] and automatically gives most weight to early lags and down-weights to the lags with a small number of observations. The second scheme assigns weights based on the criterion of goodness described by McBratney and Webster [65].

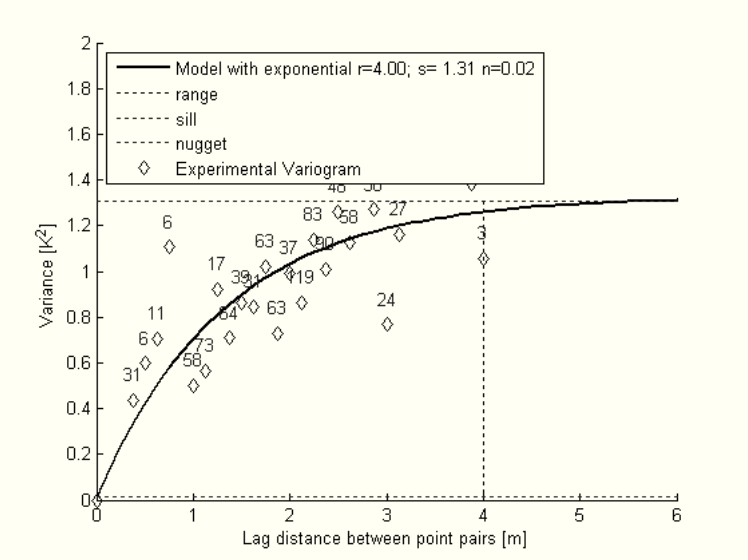

Figure 3.12 Experimental variogram for temperature measurements and its fitting by a theoretical model. The numbers indicate how many pair of points were available for a given distance.

3.4.1.2 *Source and coset space partition*

To take the binning concept into a real-valued domain, it is necessary to use a compression scheme to generate a subset of possible candidates, wherein the Euclidean distance between any pair of candidates should be as big as possible. With the exception of Chou [55], most of the research work is based on coding and decoding techniques rather than compression and recovery. Chou proposed a compression method that has very lightweight encoders.

The partition process is described mathematically using a modulo operation as in Equation 3.16.

$$\boldsymbol{coset = de2bi\left(round\left(\frac{U-lower_{limit}}{\Delta}\right) mod\ 2^{i}\right)} \quad \textbf{(3.16)}$$

Where de2bi is the decimal-to-binary conversion. Although mathematically elegant, it is equivalent to obtaining the decimal value of the truncated binary word at the i[th] LSB bit to represent the uncertainty $H(u|v)$.. The value of u can be recovered from the received information by fusing it with the information $H(v)$ available at the sink.

Similar to DSC, the source space will be partitioned into 2^N bins or cosets, each consisting of 2^{M-N} binary words. Instead of using codes, the method is based on the creation of linear spaces that are separated by a big Euclidian distance. The method starts with a linear space (LS) that contains the 2^M values separated by the quantization step Δ. The LS is then partitioned into two linear spaces; one of them corresponding the odd-indexed representation and the other to the even-indexed ones. The process is repeated M times, resulting in a final LS that contains 2^{M-N} values separated by a Euclidean distance of 2^N Δ. The descending tree process is illustrated in Figure 3.13; the original LS is shown at the top, even representations are on the bottom-right branches, and odd representations are on the bottom-left branches. By traversing the tree-based construction starting with the least-significant bit, the method will form the final LS.

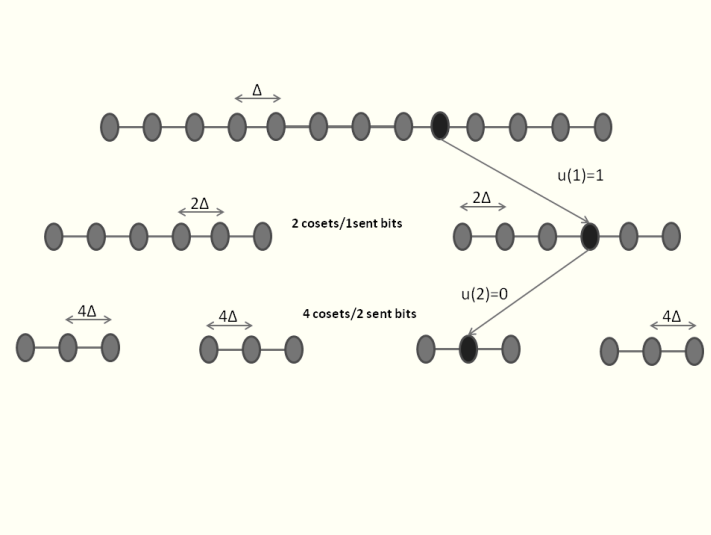

Figure 3.13 Tree-based source space partition. The value of the ith bit in u determines the construction of the linear spaces

Algorithm 1 Pseudo-code implementation of source space partition

Initialization

Create LS LS of 2^M elements separated by one Δ

$LS = linspace(0, 2^{M-1}, M)$

Build the LSs accordingly

Main loop

$for(index = 1; index \leq M; index++)$

$if(LS = 1)$

$LS = linspace(LS(2), size(LS), 2^{M-index})$

$else$

$LS = linspace(LS(1), size(LS) - 1, 2^{M-index})$

end

end

3.4.1.3 *Estimation*

The disadvantage of Chou's method lies in the decoding operation. A lookup table (LUT) is used to determine, by comparison, which one of the elements in the LS is closer to the side information available. A correlation tracking algorithm is required to find a parameter that scales the side information value and estimates U by selecting the value in the LUT that is closer. Such an algorithm requires all of the sensors to send their uncompressed data several times to calculate an estimate of the variances of the prediction error for each pair of sensors.

Their approach however is correct in the sense that an LUT-based estimation is energy-efficient but fails in terms of simplicity. The knowledge of auxiliary information and the use of information fusion will help to solve this problem.

3.5 Estimation via information fusion

The fundamental idea behind this concept is to fuse all information available to recover the real source value from a truncated received word. The data recovery unit requires the so-called auxiliary information.

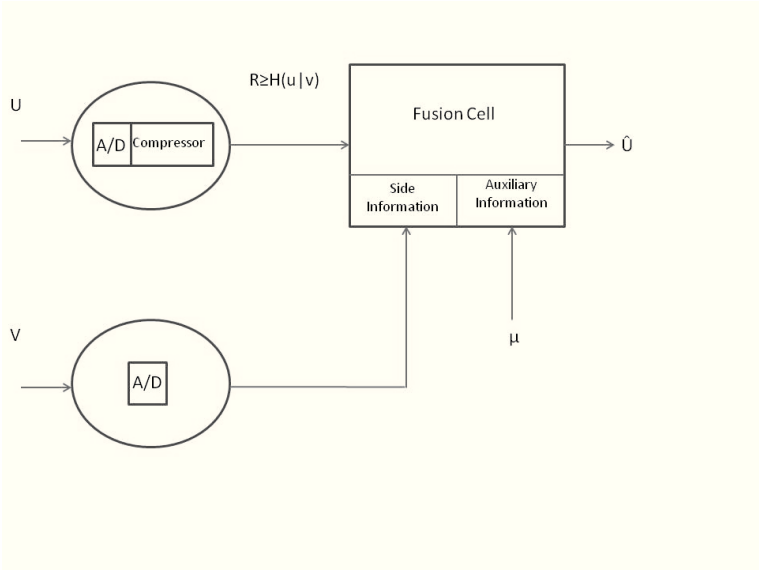

Figure 3.14 Data estimation in a fusion cell

In the 1990s, Uhlmann and Julier [66] pioneered a data fusion technique that was termed covariance intersection (CI). Later, in 2001, Hurley [67] showed its applicability to sensor measurements fusion. He demonstrated that it results in the minimization of the entropy of the fused density functions and gave an information-theoretic justification for it.

In CI, two pieces of information, labelled U and V, that are noise corrupted, are fused into an output Z to provide a better estimation of it in the presence of unknown correlation. The only information is the mean μ and the covariance of each of the estimations. We consider that the mean is the same for all three variables as they belong to the same random field.

If

$$\widetilde{\boldsymbol{U}} = \boldsymbol{U} - \boldsymbol{\mu} \qquad \widetilde{\boldsymbol{V}} = \boldsymbol{V} - \boldsymbol{\mu} \tag{3.17}$$

And

$$\mathbf{E}\{\widetilde{\boldsymbol{U}}\widetilde{\boldsymbol{U}}^{\boldsymbol{T}}\} = \widetilde{\boldsymbol{P}}_{\boldsymbol{UU}} \qquad \mathbf{E}\{\widetilde{\boldsymbol{V}}\boldsymbol{V}^{\boldsymbol{T}}\} = \widetilde{\boldsymbol{P}}_{\boldsymbol{VV}} \tag{3.18}$$

The fusion is made though a linear combination of them.

$$\mathbf{Z}=\boldsymbol{W_U\widetilde{U}+W_V\widetilde{V}} \tag{3.19}$$

It follows that

$$\mathbf{P_{ZZ}=W_UP_{UU}W_U{}^T+W_UP_{UV}W_V{}^T+W_VP_{VU}W_U{}^T+W_VP_{VV}W_V{}^T} \tag{3.20}$$

The aim of the algorithm is basically to minimize the trace of $\mathrm{P_{ZZ}}$ by choosing the weights W_U and W_V. For decompression purposes a minimization criterion has to be defined when one of the measurements is fixed and used as side information and the correlation are known.

It is observed that Equation 3.20 can be written in terms of centred covariances

$$\mathbf{C_{ZZ}(h)=W_UC_{UU}(h)W_U{}^T+W_UC_{UV}(h)W_V{}^T+W_VC_{UV}(-h)W_U{}^T+W_UC_{VV}(h)W_V{}^T} \tag{3.21}$$

If the centred covariance is considered symmetric

$$\boldsymbol{C_{UV}(h)=C_{UV}(-h)=C_{VU}(h)} \tag{3.22}$$

Also, if V is the side information, the expectation is constant as well

$$\boldsymbol{\widetilde{P}_{VV}=C_{VV}(h)=\widetilde{V}V^T=(V-\mu)^2} \tag{3.23}$$

Traditionally, a CI iterative algorithm would have a set of measurements of both variables and would find the matrix weights W_U and W_V that minimize the trace of P_{ZZ} by performing filtering of redundant data between U and V.

Because $\tilde{P}_{VV}$ is constant, the elements of $\mathrm{W_V}$ will be weighted equally, and $\mathrm{C_{VV}(h)}$ does not have an effect on the minimization. The minimization depends mainly on the trace of $C_{UV}(h){W_U}^T$

$$\mathbf{min}(\boldsymbol{C_{ZZ}(h)})=\boldsymbol{min}\left(\boldsymbol{tr}\left(\mathbf{2}\boldsymbol{W_UC_{UV}(h)W_V{}^T}\right)\right)=\boldsymbol{min}\left(\boldsymbol{tr}\left(\mathbf{2}\boldsymbol{W_UC_{UV}(h)}\right)\right) \tag{3.24}$$

V is constant and U takes all the possible 2^{M-N}values in the coset by considering the main diagonal of $C_{UV}(h)$.

$$\boldsymbol{C_{UV}(h)}=\begin{bmatrix}(\boldsymbol{V}-\mu\ )(\boldsymbol{U_1}-\mu) & \cdots & * \\ \vdots & \ddots & \vdots \\ * & \cdots & (\boldsymbol{V}-\mu\ )\left(\boldsymbol{U_{2^{M-N}}}-\mu\right)\end{bmatrix} \tag{3.25}$$

and its trace is

$$\boldsymbol{tr(C_{UV}(h))}=\sum_{\boldsymbol{i=1}}^{\boldsymbol{2^{M-N}}}(\boldsymbol{V}-\mu\ )(\boldsymbol{U_i}-\mu) \tag{3.26}$$

Minimizing the trace of $C_{UV}(h)$ will lead automatically to a minimization of $C_{ZZ}(h)$. If W_{U_i} and W_{V_i} are the i[th] elements in the main diagonal of W_U and W_U, then

$$tr(C_{ZZ}(h))=2\sum_{i=1}^{2^{M-N}} W_{U_i}(V-\mu\ )(U_i-\mu) \quad \textbf{(3.27)}$$

If an iterative algorithm were used to find the minimum of the trace of $C_{ZZ}(h)$, it would weigh fewer proportionally big values of $(V-\mu\ )(U_i-\mu)$ and consequently more small values of it. By choosing the minimum of all of them, that is, the most weighted, we automatically choose the one that contributes more to the fusion, and because all elements of U_i are possibly estimations of the source that are separated by a big Euclidean distance, there is a large possibility of finding the correct source value

The value of U_i that leads to the minimum of $(V-\mu\ )(U_i-\mu)$ is:

$$\widehat{U}=\mathbf{argmin}_{U_i \epsilon\, LS}\big((V-\mu\ )(U_i-\mu)\big) \quad \textbf{(3.28)}$$

And because $(V-\mu\ )$ is constant,

$$\widehat{U}=\mathbf{argmin}_{U_i \epsilon\, LS}\big((U_i-\mu)\big) \quad \textbf{(3.29)}$$

Equation 3.29 leads to the conclusion that the estimation in the linear space that is closer to the mean value is the one that has a higher probability of being the correct one. It also leads to the conclusion that the side information plays no role in the minimization process.

3.5.1 Rate allocation

Because U and V are in fact two outcomes of the same random variable, $C_{ZZ}(h)$ is in fact the variogram $\gamma_U(h)$ of the random field.

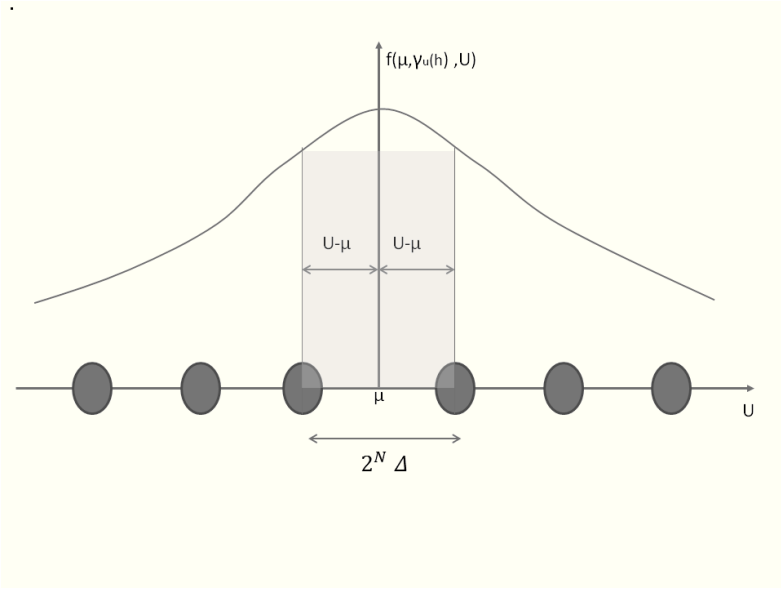

Figure 3.15 Probability density function of the random variable U and its relation with the coset partition.

Given the distance between two measured points and a fitted variogram model, it is possible to have an estimate of the number of bits required to represent the source U given by the following equations.

The expected value of $(U-\mu)^2$ is in fact the value of the fitted variogram at a distance h.

$$\boldsymbol{E(U-\mu) =\approx \sqrt{\gamma_U(h)}} \tag{3.30}$$

According to equation 3.29, the minimum value of $(U-\mu)$ must selected, and beacause$2^N\,\Delta$ is the Euclidian distance between all the elements in the coset, a correct estimation is made when

$$\boldsymbol{E(U-\mu) < \frac{2^N\,\Delta}{2}} \tag{3.31}$$

which leads to

$$\boldsymbol{\sqrt{\gamma_U(h)} < \frac{2^N\,\Delta}{2}} \tag{3.32}$$

and the assignment of rates is made by rounding the result of equation 3.32 to the next integer and adding one to compensate for modelling inaccuracies.

$$\boldsymbol{N > ceil\left(log_2\left(\frac{2\sqrt{\gamma_U(h)}}{\Delta}\right)\right) + 1} \tag{3.33}$$

3.6 Simulation Results

In this section simulation results are provided. We wanted to measure compression rates due to bit transmission and the percentage of failed estimations for different fitted variogram models and weighting schemes. For experimental confirmation of the developed compression method, a binary word size of 11 bits was selected. The following table shows the upper and lower limits used for linear quantization and the corresponding quantization steps for humidity and temperature

Table 3.1 Limits used for linear quantization and respective quantization steps

4	Upper limit	Lower limit	Δ
Temperature (K)	25	0	0.0122
Humidity (%RH)	75	0	0.0366

4.1.1 Compression rates

For a word size M of eleven bits and the mentioned quantization steps, the entropies and their values ranges are summarized in the next table.

Table 3.2 Binary entropies and respective temperature and humidity ranges

	Temperature variance		Humidity variance	
Entropy(bits)	**Minimum**	**Maximum**	**Minimum**	**Maximum**
5	.0034	.009	0.04	0.09
6	.009	.03	0.09	0.34
7	.03	.1527	0.34	1.37
8	.1527	.61	1.37	5.50
9	.61	.82	5.50	12.03

Figure 3.16 shows the variogram fitting for an exponential model with weighting as described by McBratney and Webster [65] for the temperature measurements in the experiment with pallets on the floor if the variogram and the mean value are updated at every sampling time.

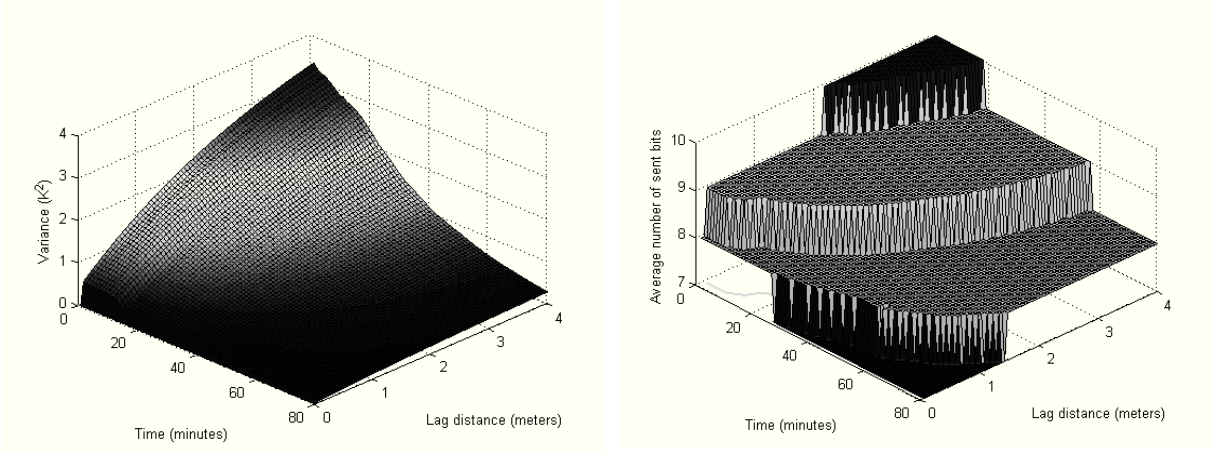

(a) **(b)**

Figure 3.16 Results for temperature when the container is filled with pallets: (a) spatio-temporal variogram; (b) rate allocation.

The selection of the variogram model has no impact on the average compression, as can be seen in Table 3.3

Table 3.3 Average achieved compression rates for three fitted variogram models

	Average compression rate ´R			
Variogram model	**Δ**	**2 Δ**	**3 Δ**	**4 Δ**
Gaussian	0.76	0.67	0.61	0.58
Spherical	0.75	0.66	0.61	0.57
Exponential	0.76	0.67	0.62	0.58

4.1.2 Percentage of failed estimations

Regarding the percentage of failed estimations, the exponential model provides better results for both experiments and for both environmental variables. The weighting scheme based on McBratney and Webster [65] also reduces the percentage of failed estimations in all cases.Table 3.3 shows the results for temperature when the container is filled with pallets on the floor for different quantization steps.

Table 3.4 Percentage of failed estimations for three models and two weighting schemes for temperature measurements when the container is filled with pallets on the floor

	McBratney and Webster				Cressie			
	Δ	**2 Δ**	**3 Δ**	**4 Δ**	**Δ**	**2 Δ**	**3 Δ**	**4 Δ**
Gaussian	10.63	10.66	9.75	10.70	13.86	13.89	12.13	13.95
Spherical	11.44	11.47	7.50	11.53	12.55	12.58	9.44	12.67
Exponential	7.53	7.53	5.58	7.64	9.95	9.97	7.23	10.03

The next table summarizes the results for both experiments and for temperature (T) and humidity (H) when the exponential model is fitted using the criterion of McBratney and Webster. Every possible combination of source–sink pairs was simulated. The percentage energy savings is calculated by averaging the N sent bits over the duration of the experiments. It can be seen that energy savings up to 57% for temperature and up to 50% for humidity are possible without exceeding an estimation failure rate of 10%. In the best cases it is possible to achieve an estimation failure rate of 4% with 40% energy savings.

Table 3.5 Summary of accuracy and energy saving results for an exponential variogram model fitted using the criterion of McBratney and Webster

		Percentage of error				Energy savings (%)			
		Δ	**2 Δ**	**3 Δ**	**4 Δ**	**Δ**	**2 Δ**	**3 Δ**	**4 Δ**
Container with pallets	**T**	7.53	7.53	5.58	7.64	23.82	32.79	37.95	41.77
	H	6.16	6.27	7.45	6.08	26.65	35.63	41.26	44.61
Empty container	**T**	7.41	7.95	9.14	7.72	39.22	48.20	53.01	57.18
	H	3.91	4.06	5.42	4.42	31.96	40.93	46.61	49.91

4.1.2.1 *Robustness against non-stationarity*

The previous results assume that information about the mean and variogram is updated continuously for every sample. However, because the aim is to compress data to reduce communication, the acquisition of uncompressed data from all sensors has to be avoided as much as possible. The datasets used in the present research work are very useful to study the

robustness of the method because the variances and mean of the environmental field are changing drastically over time.

An experimental variogram data-aggregation query is far more energy-consuming than a mean value one. However, the mean value plays a bigger role in performing a correct estimation. It makes sense to update the mean value more often than the variogram. To test the robustness against non-stationarity, the variogram is updated only at the times when the sill of the fitted variogram model reaches one of the entropy transition values shown in Table 3.6. The mean is updated at regular intervals of 10 and 15 minutes.

Table 3.6 Summary of accuracy and energy savings results for an exponential variogram model fitted using the criterion of McBratney and Webster when the mean is updated at discrete intervals

		Percentage of error			Energy savings (%)		
		Stationary-like	**10 minute interval**	**15 minute interval**	**Stationary-like**	**10 minute interval**	**15 minute interval**
Container with pallets	**T**	7.53	6.82	10.26	23.82	18.95	18.95
	H	6.16	9.51	12.20	26.65	23.89	23.89
Empty container	**T**	7.41	6.76	11.01	39.22	34.66	34.66
	H	3.91	7.23	11.71	31.96	29.41	29.41

Table 3.6 summarizes the results when the variogram and the mean are updated at every sampling, that can be considered a stationary-like process, and when the variogram is updated according to the binary entropy and the mean is updated at discrete intervals. It can be seen that, as expected, the percentage of estimation errors increases, but in the worse case it is only 12%. The energy saving decreases, but in the worse case only about 5% is not saved in comparison with the stationary-like case,

4.1.3 Comparison with DSC coding

In order to compare both approaches for distributed compression, the temperature measurements for the container with pallets on the floor are selected. The rates are adapted according to our method for the last sampling time. The probability of bit flip in DSC is fixed at 0.45. An implementation of the decoder provided by [68] and geometric codes described in [69] are used.

Figure 3.17(a) shows that for the statistical approach almost all combinations are perfectly recovered; correct estimations are represented by blue squares and failures by red ones.

Figure 3.17 (b) illustrates the results for the Slepian-Wolf approach; it can be observed that the percentage of errors is high. Another selection of the probabilities of bit-flip helps in some sensor combinations, but its detrimental in others.

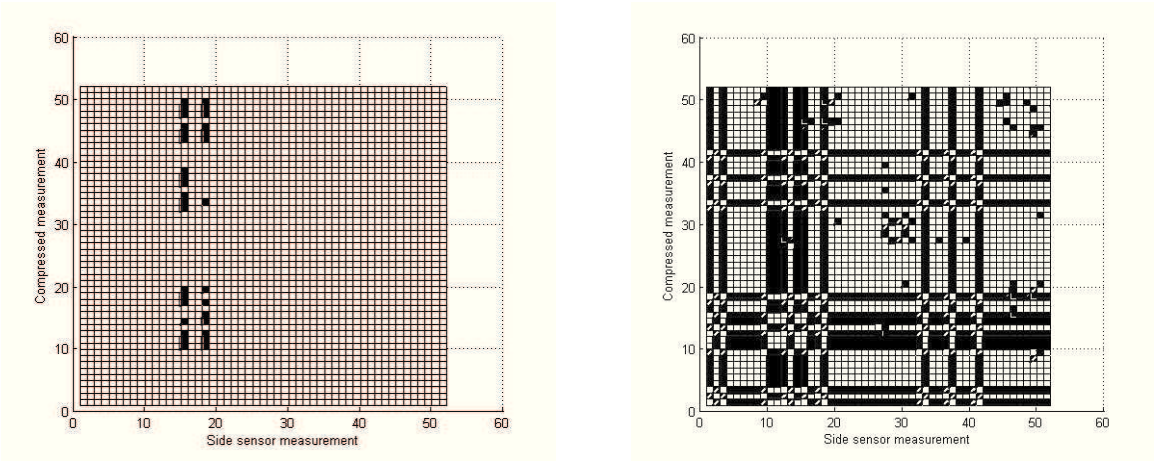

(a) **(b)**

Figure 3.17 Correct estimations for all possible combinations of sensor pairs: (a) using continuous-valued approach; (b) using the Slepian-Wolf approach

4.2 Summary and conclusion chapter 3

Methods in the geosciences and data fusion fields can be combined for application in key technologies such as sensor networks to cope with inherent constraints such as the need to reduce radio communication. By doing this and shifting from the binary to the real-valued domain it is possible to achieve not only efficient data compression but also easy data recovery suitable for performance in constrained devices.

Parallels exist between performing distributed sensor compression in digital and real-valued domains. In the binary domain, the environment is modelled as a wireless communication channel, where the source is corrupted by noise during transmission, arriving at the decoder with some of the bits flipped due to the noise power. The bigger the noise, the more bits are likely to be flipped. In a real-valued domain, the environment is first “explored”; an experimental variogram is acquired from the actual measurements and automatically fitted to a theoretical model to determine the spatial relationships.

In the binary domain, rate allocation is bounded for example by Chebyshev’s inequality, in which it is necessary to establish a prediction error and the value of the quantization step. In

the real-valued domain the fitted variogram model together with the mean value is required to allocate ratios.

Both approaches use the concept of partitioning the source space into cosets; each element belonging to a specific coset is “far away” from the others using a specific metric; in the digital domain the metric used is the Hamming distance, whereas in the real-valued domain it is a Euclidean one.

In both cases, the task of the data estimation unit is to utilize the available information properly to select the element inside the coset that best complies with a given criterion. In the binary domain the decoder uses complex techniques such as belief propagation to determine which binary word is more likely to be the one sent, given the probability of bit flip during transmission. In the real-valued domain, all elements of the coset are used together with the auxiliary information to build a lookup table from which the minimum element is selected.

The results show that is possible to achieve perfect estimations of at least 90% of the possible sensor combinations while reducing communication by up to 60% without needing a simple algorithm that can be deployed in sensor nodes. It is also shown that the method is robust against non-stationarity.

5 Theoretical-guaranteed Increased Coverage in WSN

5.1 Relation between Information Fusion and Kriging Methods

Information Fusion (IF) has found applicability in Geographical information systems (GIS). In [68] several research papers regarding IF and GIS are discussed, surprisingly, Kriging interpolation, developed for geo-statistics, is not considered. Kriging methods are IF ones, but they have not been fully appreciated by the general fusion community. The Ordinary Kriging method (OK) can be considered as a spatial statistical fusion method across sensors whereas Cokriging interpolation (CK) can be considered a spatial statistical method for fusion across attributes and sensors.

Kriging methods are based on statistical descriptions of the spatial dependencies of the attributes, the so called variograms. They are Best Linear Unbiased Estimators (BLUE), where "best" basically means that the estimation gives the lowest variance possible and therefore gives strong theoretical guarantees. The condition of unbiasedness is assured by constraining the sum of all weights of the primary attributes to be equal to one. The minimization of the variance is then constrained to the unbiasedness condition, by using Lagrange multipliers the problem of constrained minimization turns into a problem of unconstrained minimization.

5.1.1 Conditions for Theoretical Guarantees

Kriging and cokriging errors have Gaussian distributions; it is determined by the mean μ and the resulting Kriging variances. A correct tuning of the variogram models and parameters is a necessary condition to the correctness of the estimation. Such correctness, can be evaluated by cross-validating the predicted Kriging standard deviation σ_i and the actual error $\boldsymbol{\varepsilon_i}$ for each destination point i [69]. The relation θ should be unitary.

$$\boldsymbol{F(i) = \frac{\varepsilon_i}{\sigma_i}} \tag{5.1}$$

$$\boldsymbol{\theta = \frac{\sum_{i=1}^{n} F(i)}{N_z}} \tag{5.2}$$

5.1.2 Definition of Interpolation Error

The interpolation error ε_i at each point is defined as the average squared error between the estimated value $\hat{z}_i(k)$ and the real value $z_i(k)$ over N_k samples.

$$\varepsilon_i^2 = \frac{\sum_{k=1}^{N_k}(\hat{z}_i(k) - z_i(k))^2}{N_k} \quad \textbf{(5.3)}$$

The average prediction error $\bar{\varepsilon}$ over N_z destination points was selected as a measure of the quality of the interpolation.

$$\bar{\varepsilon} = \frac{\sum_{i=1}^{n} \varepsilon_i}{N_z} \quad \textbf{(5.4)}$$

5.2 Ordinary Kriging vs. Deterministic Models

Kriging [48, 69] performs linear interpolation to estimate the value in one destination point by multiplying the available measurements with a set of weighting factors. Weights are proportional to the correlation between the estimated points and the measurements; if there is no spatial correlation all weights are equal and the estimates yield to the average value of all measurements. In comparison with deterministic interpolation techniques such as Null-model and Inverse Distance Weighting (IDW), provides two estimates: the values at a specific location and the uncertainty of such estimation. The results were published in a joint paper [70]. The contributions of the author of this thesis were on the research of the accuracy of the Nelder-Mead method to automatically fit the variogram to the experimental data and on the comparison with the accuracy achieved by other methods.

5.2.1 Deterministic Interpolation Methods

There are plenty of interpolation techniques, we have selected only two, IDW that takes into account the distances between the source points and a null-model that averages all the sources.

IDW is the most common method used to interpolate the value at an unknown location; it uses only the geometrical distances h_{iP}^2 between the source points and the destination. The estimation at an unknown location is given by

$$\hat{U}_P = \sum_{i=1}^{n} a_i U_i \quad \textbf{(5.5)}$$

And the weighting coefficients are given by:

$$a_i = \frac{1/h_{iP}^2}{\left(\sum_{i=1}^{n} \frac{1}{h_{iP}^2}\right)} \quad \textbf{(5.6)}$$

It assumes that the influence of a source point on a destination point decreases with the square of their distance.

Null-Model is a simpler model, that ignores the influence of the distances in the estimation calculates the average of the source points to estimate the value at a specific location.

$$\widehat{\mathbf{U}}_{\mathbf{0}} = \frac{\mathbf{1}}{\boldsymbol{n}} \sum_{\boldsymbol{i}=\mathbf{1}}^{\boldsymbol{n}} \boldsymbol{U_i} \tag{5.7}$$

The Ordinary Kriging method (OK) can be considered as a statistical fusion method across sensors due to the fact that it improves the completeness of the information: it estimates the value at a specific location and provides the so called kriging variance (KV), that is a measure for the certainty of the estimations. The subsequent curve fitting is restricted to a limited set of the guaranteed consistency. Variogram values for distances between the measured points are combined in a linear equation system. The interpolation is calculated by weighing the existing measurements by a set of coefficients, given by the solution of the equation system. For a detailed introduction to the Kriging method, see [71].

5.2.2 Kriging interpolation

Kriging [48, 69] applies a linear interpolation to predict the temperature in one destination point by multiplying the available measurements with a set of weighting factors. An experimental Variogram is calculated from the measurements and then fitted with a theoretical model in a way to minimize the error between experimental and theoretical Variogram. The application of the Variogram to set the Kriging weights provides a statistically correct estimator for the weighting factors, and therefore, is the best linear estimator under the condition that the expected value for the difference between two points depends only on their distance vector and not on their absolute position.

Variogram values for distances between the measured points are combined in a linear equation system. The interpolation is calculated by weighing the existing measurements by a set of coefficients, given by the solution of the equation system.

$$\begin{bmatrix} \boldsymbol{\gamma_U(0)} & \boldsymbol{\gamma_U(h_{AB})} & \boldsymbol{\gamma_U(h_{AC})} & \dots & \mathbf{1} \\ \boldsymbol{\gamma_U(h_{AB})} & \boldsymbol{\gamma_U(0)} & \boldsymbol{\gamma_U(h_{BC})} & \dots & \mathbf{1} \\ \boldsymbol{\gamma_U(h_{AC})} & \boldsymbol{\gamma_U(h_{BC})} & \boldsymbol{\gamma_U(0)} & \dots & \mathbf{1} \\ \vdots & \vdots & \vdots & \vdots & \vdots \\ \mathbf{1} & \mathbf{1} & \mathbf{1} & \dots & \mathbf{0} \end{bmatrix} \begin{bmatrix} \boldsymbol{a1} \\ \boldsymbol{a2} \\ \boldsymbol{a3} \\ \vdots \\ \boldsymbol{an} \\ \boldsymbol{\lambda} \end{bmatrix} = \begin{bmatrix} \boldsymbol{\gamma_U(h_{AP})} \\ \boldsymbol{\gamma_U(h_{BP})} \\ \boldsymbol{\gamma_U(h_{CP})} \\ \vdots \\ \boldsymbol{\gamma_U(h_{nP})} \\ \mathbf{1} \end{bmatrix} \tag{5.8}$$

The unbiasedness is guaranteed by:

$$\sum_{\boldsymbol{i}=\mathbf{1}}^{\boldsymbol{n}} \boldsymbol{a_i} = \mathbf{1} \tag{5.9}$$

And the KV is obtained by:

$$\sigma_{OK}^2 = \sum_{i=1}^{n} a_i \gamma_U(h_{iP}) + \lambda \quad \textbf{(5.10)}$$

Where λ is the lagrange multiplier

5.2.3 Variogramm fitting algorithms

As mentioned before a correct variogram model and proper fitting of its parameter is highly important. Besides Nelder-Mead algorithm described in [63], we selected two more methods.

5.2.3.1 *Grid-search*

A *brute-force* grid search was implemented. The grid search tests all combinations of range, nugget and sill for the lowest fitting error between a given set of boundaries. For an adequate setup of the boundaries, The algorithm searched for a sill value between 60% and 180% of the measurement variance all measurements. The lower and upper grid boundaries for the nugget value were set to 2% and 20% of the measurement variance, respectively; the search for the variogram range values was performed between 1 and 10 meters.

5.2.3.2 *Fixed Parameters*

A third method that only adapts the sill value was implemented. Based on the resulting range of the fitting-algorithms, the fixed range was set to the average range value of the fitted experiments. The nugget was directly set to the square of the measured sensor tolerances. The sill was calculated to fit the average value of the theoretical model to the experimental Variogram for large distances.

5.2.4 Datasets

In total 14 datasets were recorded to test the Kriging procedures on different conditions: eight in cold storage rooms and six during regular food transports.

The dimension of the cold storage rooms are of 2.6 × 2.2 × 2.3 meters. Between 54 and 68 temperature probes of PT100 type were installed at the walls. Zero and six degree Celsius were programmed as set point temperatures, empty and loaded conditions as well as on-of an modulated cooling modes were tested. Specific Details can be found in [72].The performance conditions to validate the tests are the loading state (empty/full), set-points of 6 and -29 °C

The six experiments performing during food transports were acquired in collaboration with food supplier companies and consists of two datasets recorded during terrestrial transport of frozen-meat and four recorded during overseas transport of bananas.

The tests consisting of terrestrial transport of frozen meat was performed inside delivery trucks provided by the German company Rungis Express. The trucks is separated into three separate chambers, the experiments were performed in the deep freezer chamber with dimensions of $2.9 \times 2.5 \times 2.35$ meters. Forty TurboTag [73] data loggers were placed with a set point of -29 °C.

Two of the datasets tests consisting of overseas transport of bananas were provided by Maersk, in it forty-five sensors were placed inside the freight. The rest two datasets were recorded within a cooperation project with Dole from Costa Rica to Antwerp. Twenty-seven and thirty-one iButton [74] data loggers were placed in the centre of banana boxes in experiments perform in 2010 and 2011, respectively.

5.2.5 Resulting variogram models

The resulting variogram models and range value depend basically of the loading conditions, dimensions of the closed, controlled environment and set point. Table 5.1 shows the average range of the grid search Variogram models sorted by groups of experiments. It can be seen that if the air circulates without obstacles, the temperature variations spread over a wider range. A clear comparison is the resulting ranges of the cold storage room the average range decreases from 4.7 to 3.4 meters in the presence of cargo. The highest range of 4.7 metre was measured in empty cold storage rooms. Partially filled cold storage rooms and trucks showed almost the same range of 3.25 to 4 meter. For densely packed cargo such as bananas in sea containers the range dropped to 1.65 or 1.125 meter.

An important figure of merit is the number of neighbours that lie into the resulting variogram range; neighbours lying above the average range have little effect on the interpolation because their assigned weights are very low. In a worst-case scenario, if all neighbours are outside the variogram range, all neighbours will be assigned with the same weights; the resulting interpolation would be equal to the average of the values of the neighbours.

Table 5.1 Fixed range parameter for groups of experiments

Group	Range	Model type	Neighbours in range
Empty cold storage room	4.7 metre	Spherical	29.9
Loaded cold storage room	3.4 metre	Spherical	24.7
Trucks	3.25 metre	Gauss	24.5
Container Maersk, inside bananas	1.65 metre	Gauss	3.8
Container Dole, inside bananas	1.125 metre	Gauss	4.0

Figure 4.1 show some representative resulting variogram models. It can be observed how in the case of cold storage rooms the variogram models fit well to the experimental data, only some measurements lie outside the model. The experimental Variograms for the container tests turned out to be very sparse which might be caused by either anisotropic dependencies of the variance from the direction of the distance vector between the pair of point or by the lack of enough probe points in the container.

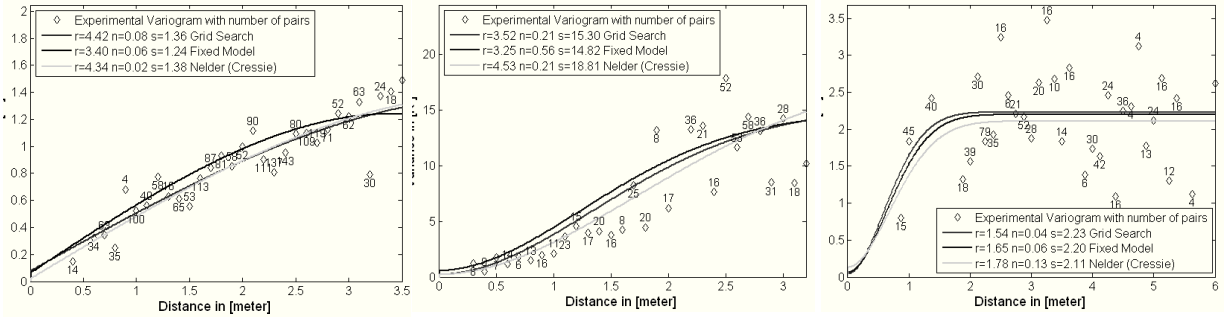

(a) **(b)** **(c)**

Figure 5.1 Experimental Variogram and models resulting from different estimator algorithms: (a) Spheric for experiment 8(loaded cold storage room), (b) Gauss for partly filled truck (experiment 10) and (c) Gauss for sea container loaded with bananas (experiment 11)

5.2.5.1 *Accuracy of the estimations*

The robustness of Kriging interpolation is highly dependent of the variogram model and its parameters and therefore of the method used to fit it to the experimental data. The prediction errors of the resulting variogram parameter for the grid search, the fixed model and Nelder/Cressie search algorithms were compared with the Null-model and the Inverse-Distance-Weighting model. The results are shown in Figure 5.2.

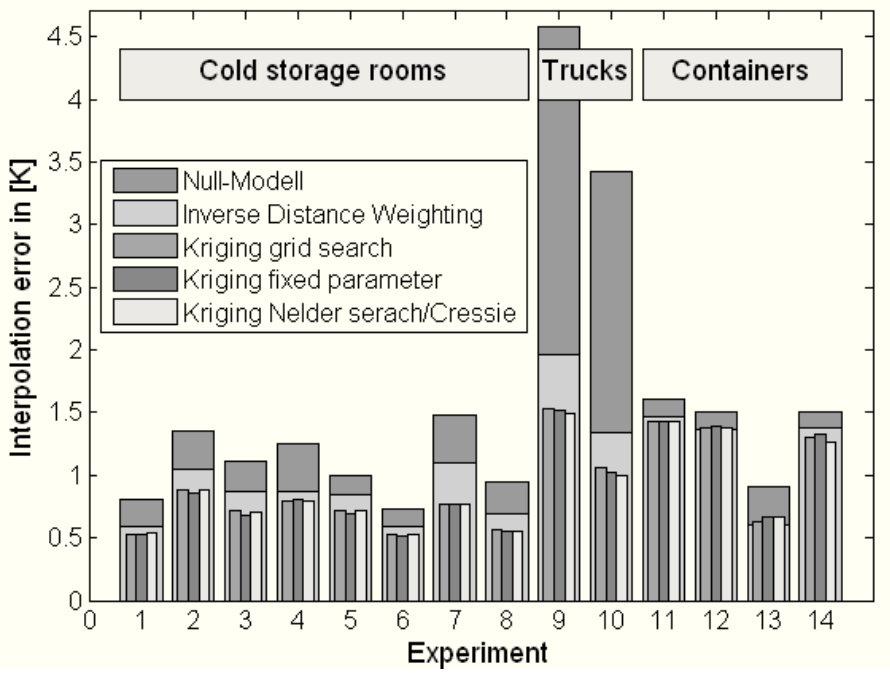

Figure 5.2 Error between prediction and measurements for different methods for Variogram estimation. Compared with the Null- and the IDW-model.

A significant improvement using Kriging interpolation can be observed for the truck tests. Kriging method brought a smaller but still remarkable improvement compared with Deterministic models for the test in cold storage room. The worst results for Kriging was for the container tests; it brought only little advantage compared to the Null-model and was sometimes even worse than the Inverse-Distance-Weighting. The results are summarized inTable 5.2

Table 5.2 : List of methods that gave the best relation θ for the different types of experiments

.

Type	**Best method**	**Model type**	**Improvement over Null-model**	**Improvement over IDW-model**
Cold storage room	Nelder/Cressie	Spherical	35.8 %	16.0 %
Truck	Fixed parameters	Gauss	68.5 %	23.4 %
Container	Grid search	Gauss	16.1 %	1.4 %

5.2.5.2 *Theoretical Guarantees of the estimations*

A theoretical guaranteed estimation is only given if the relation θ between Kriging Variance and actual interpolation error is close to the unity. The results are summarized in Figure 5.3.

The best results were achieved for the tests in the cold storage room where they are almost unitary. The worse results are for the last two container experiments at Dole, the relation θ increased to values of up to 3.5; this is explained by the low number of neighbors that lie inside the variogram range, with a higher number of sensors the relation should increase.

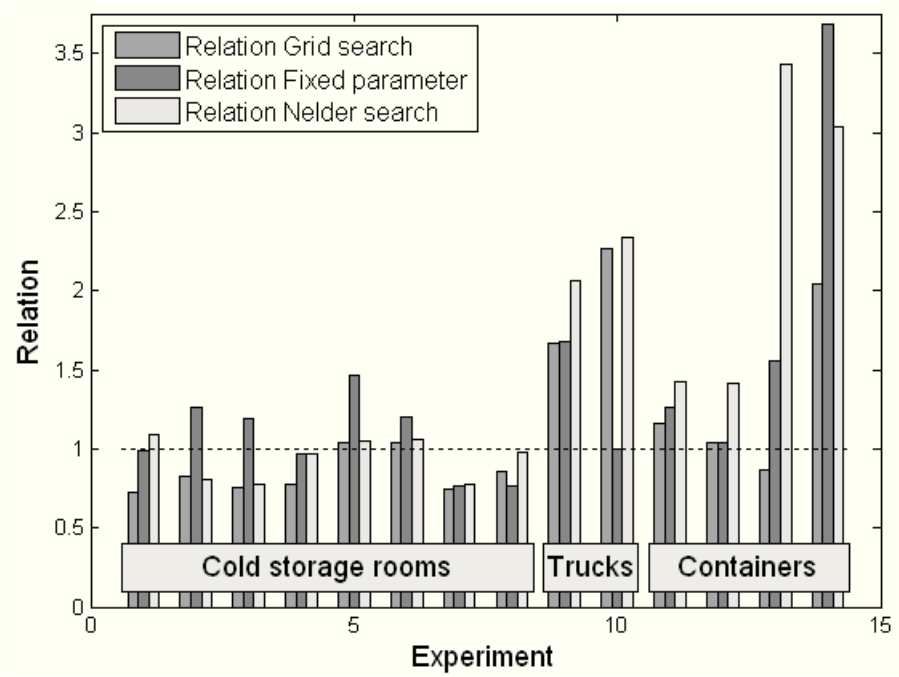

Figure 5.3 Relation between Kriging Variance and actual interpolation error θ for different methods for Variogram estimation.

As can be seen in Figure 5.3, depending on the type of experiment, different methods for Variogram estimation gave the best result for the relation θ. Without taking into account the container tests, the interpolation error can be reduced by up to 68.5 % if Kriging is used for interpolation compared with the deterministic models, the Kriging interpolation is in average 20% better except for the container tests. The weighting according to [65] was rejected because it gave only inaccurate Variogram parameter for two tests in the cold storage room. Furthermore, the relation was worse than by all other methods.

5.2.6 Minimum number of required sensors

The number of neighbours within the variogram range is a good indicator of a good sensor deployment; similar number of probe points were used for different experiment, however only those with many sensor inside the range gave a good estimation as they have the most influence on the interpolation result. The cold storage rooms and trucks had an average number of neighbours in range between 24 and 30, whereas the sensor setup for the containers had only 3.8 or 4 neighbours in range as listed in Table 5.1

In Figure 5.4. the number of source points was incremented step by step. In order to estimate a threshold for the index value, Every time a point was added, the horizontal axis was recalculated in order to directly display the number of neighbours in range instead of the total number of source points. It can be observed that if the number of neighbours in range is higher than 10 (dotted line), the Kriging interpolation results in a lower error than the Inverse-Distance-Weighting. At this index value, Kriging has also a clear benefit compared to the Null-model.

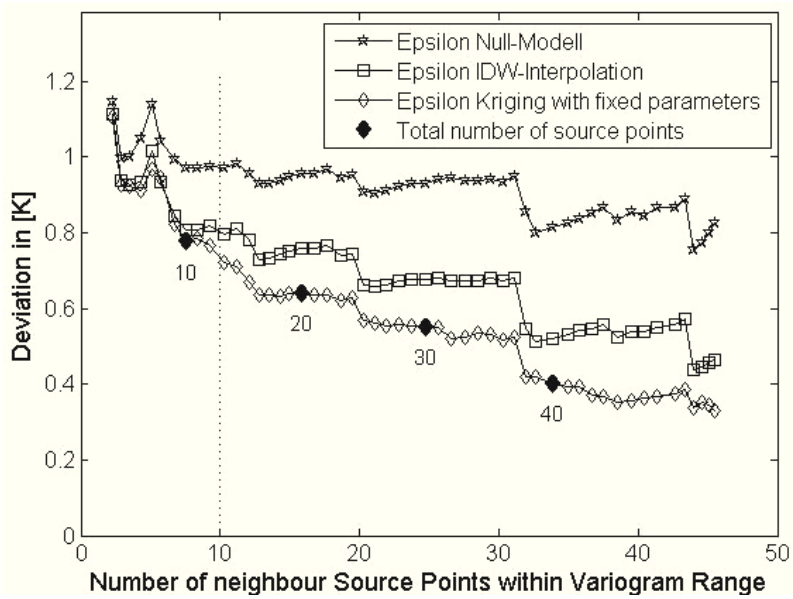

Figure 5.4 Interpolation error as function of the number of neighbours in range for experiment 8 (loaded cold storage room). Total number of source points marked by diamonds.

5.3 Cokriging vs. Ordinary Kriging

Ordinary Kriging is a Best Linear Unbiased Estimator, it is more accurate than deterministic methods under two basic conditions: a correct fitting of an experimental variogram to a theoretical model, and enough number of informative sources. Assuming a correct theoretical

model of the variogram, one way to improve the accuracy is by finding the optimal positions of the sensing points.

However, repositioning of the sensors is not always possible after deployment; to solve this problem, it is proposed to exploit the spatial cross-correlations between the attributes; an attribute of interest that is sparsely sampled and a secondary attribute that is densely sampled. For instance, instead of deploying 50 humidity sensors, collocated temperature sensors might help predict humidity levels for 40 of the positions by using only 10 genuinely acquired measurements.

Cokriging interpolation (CK) can be considered as a method for fusion across attributes and sensors. In the context of sensor networks it might bring some interesting advantages: according to [69], adding data from a secondary attribute to estimate the primary one, could only increase precision; the so-called cokriging variance can only be less than or equal to the KV of the same primary attribute; that also means that the certainty of the fusion is improved.

5.3.1 The linear Model of coregionalization

The cross-variogram $\gamma_{UV}(h)$, that describes the statistical dependency across attributes, U and V corresponding to two different attributes viewed as two random processes, comprises the bivariate computation of variograms. Its estimation requires measuring both attributes at each lag distance, subtracting the values for each attribute at each pair of points and computing the statistical dependency as in the univariate case; unlike the variogram, a cross-variogram might be negative.

$$\boldsymbol{\gamma_{UV}(h) = \frac{1}{2} E\{U(k+h) - U(k)\}\{V(k+h) - V(k)\}} \quad \textbf{(5.11)}$$

The expected value E can be estimated for one pair of points by the experimental data, which are present in the form of a time series.

$$\boldsymbol{\gamma_{UV}(h) = \frac{1}{2N_k} \sum_{k=1}^{N_k} \Big((U(k+h) - U(k)\,)\big(V(k+h) - V(k)\big)\Big)} \quad \textbf{(5.12)}$$

Multivariate models might present more varied shapes than the authorised ones and must be modelled jointly. One simple way to do this is as a linear combination of the basic ones, the so-called linear model of co-regionalisation, that is interpreted as decomposition of components; if a particular element of an attribute is not present in the co-regionalisation model, the coefficient is set to zero. Suppose we have S number of basic γ(h) models for the two attributes involved, the coregionalisation matrix for that model is:

$$\begin{bmatrix} \boldsymbol{\gamma_{Uj}(h)} & \boldsymbol{\gamma_{UVj}(h)} \\ \boldsymbol{\gamma_{UVj}(h)} & \boldsymbol{\gamma_{Vj}(h)} \end{bmatrix} = \begin{bmatrix} \boldsymbol{u_j} & \boldsymbol{uv_j} \\ \boldsymbol{uv_j} & \boldsymbol{v_j} \end{bmatrix} \begin{bmatrix} \boldsymbol{\gamma_j(h)} & \mathbf{0} \\ \mathbf{0} & \boldsymbol{\gamma_j(h)} \end{bmatrix} \quad \textbf{(5.13)}$$

If we define $\Gamma_j(h)$ as a matrix of simple and cross variograms at lag h and $\gamma_j(h)$ as the set of basic variogram models, equation 4.13 can be written as following:

$$\boldsymbol{\Gamma_j(h)} = \mathbf{B_j}\boldsymbol{\gamma_j}(\mathbf{h}) \quad \textbf{(5.14)}$$

In cokriging, the matrix $\Gamma(h)$ has to comply with the mentioned restrictions. The conditions necessary for the matrix to be positive-definite are:

$$\boldsymbol{u_j > 0 \; and \; v_j > 0 \, , for \; all \; j = 0,..,S} \quad \textbf{(5.15)}$$

$$\boldsymbol{(u_j)(v_j) > (uv_j)(uv_j), for \; all \; j = 0,..,S} \quad \textbf{(5.16)}$$

and the linear model of co-regionalisation given by the following equation is also positive-definite.

$$\boldsymbol{\Gamma(h)} = \sum_{\mathbf{j=1}}^{\mathbf{S}} \mathbf{B_j}\, \boldsymbol{\gamma_j}(\mathbf{h}) \quad \textbf{(5.17)}$$

5.3.2 Cokriging interpolation

In order to understand how cokriging interpolation works, consider two attributes: U and V, each of them measured separately on two sets of coordinates of n and m dimensions, respectively. The linear estimations for each attribute at point P is given by:

$$\boldsymbol{\hat{U}_P = \sum_{i=1}^{n} a_i U_i + \sum_{j=1}^{m} b_j V_j} \quad \textbf{(5.18)}$$

$$\boldsymbol{\hat{V}_P = \sum_{i=1}^{m} c_i V_i + \sum_{j=1}^{n} d_j U_j} \quad \textbf{(5.19)}$$

Similar to ordinary kriging interpolation, cokriging calculates the solution of its weights by assuming the following: the mean of the measurement values is independent of space and the expected value for the attribute difference between two points depends solely on their spatial distance vector. The unbiasedness condition is satisfied by:

$$\boldsymbol{\sum_{i=1}^{n} a_i = 1} \qquad \boldsymbol{\sum_{j=1}^{m} b_j = 0} \qquad \boldsymbol{\sum_{i=1}^{m} c_i = 1} \quad \textbf{and} \quad \boldsymbol{\sum_{j=1}^{n} d_j = 0} \quad \textbf{(5.20)}$$

The weighting factors a_i, b_i and c_i can be calculated by solving a linear matrix equation.

The solution of the system equation is similar to the uni-attribute case, each element of the solver is replaced by a 2-by-2 matrix with the main diagonal containing the values of the two single-attribute variograms and the two elements of the minor diagonal containing the cross-variogram values; matrix elements containing the value of 1 and 0 are replaced by the identity and zero matrices, correspondingly.

$$\boldsymbol{\Gamma(h)} = \begin{bmatrix} \boldsymbol{\gamma_U(h)} & \boldsymbol{\gamma_{UV}(h)} \\ \boldsymbol{\gamma_{UV}(h)} & \boldsymbol{\gamma_V(h)} \end{bmatrix} \boldsymbol{W_{i,p}} = \begin{bmatrix} \boldsymbol{a_{i,p}} & \boldsymbol{b_{i,p}} \\ \boldsymbol{d_{i,p}} & \boldsymbol{c_{i,p}} \end{bmatrix} \boldsymbol{v_{i,p}} = \begin{bmatrix} \boldsymbol{\gamma_U(h_{i,p})} & \boldsymbol{\gamma_{UV}(h_{i,p})} \\ \boldsymbol{\gamma_{UV}(h_{i,p})} & \boldsymbol{\gamma_V(h_{i,p})} \end{bmatrix} \tag{5.21}$$

$$\begin{bmatrix} \gamma_{\mathrm{U}}(\mathbf{0}) & \gamma_{\mathrm{UV}}(\mathbf{0}) & \gamma_{\mathrm{U}}(h_{AB}) & \gamma_{\mathrm{UV}}(h_{AB}) & \cdots & \gamma_{\mathrm{U}}(h_{AC}) & \gamma_{\mathrm{UV}}(h_{AC}) & 1 & 0 \\ \gamma_{\mathrm{UV}}(\mathbf{0}) & \gamma_{\mathrm{V}}(\mathbf{0}) & \gamma_{\mathrm{UV}}(h_{AB}) & \gamma_{\mathrm{V}}(h_{AB}) & & \gamma_{\mathrm{UV}}(h_{AC}) & \gamma_{\mathrm{V}}(h_{AC}) & 0 & 1 \\ \gamma_{\mathrm{U}}(h_{AB}) & \gamma_{\mathrm{UV}}(h_{AB}) & & & \ddots & & & 1 & 0 \\ \gamma_{\mathrm{UV}}(h_{AB}) & \gamma_{\mathrm{V}}(h_{AB}) & & & & \vdots & & 0 & 1 \\ \vdots & & & & & & & & \\ \gamma_{\mathrm{U}}(h_{AC}) & \gamma_{\mathrm{UV}}(h_{AC}) & & & & \gamma_{\mathrm{U}}(\mathbf{0}) & \gamma_{\mathrm{UV}}(\mathbf{0}) & 1 & 0 \\ \gamma_{\mathrm{UV}}(h_{AC}) & \gamma_{\mathrm{V}}(h_{AC}) & & & \cdots & \gamma_{\mathrm{UV}}(\mathbf{0}) & \gamma_{\mathrm{V}}(\mathbf{0}) & 0 & 1 \\ 1 & 0 & & 1 & 0 & 1 & 0 & 0 & 0 \\ 0 & 1 & & 0 & 1 & 0 & 1 & 0 & 0 \end{bmatrix} \begin{bmatrix} a1 & b1 \\ d1 & c1 \\ a2 & b2 \\ d2 & c2 \\ \vdots & \\ an & bn \\ dn & cn \\ \lambda_{\mathrm{U}} & \lambda_{\mathrm{VU}} \\ \lambda_{\mathrm{UV}} & \lambda_{\mathrm{U}} \end{bmatrix} = \begin{bmatrix} \gamma_{\mathrm{U}}(h_{AP}) & \gamma_{\mathrm{UV}}(h_{AP}) \\ \gamma_{\mathrm{UV}}(h_{AP}) & \gamma_{\mathrm{V}}(h_{AP}) \\ \gamma_{\mathrm{U}}(h_{BP}) & \gamma_{\mathrm{UV}}(h_{BP}) \\ \gamma_{\mathrm{UV}}(h_{BP}) & \gamma_{\mathrm{V}}(h_{BP}) \\ \vdots & \\ \gamma_{\mathrm{U}}(h_{CP}) & \gamma_{\mathrm{UV}}(h_{CP}) \\ \gamma_{\mathrm{UV}}(h_{CP}) & \gamma_{\mathrm{V}}(h_{CP}) \\ 1 & 0 \\ 0 & 1 \end{bmatrix} \tag{5.22}$$

The cokriging variances for the estimation of U and V at point P are giving by:

$$\boldsymbol{\sigma_{CK}^2} = \sum_{i=1}^{n} \boldsymbol{a_i \gamma_{\mathrm{U}}(h_{iP})} + \sum_{j=1}^{m} \boldsymbol{b_j \gamma_{\mathrm{UV}}(h_{jP})} + \boldsymbol{\lambda_{\mathrm{U}}} \tag{5.23}$$

For attribute U at destination point P.

$$\boldsymbol{\sigma_{CK}^2} = \sum_{j=1}^{m} \boldsymbol{c_j \gamma_{\mathrm{V}}(h_{jP})} + \sum_{i=1}^{n} \boldsymbol{d_i \gamma_{\mathrm{UV}}(h_{iP})\, \lambda_{\mathrm{V}}} \tag{5.24}$$

For attribute V at destination point P. Where $\lambda_{\mathrm{U}}$and $\lambda_{\mathrm{V}}$are Lagrange multipliers

5.3.2.1 *CK interpolation under incompleteness of information*

In cross-attribute fusion terminology, the completeness can be improved by bringing new information where there is lack of it. CK is able to perform such task by supporting the primary variable interpolation with measurements of the second one, the so called under-sampling case. However, several factors regarding the cokriging interpolation procedure have to be taken into account; the calculation of experimental cross-variogram pairs can only be calculated for those measurement points where both variables are available. If, for example, variable V is not present at the measuring point, the elements $\gamma_{UV}(h)\ and\ \gamma_V(h)$ in matrix $\Gamma(h)$ cannot be calculated.

$$\boldsymbol{\Gamma(h)} = \begin{bmatrix} \boldsymbol{\gamma_U(h)} & * \\ * & * \end{bmatrix} \tag{5.25}$$

The first implication requires only the inclusion of an additional algorithm to group those measurements points in which both measurements are available. However, the second requires more complex modifications in the cokriging solver and the fitting algorithm.

Regarding the solver, each non-common measurement reduces the dimensions of the left matrix by one row and column and the column dimensions of the other by one column. Suppose that there is no measurement for variable V at point P when we have three source points, then the solver is as follows:

$$\begin{bmatrix} \gamma_U(0) & \gamma_{UV}(0) & \gamma_U(h_{AB}) & \blacksquare & \cdots & \gamma_U(h_{AC}) & \gamma_{UV}(h_{AC}) & 1 & 0 \\ \gamma_{UV}(0) & \gamma_V(0) & \gamma_{UV}(h_{AB}) & \blacksquare & & \gamma_{UV}(h_{AC}) & \gamma_V(h_{AC}) & 0 & 1 \\ \gamma_U(h_{AB}) & \gamma_{UV}(h_{AB}) & & \ddots & & \vdots & \vdots & 1 & 0 \\ \blacksquare & \blacksquare & & & & & & \blacksquare & \blacksquare \\ \vdots & & & & & & & & \\ \gamma_U(h_{AC}) & \gamma_{UV}(h_{AC}) & & & & \gamma_U(0) & \gamma_{UV}(0) & 1 & 0 \\ \gamma_{UV}(h_{AC}) & \gamma_V(h_{AC}) & & \cdots & & \gamma_{UV}(0) & \gamma_V(0) & 0 & 1 \\ 1 & 0 & 1 & \blacksquare & & 1 & 0 & 0 & 0 \\ 0 & 1 & 0 & \blacksquare & & 0 & 1 & 0 & 0 \end{bmatrix} \begin{bmatrix} a1 & b1 \\ d1 & c1 \\ a2 & b2 \\ \blacksquare & \blacksquare \\ \vdots & \\ an & bn \\ dn & cn \\ \lambda_U & \lambda_{VU} \\ \lambda_{UV} & \lambda_U \end{bmatrix} = \begin{bmatrix} \gamma_U(h_{AP}) & \gamma_{UV}(h_{AP}) \\ \gamma_{UV}(h_{AP}) & \gamma_V(h_{AP}) \\ \gamma_U(h_{BP}) & \gamma_{UV}(h_{BP}) \\ \blacksquare & \blacksquare \\ \vdots & \\ \gamma_U(h_{CP}) & \gamma_{UV}(h_{CP}) \\ \gamma_{UV}(h_{CP}) & \gamma_V(h_{CP}) \\ 1 & 0 \\ 0 & 1 \end{bmatrix} \quad \textbf{(5.26)}$$

5.3.3 Fitting the linear model of coregionalization

Curve fitting is an important technique in multi-sensor data fusion [42]. It is commonly used to fuse across one single attribute. In order be able to perform cross-attribute fusion using cokriging interpolation is required to find the set of S positive-definite coregionalisation matrices that fits the best the experimental variograms. The followed approach was proposed by Goulard and Voltz (GV) [75]; they use an iterative algorithm to fit the S coregionalisation matrices B that minimize the following weighted sum of squares (WSS):

$$\boldsymbol{WSS = \sum_{k=1}^{K} w_k \left\| \hat{\Gamma}(\mathbf{h_k}) - \Gamma(\mathbf{h_k}) \right\|^2 = \sum_{k=1}^{K} w_k} \quad \textbf{(5.27)}$$

The weights are positive and/or proportional to the number of pairs at each lag h. The idea of the algorithm is to minimise the weighted sum of squares by optimising each matrix at each iteration and stopping when WSS cannot decrease any more. The algorithm converges to a unique solution that is always reached [76].

The core part of the algorithm lays the decomposition of each matrix B_k into a scalar product between matrices, being V, a positive-definite matrix.

$$\boldsymbol{B_k = U_k \Delta_k U_k^T \text{ with } U_k V U_k^T = I} \quad \textbf{(5.28)}$$

Δ_k is a diagonal matrix containing the eigen values in decreasing order and U_k is the matrix of eigenvectors. The constrained solution is obtained by setting to zero any negative entry in Δ_k to obtain Δ_k^+ and by replacing B_k with B_k^+

$$\boldsymbol{B_k^+ = U_k \Delta_k^+ U_k^T} \quad \textbf{(5.29)}$$

The disadvantage of such a method is that the algorithm requires knowledge of all measurements, which is impossible in the case of under-sampled sampling.

Automatic fitting in the presence of under-sampled sampling implies dealing with missing values in the sample variogram matrices. An approach to solve this problem is proposed by Emery [77]. He solved the heterotopy problem by modifying the Goulard-Voltz algorithm to

minimise the weighted sum of squares for each one of the elements in matrix B and extending the WSS to the double of the lags.

$$\boldsymbol{WSS} = \sum_{k=1}^{2K} \sum_{ij=1}^{N} \boldsymbol{w_{ijk}} \left[\widehat{\boldsymbol{\gamma}}_{ij}(\mathbf{h_k}) - \boldsymbol{\gamma_{ij}}(\mathbf{h_k}) \right]^2 \quad \textbf{(5.30)}$$

Where the lags and weights from the K-th element are set conveniently as:

$$\mathbf{h_{k+K}} = \mathbf{h_k}, \qquad \widehat{\boldsymbol{\gamma}}_{ji}(\mathbf{h_{k+K}}) = \widehat{\boldsymbol{\gamma}}_{ji}(\mathbf{h_k}) \qquad \text{and} \qquad \boldsymbol{w_{ji(k+K)}} = \boldsymbol{w_{ijk}} \quad \textbf{(5.31)}$$

Each optimal element of the matrix Bs is found by cancelling out the partial derivative of WSS with respect to b_{ijs}:

$$\widetilde{\boldsymbol{b}}_{\boldsymbol{ijs}} = \frac{\sum_{k=1}^{2K} \boldsymbol{w_{ijk}} \boldsymbol{g_s}(\mathbf{h_k}) [\widehat{\boldsymbol{\gamma}}_{ij}(\mathbf{h_k}) - \sum_{\substack{u=1 \\ u \neq s}}^{S} \boldsymbol{b_{iju}} \boldsymbol{g_u}(\mathbf{h_k})]}{\sum_{k=1}^{2K} \boldsymbol{w_{ijk}} \boldsymbol{g_s}(\mathbf{h_k})^2} \quad \textbf{(5.32)}$$

5.3.4 Resulting Coregionalisation Models

Firstly, it was decided to find the proper linear co-regionalisation model for each of the experiments. As mentioned in [76], in practice, the number of selected structures should not exceed three. Combinations of Spherical, Gaussian and Exponential models were tested; additionally, the nugget model is always taken into consideration as a contributor. Linear combinations of these basic structures will be able to present more complex shapes than simple structures [69].

Through simulations, it was observed that a good fitting is not necessarily an indicator of a good variogram model, as the nugget might result to be excessively high. However, it was decided to always include a nugget model and use it as an indicator of a correct selection model. The rest of the models were included to determine whether they achieve a good fitting without increasing the nugget. An Exponential model better characterised the variations inside the container for large ranges. It was able to fit a wide interval of range values without increasing the nugget value and was taken as the main variogram. The following task was to determine the third variogram model with a lower range. The Gaussian model always had bad fitting results, whereas the Exponential model with lower ranges often led to a good fitting.

Table 5.3 and Table 5.4 show the automatic fitting results for both experiments. The average relation between the predicted CK standard deviation and the actual error ε_i for each destination point is used as a measure of the accuracy of the model as suggested by Wackernagel [69]; it should be about 1.

Table 5.3 Automatic fitting results for an empty container

Ranges		Predominant Model?	WSS	θ		ε_i	
Exponential	Spherical			Min	Max	Min	Max
5.5	4.7	No	.1044	1.7	2.19	1.44	2.46
5	4	Spherical	.099	1.63	1.84	1.6	2.43
4	2.7	No	.098	1.42	1.76	1.42	2.39
3	2	No	.107	1.23	1.74	1.42	2.39
3	1.7	Exponential	.108	1.21	1.77	1.44	2.39

Table 5.4Automatic fitting results for a container with pallets on the floor

Ranges			WSS	θ		ε_i	
Exponential	Spherical			Min	Max	Min	Max
5.5	4.7	Spherical	.30	.34	1.06	.76	2.14
5	4	Spherical	.39	.32	.98	.76	2.12
4	2.7	Exponential	.57	.17	.94	.70	2.18
3	2	Exponential	.71	.15	.94	.69	2.19
3	1.7	Exponential	.71	.15	.94	.69	2.19

They show whether the results sills are predominantly spherical or exponential and also offer a quick overview of the maximum and minimum relation and epsilon results after applying cokriging interpolation.

The selected ranges are highlighted in the tables; Table 5.5 shows the numerical values of the sills for both experiments using those ranges and Figure 5.5 shows the experimental and co-regionalisation model for the experiments when pallets are placed on the floor.

Table 5.5 Resulting sill and range values for the best selected model

	Empty Container			Container with pallets		
	T	T-H	H	T	T-H	H
Nugget	0	0	0	.01	0	0
Exponential	0.17/3	-.46/3	1.4/3	0.03/5	.016/5	0/5
Spherical	0.07/2	-.29/2	1.24/2	1.42/4	-2.86/4	5.75/4

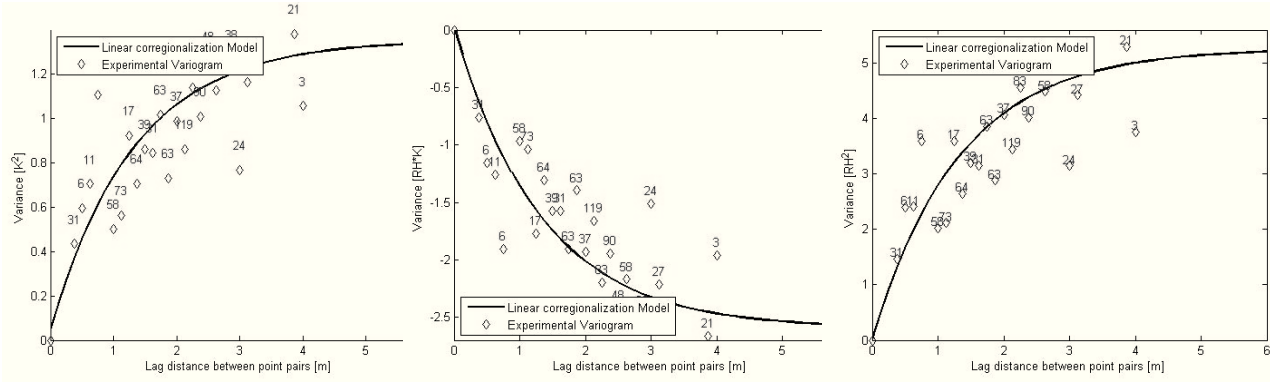

(a) **(b)** **(c)**

Figure 5.5 Experimental and theoretical variogram and cross-variogram for container with pallets on the floor: (a) Temperature, (b) Temperature-Humidity and (c) Humidity. The theoretical variogram is calculated as the sum of an exponential and a spherical model with parameters according to Table 3 and nugget = 0.

5.3.5 Accuracy of the estimations

In order to determine if CK interpolation brings any advantage over single-attribute kriging when humidity is taken as the primary attribute and temperature as the support attribute, the resulting average error was plotted against the number of source humidity sensors used for interpolation. Two cokriging cases are plotted on the same graph: when the same number and positions of humidity and temperature measurements are used (isotopic case) and when the same number of humidity measurements is used but when the complete set of temperature measurements is taken as support. Figure 5.6 shows the three mentioned plots for both experiments and two important observations can be made. Firstly, CK interpolation does not bring any advantage over OK if the temperature and humidity measurements are collocated (isotopic case), the plots are superposed, containing practically the same values and making hard to visualize the differences between them; secondly, the interpolation error improves significantly in the heterotopic case when all temperature measurements are taken as support.

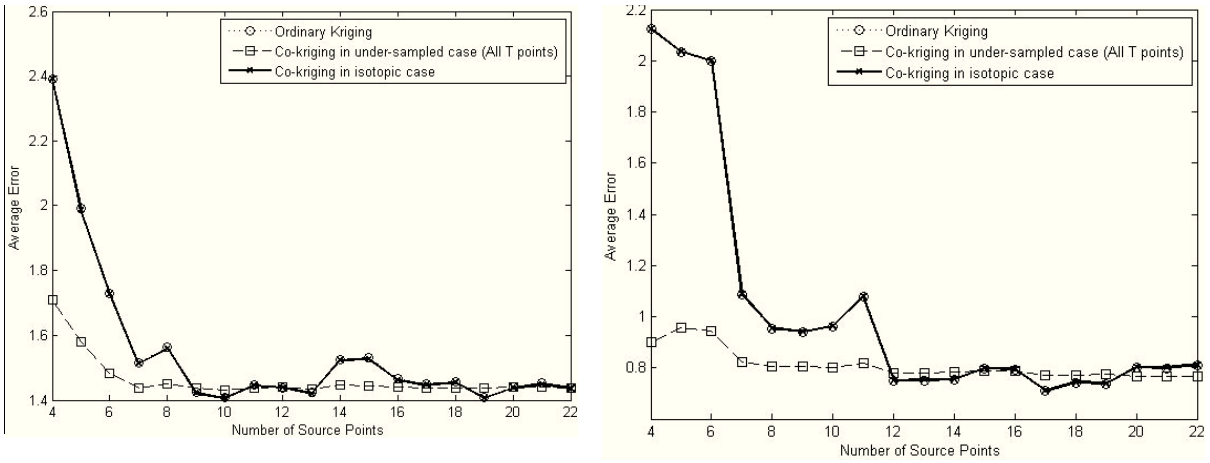

(a) **(b)**

Figure 5.6 Comparison of Average Interpolation Errors of single-variable kriging and cokriging: (a) Empty Container, (b) Container with pallets on the floor

For the best case for the container with pallets on the floor, if only four humidity sensors are available, the interpolation error improves from about 2.1 to 0.9. For comparison, if OK is applied, twelve humidity sensors are required to achieve an interpolation error lower than one.

Despite the demonstrated significant advantage of using CK to reduce the number of humidity sensors while reducing the average error, the previous exemplification was done using all of the temperature points as a support. In general, adding either temperature or humidity measuring points reduces the average interpolation error and the CK variance.

Figure 5.7 shows the three-dimensional plots for the CK interpolation error for both experiments when both the humidity and temperature measurement points are increased from four to twelve. As expected, the higher the number of sensors, the lower the interpolation error; the method shows to have *submodularity*, the rate at which it decreases seems to be non-linear. A small decreasing rate is obtained with more than twelve sensors, that is the reason why these points are not plotted. The next step is then to determine the minimum number of sensors required in order to achieve an interpolation error lower than a selected threshold.

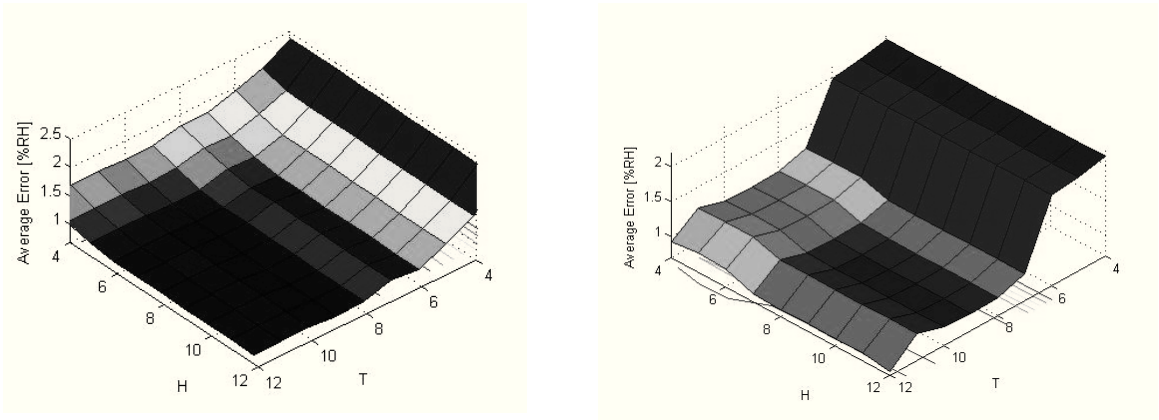

(a) **(b)**

Figure 5.7 Average Interpolation Errors of cokriging vs. Number of Humidity and Temperature Sensors: (a) Empty Container, (b) Container with pallets on the floor.

5.3.5.1 *Certainty of the estimations*

Figure 5.8 shows the three-dimensional plots for the estimation variance in both experiments when both the humidity and temperature measurement points are increased from four to twelve. As Figure 5.7 the higher the number of sensors, the lower variance, if the 3D accuracy graphs and the estimation graphs are compared, it can be observed that they are very similar in shapes and values, that is an indicator of a proper fitting of experimental data to the linear model of coregionalization and cross-validates the theoretical guarantees of the methods with the experimental results.

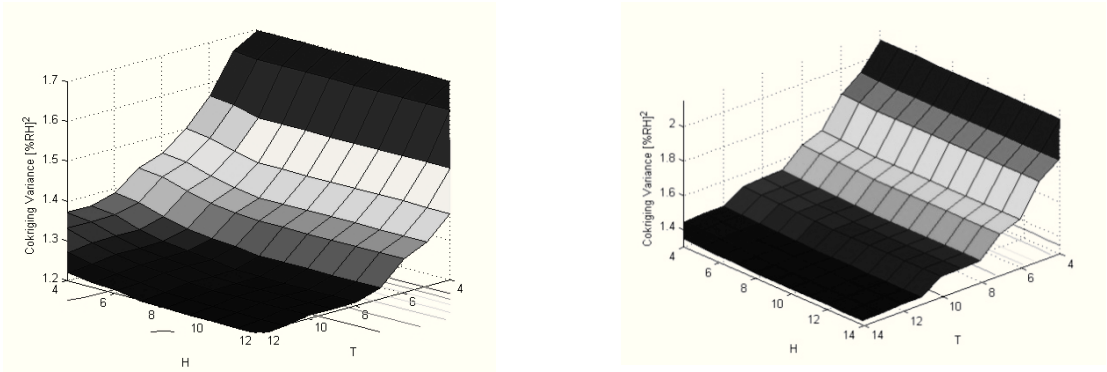

(a) **(b)**

Figure 5.8 Average CK Variance vs. Number of Humidity and Temperature Sensors: (a) Empty Container, (b) Container with pallets on the floor

5.3.6 Accuracy of the estimation under incompleteness

As it can be seen in Figure 5.7 and Figure 5.8, CK interpolation does bring more accurate interpolation errors over OK. It tends towards the same accuracy value with only a few sensors but it does not improve in a significant way the lowest interpolation error achieved by ordinary kriging, which is 1.42 and 0.76 for an empty container and a container with pallets, respectively. The main advantage is in reducing the required number of humidity sensors.

In order to illustrate the applicability of CK in reducing the number of measuring points, two thresholds: 1.55 and 0.85, that correspond to a 10% increase of the interpolation errors obtained for both experiments, were selected. The same Matlab scripts that produced the plots in Figure 5.7 were run but in this case, with the aim of clarity, all points exceeding the respective threshold were set to NaN (Not-a-Number). The plots then were rotated so as to be viewed from above and Figure 5.9 shows that view: It can be seen that robustnees of the CK method to achieve good estimates with low variability, due to the submodularity, adding more measurements does not necessarily increase the accuracy of the estimation. The areas where the submodularity is not achieved are the ones inside the red circles. Only 3 combinations for the empty container and 6 of the container with pallets exceeded the established thresholds.

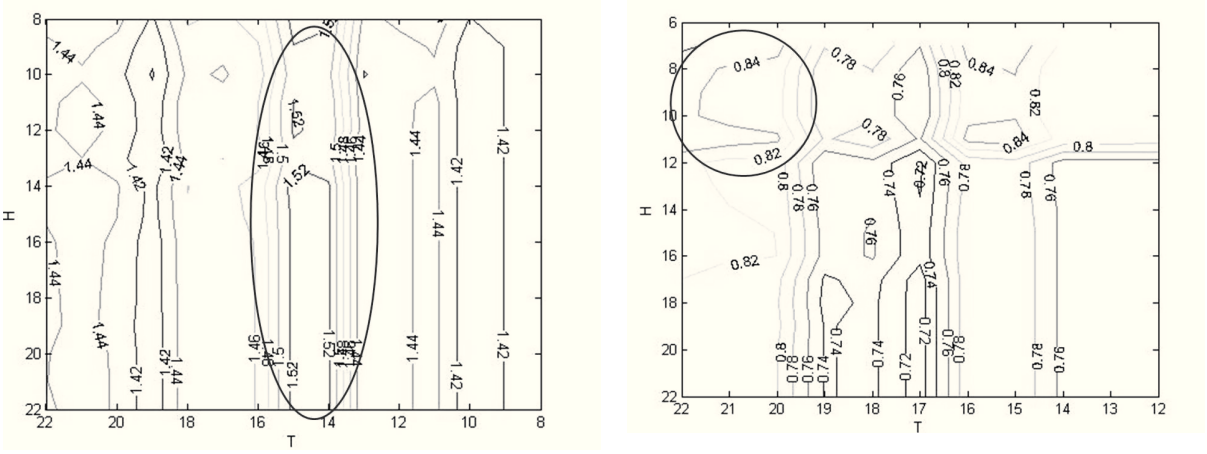

(a) **(b)**

Figure 5.9 Average Interpolation Errors lower than the threshold: (a) Empty Container, (b) Container with pallets on the floor.

Table 5.6 shows that in the case of the empty container, that has low variability, the use of CK does not bring any advantage in reducing the number of humidity sensors; however, it can achieve more accurate predictions with the same number of humidity measurements when taking the temperature measurements as support.

Table 5.6 Number of Humidity Sensors required for OK and CK interpolations that comply with different thresholds when the container is empty.

Threshold	Number of combinations	Combination with minimum sensors for humidity		Number of humidity points required for kriging
			T	
1,43	66	7	9	-----
1,44	111	7	9	7
1,49	201	6	9	6
1,59	283	5	9	5
1,71	297	4	9	4

Table 5.7shows that when the variations are higher, cokriging interpolation is able to reduce the number of humidity sensors required for OK.

Table 5.7: Number of Humidity Sensors required for Ok and CK interpolations that comply with different thresholds when the container has pallets on the floor.

Threshold	Number of combinations	Combination with minimum sensors for humidity		Number of humidity points required for kriging
		H	T	
0,76	68	8	17	---------
0,77	74	7	17	18
0,8	103	7	17	12
0,82	143	7	12	8
0,9	180	4	17	7

5.3.7 Fitting the linear model of co-regionalisation under incompleteness

As mentioned before, fitting the proper co-regionalisation model is the basis for CK interpolation. The theoretical guarantees of the interpolation are void if the model is not properly fitted. The main factor affecting this is the lack of sufficient measurements either from the primary or secondary attribute. The method developed by Emery takes into account the absence of such measurements but still needs to be verified as to whether the method fits proper sills under highly heterotopic cases.

In order to do so, the method described in section 4.3.5 was run again. However, this time, at each combination of number of humidity and temperature points the variogram fitting procedure, described in section 4.3.3, is run and the resulting sills are used for the CK interpolation at that specific point. In order to compare the interpolation errors obtained when all measurement points are available with those resulting from the heterotopic case, the absolute value of the difference between them is plotted. The results are surprisingly good; the difference is close to zero in most of the combinations. Figure 5.10 shows the difference between the interpolations errors when the point combinations exceeding a threshold of 0.05 are set to Nan. It can be observed that approximately 8 humidity and 10 temperature measurements are required in order to achieve the same results as in the fully-sampled case.

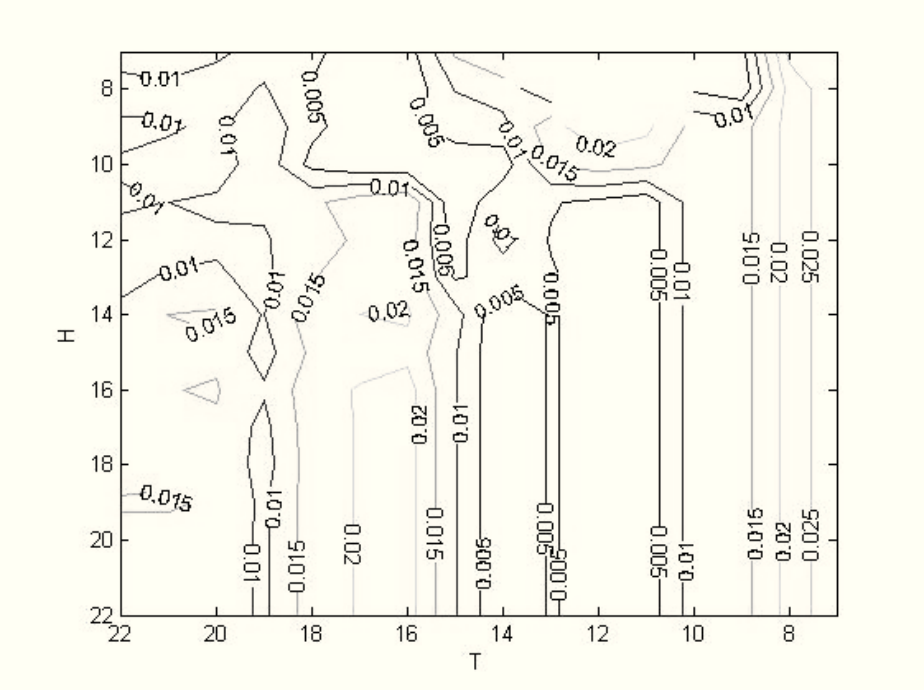

Figure 5.10 Difference between Interpolation Errors when the model is fitted with all measurements and when it is fitted in the under-sampled case for the empty container.

5.4 Summary and conclusions chapter 4

One of the inherent constraints in WSN is the impossibility of deploying dense number of sensors; to cope with it; spatial interpolation is proposed to estimate the value at the positions that are not covered by a sensor. Deterministic methods exist but their disadvantage is the lack of theoretical guarantees.

The Kriging method is a useful tool to interpolate a physical property for points where no sensor is available and provides theoretical guarantees through the use of the so-called Kriging variance. It can be used as an offline-tool to estimate to which amount the number of sensors can be reduced for a supervision task. The theoretical guarantees are only valid if the theoretical model is properly fitted to an experimental variogram and if sufficient number of neighbours lie into the variogram range.

The most suitable method to verify the correctness of the variogram model is based on the $\varepsilon i/\sigma k$ relation. The best results were achieved either by the Nelder-Mead algorithm combined with the weighting according to Cressie or by setting the nugget by known sensor tolerances and the range by an average value of previous experiments. If the average number of neighboring sensors within the Variogram range is sufficient, the Kriging method provides an interpolation, that is in average 20% more accurate than that of the inverse-distance-weighting used as the reference method.

If the attribute of interest is not densely sampled, and only few sources are inside the variogram range, Kriging interpolation offers few or no advantage over deterministic methods. Fortunately, by fusing the available information with the information a secondary correlated attribute is possible to perform accurate and theoretical guaranteed estimations

Cokriging interpolation, considered as a cross-attribute fusion technique, guarantees theoretical performances under the assumptions that the experimental variograms are correctly fitted to a theoretical co-regionalisation model, that has to be positive-definite. This makes it possible to fuse different attributes to improve spatial coverage of an “expensive” attribute with observations at a finite number of locations of a “cheap” one without the repositioning of the sensors. It produces Best Linear Unbiased Estimation (BLUE) and estimate corresponding variances.

The best fitting results in the fully-sampled case are obtained when the weights are set directly proportional to the number of pairs and inversely proportional to the distance. The Exponential model gives good fitting without increasing the nugget for several sets of ranges;

it is preferred if a Spherical model is added. The algorithm developed by Emery has shown to be robust against the lack of primary and support attributes.

The cross-attribute fusion process proved to improve the completeness of the system. In the case of under-sampled humidity points, such that all temperature points are used and only some humidity ones, both the accuracy and variance are significantly improved, if the number of humidity sensors is fixed, adding temperature sensors improves the accuracy. It can be concluded that if high accuracies are required, cokriging interpolation is able to reduce the number of humidity sensors. As an example, to achieve an accuracy of 0.76, the number of humidity sensors can be reduced from eighteen to seven.

6 Feasibility of the use of Java-based deployments in Ubiquitous applications

6.1 Introduction

It can be said that ubiquitous applications are inherently heterogeneous. There are three common types of heterogeneity in wireless sensor networks: computational heterogeneity, link heterogeneity and energy heterogeneity [78].

Energy heterogeneity: means that some nodes are battery operated and have lifetime expectancy, while others are line powered.

Computational heterogeneity: means that some of the nodes have more computational capabilities than others. They may have more powerful microprocessor and biggest memory capacity.

Link heterogeneity: means that some nodes have limited communication ranges and bandwidths.

The Java programming language was developed by Sun Microsystems and was designed to offer a programming language, able to support flexible solutions to address diverse hardware (heterogenous) devices. In some cases, when the algorithms are so complex to be deployed in sensor nodes, the gateway must perform centralized processing.

6.2 Relation with Flexibility and Maintenance

On one hand, as mentioned in chapter 2, the main issues to consider for flexibility and maintenance in WSN are [8]: *Integrity checking, version control, heterogeneity management, activation mode, and performance.* On the other hand, the main characteristics of Java are [79]: *portability, robustness, security, object orientation, multithreading and synchronization.*

- *Version control and Integrity checking*, that is, prevention of version mismatch. *The use of java-based technologies* such as *OSGi* allows version control, high modularity, and dynamic programming.
- *Heterogeneity management* of sensor nodes. The high acceptance of Java in the programming community is mainly due to its *portability*. It is based on the concept of "write once, run anywhere" (WORA). Java applications are capable of executing in diverse hardware and operating systems.

- *How software would be activated*. Depending of the Java technology and configuration used the activation can be *automated* after installation or *remotely activated* by an on-line command.
- *Performance.* The time required to update nodes as wells as tradeoffs between time and energy Being Java an interpreted language, it requires a Java virtual machine (JVM) and the required application programming interfaces (APIs) to be installed, implying minimum requirements in memory and lower energy performances. One way to make a trade off is by *measuring the time required for the algorithms to run* in the hardware platforms to calculate the total current draw and estimate life expectancies.

6.3 Java Technologies

Java is an interpreted language. The program code is compiled into bytecode that is a code that can be executed in a platform-independent way. The bytecode can be interpreted in any computer that has a Java virtual machine (JVM) and all required application programming interfaces (APIs) installed. Together the JVM and the APIs form the Java platform.

Insulation the application from the platform comes with a cost: Java solutions are often associated with high costs in terms of resource consumption [80]. Only some devices can benefit from the solutions Java environments offers in terms of connectivity, modularity and dynamic features.

Java was split into four core technologies shown in Figure 6.1 [79]. JavaSE is the standard platform for programming in the Java language. It consists of a Java virtual machine for executing the compiled class-files (the Java program) and a set of libraries that makes it possible to access, e.g. the file system, graphical or network interfaces from a Java program. We will focus on Java Micro Edition (JavaME) which was created to be deployed in resource constrained devices.

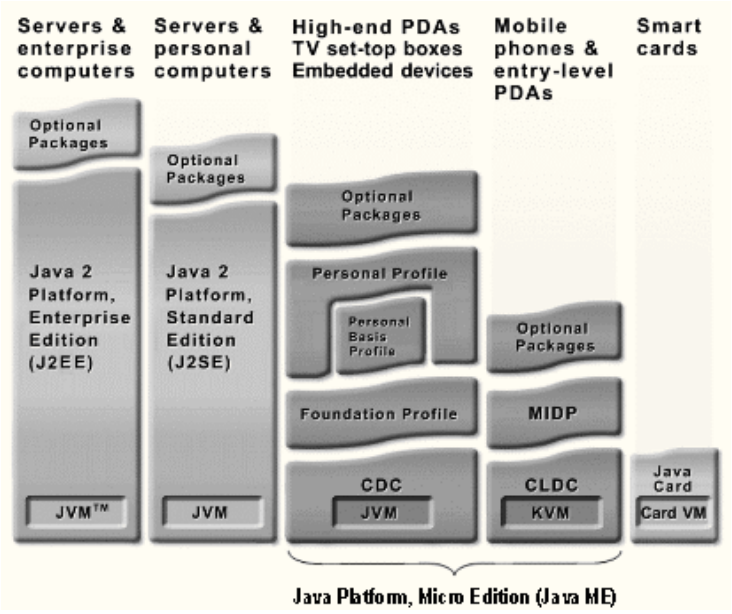

Figure 6.1 Java technologies [79]

6.3.1 JavaME

The Java Micro Edition (JavaME) is aimed at embedded systems, e.g. mobile phones with limited resources. Sun released a cut-down version of the JVM that required less than 10% of the resources required for Java SE. The removed functionalities from JavaSE include those allowing dynamic software updates such as reflection, advanced thread control and user-defined class loaders; memory management such as automatic object finalization and calls from and to a native application through the use of the Java Native Interface (JNI).They also opted for creating a pluggable architecture to make it more flexible. Java ME consists of:

Configurations: The Connected Device Configuration (CDC) includes almost the entire scope of JavaSE except for GUI-related libraries. The Connected Limited Device Configuration (CLDC) only contains the minimum amount of classes necessary to enable the operation of a JVM.

Profiles: Adds a certain set of API, and optional packages for additional functionality in regards to the profile scope. A profile can be chosen that fits the desired target application. For example, the Mobile Information Device Profile (MIDP) for mobile devices such as mobile phones, or the Personal Profile for consumer electronics. Applications written based on the former profile are called MIDlets.

Optional packages: These APIs provide general-purpose functionalities and add extra functionalities

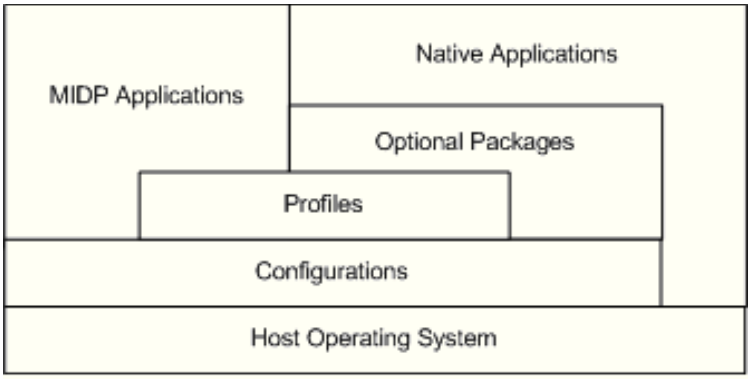

Figure 6.2 Architecture for CLDC and MIDP [79]

6.3.1.1 *Activation of MIDLETs:*

In JavaME, the activation and deactivation of the programs is done by commands. A device running a Mobile Information Device Application (MIDlet) has an environment that enables the user to choose MIDlets for installing, starting and removing. This so called Application Management Software (AMS) to control the life-cycle is responsible for the interaction with the user as well as for error handling. MIDlets have three possible states paused, active and destroyed.

In paused state, the application is non-active; this state is entered in one of three ways: after the MIDlet has been instantiated, if the AMS calls pauseApp() method, if an exception has been thrown. The active state is entered once the AMS invokes the startApp() method. When a MIDlet is in paused mode, it can be turned active by calling the startApp() method. The destroyed state can only be entered once and is done when the AMS invokes the destroyApp() method, all resources used by the MIDlet are released.

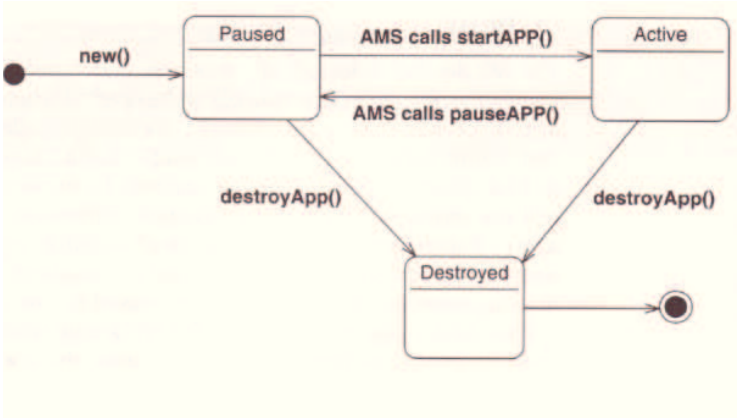

Figure 6.3 MIDlet Lifecycle [79]

6.3.1.2 *Modularity*

Strictly speaking, JavaME is not modular, however by using the so-called Record Management System (RMS), introduced from MIDP2.0, it is possible to establish communication between MIDLETs. It allows a MIDLET to store persistent data without compromising system security. It stores binary data in a record: MIDLETS can add, remove, and updates the records.

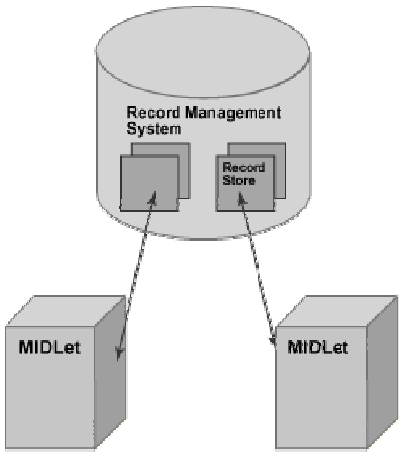

Figure 6.4 . Overview of J2ME RMS and MIDlet interfacing [81]

With RMS, a MIDlet can access record stores created of other MIDlets. It is also possible to access MIDLETs of other suites if the MIDlet that created it allows it. The data inside the record is like nonvolatile device memory, it stays in the device even if it is switched-off. The only way to destroy the data is if its programmatically removed.

6.3.2 OSGi

"Java runs everywhere" is not completely true. Java technologies has been divided into Java EE, SE and ME to cope with computational heterogeneity. Ubiquitous applications must be modular, version-controlled and dynamic. To add such functionalities, the Open Services Gateway initiative framework (OSGi) can be used. OSGi enables the update, addition or replacement of Java-based applications during runtime, for example over an internet connection without being on site and without requiring restarting the devices.

The OSGi specifications are produced by the OSGi Alliance [82]. There are open source frameworks available for the current specification "OSGi Service Platform Release 4" (R4), namely Apache Felix, Eclipse Equinox and Makewave Knoplerfish and commercial OSGi frameworks such as ProSyst Software mBedded Server and Makewave Knopflerfish Pro to name two of them.

6.3.2.1 *OSGi concept of modularity*

To achieve modularity, the OSGi framework utilizes a so-called Service Registry and the concepts of bundles and services. Bundles executing within OSGi are independent of each other, yet they communicate. They are basically Java JAR files equipped with a manifest that describes their identity, version and dependencies form and to other bundles. I*mport* packages states that the bundle depends on the specified bundles, *exporting* states that bundles are required by other bundles. Versions and version ranges can be specified for each package.

Bundles can be installed started, updated and uninstalled dynamically. Once a bundle is successfully installed, it becomes resolved if all dependencies are met. Once resolved, it can be automatically or manually started. At any point the bundles can be stopped, restarted or uninstalled.

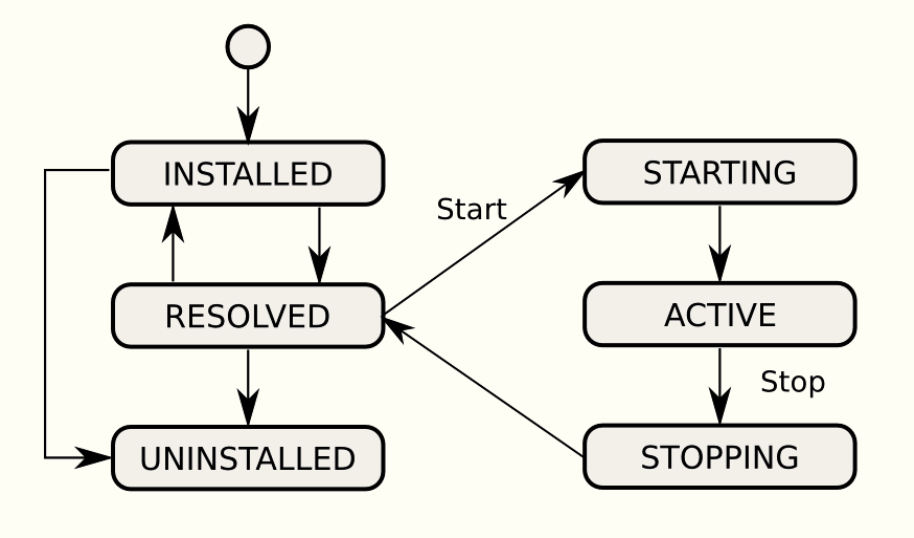

Figure 6.5 Bundle Lifecycle [83]

Dynamic communication can be done by using *services.* A bundle dynamically registers/acquires and unregister/releases the services it provides and consumes in the so-called OSGi service registry.

6.4 Selected Hardware Platforms

One of the basics of autonomous control in logistics is to shift processes from a centralized unit to distributed platforms [84]. Regarding ubiquitous systems, shifting the processes from the Gateway level to the sensor level, if the data is processed locally, radio communication is reduced and the life-time of the nodes preserved. The high-level programming language Java enables platform independent object oriented programming. To verify the suitability for shifting the process to the sensor level, off-the-shelf gateways and sensor nodes have been selected, JVM and OSGI installed if required and time measurements were performed.

6.4.1 Server Level

The selected telematics units are equipped with extended communications possibilities like 3rd generation mobile telecommunications (GSM / UMTS) and wireless LAN. Additionally, it is possible to get geodata via the global positioning system (GPS) and hard disk storage allows extensive data-logging. Table 6.1 shows selected characteristics for each hardware platform. The VTC 6100 from Nexcom is used as a reference platform; tt is equipped with an Atom processor (1.6 GHz) and 2 GB of main memory. The DuraNAV serves as an exemplary platform for lower power consumption; it utilizes an ARM architecture CPU (400 MHz) and 64 MB of RAM [85]. Both can run different Java VMs and different OSGi implementations.

Table 6.1 Telematic platforms

	DuraNAV	VTC6100
CPU (MHz)	PXA255 (400)	N270 (1600)
RAM	64 MB	1 GB
OS	Linux	Linux
Java Edition	SE	SE

Figure 6.6 VTC 6100 Plattform [86]

6.4.2 Sensor Level

The selection of the sensor nodes is of crucial importance for the analysis of the performance of the required algorithms in terms of energy consumption. Regarding java-enabled sensor nodes, the installed Java virtual machine (JVM) and the required application programming interfaces (APIs) play also a role regarding the memory and CPU requirements. Factors affecting the performance metrics can be:

- Hardware configuration in terms of processor model, clock speed and memory size
- The operating systems environment
- The algorithm being tested
- The Java Virtual Machine being used
- The Java libraries being used (if any)

Three sensor nodes platforms were selected. Two of them are Java-enabled and provide a virtual machine to execute Java code: The Oracle SunSPOT [87] and Virtenio Preon32 [88] that are described below. As a third option, Linux operating system, JamaicaVM [89] and JavaSE was installed an iMote2 sensor from Crossbow [90]. Details can be seen in Table 6.2

Table 6.2 Sensor Plattforms

	Imote2	Sun SPOT	Preon32
CPU (MHz)	PXA 271 (416)	SAM 9G20 (400)	Cortex-M3 (72)
RAM	32 MB	1 MB	64 kB
OS	Linux	None	None
JVM	any	Squawk	Custom
Java Edition	SE	ME CLDC 1.1	ME almost CLDC 1.1

6.4.2.1 *Oracle SunSPOT*

The sensor node "Sun Small Programmable Object Technology" (SunSPOT)) is a mote developed by Sun Microsystems, currently available in an 8th revision. As can be seen in Figure 6.7, it has a modular setup with three different layers: processor board, sensor board, and a 3.6V Li-Ion Battery that can be charged via USB. The processor board contains as a CPU an ARM-architecture AT91SAM9G20 with a clock rate of 400 MHz , 1 MB of RAM and Flash memory of 8 MB.

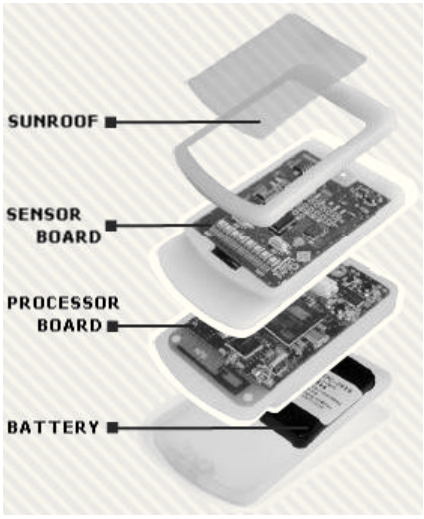

Figure 6.7 Oracle SunSPOT is Squawk sensor node [87]

Its proprietary Java Virtual Machine (JVM), called Squawk runs without an operating system. Squawk is a JavaME VM that is targeted from small resource constrained devices. Its core is mostly written in Java. Squawk utilizes the concept of isolates, where an application can be represented as an object. This allows common suites to be shared between multiple applications that run in the single JVM that can lead to a significantly reduced memory footprint. Furthermore, Java classes are not transferred directly to the execution environment but combined in a suite and prelinked to each other, that results in a reduced size of around one third of the original size. The omission of dynamic class loading in these immutable suites significantly decreases the start up time of the applications. For wireless communication the CC2420 radio chip is utilized; it supports IPv6. It has an current consumption in run mode with all processors and radio running between 70mA and 120 mA. [87]

6.4.2.2 *Virtenio Preon32*

The Preon32 developed by the company Virtenio is depicted in Figure 6.8 has also a modular system. The main board can be connected to a sensor board with several available sensors like temperature, humidity, acceleration, light and many more. It has, as a CPU a Cortex-M3 ARM-CPU at 72 MHz. The working memory has a size of 64 kB and it is extended by a flash memory of 256 kB.

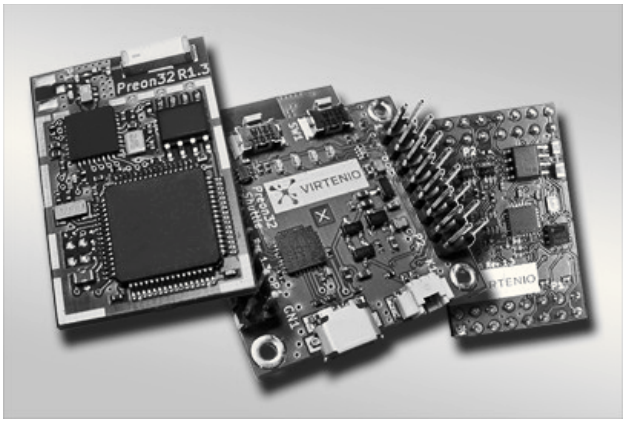

Figure 6.8 Virtenio Preon32 Sensor Node [88]

Virtenio developed for it a proprietary Java virtual machine. Unlike, SunSPOT, that is JavaME based and access to native applications is not possible, Virtenio's implementation allows access to hardware components like the radio that are written in C and through the Java Native Interface (JNI). For wireless communication the ATRF231 radio chip is utilized. Support for IPv6 is currently under development. It has an current consumption in active model of 28,3mA(at 72 MHz).

6.4.2.3 *iMote*

iMote2 sensor node from Crossbow [90] is a sensor platform with a powerful ARM PXA271 XScale processor that can run at a clock speed of up to 416 MHz , it is integrated with volatile and non-volatile memory, a power management IC to go to deep-sleep mode, a transceiver, and an antenna. Furthermore, it allows stack ability of additional modules to interconnect additional devices, such as, temperatures sensor cards.

The devices were enabled with JamaicaVM, running over a Linux operating system. On top of it, OSGi framework was installed to enable features such as dynamic software updates. Linux operating system for the iMote2 does not support low-power deep sleep modes of the ARM processor. For the evaluation of power consumption of the iMote2 the supply current was measured over a 1 Ohm resistor in series with the power supply wire, with a test probe connected in parallel to it. The CPU of the iMote2 consumes 50 mA running on full clock speed.

Figure 6.9 Crossbow iMote2 sensor node [90]

6.5 Algorithms for data fusion, analysis and reduction

Several algorithms have been selected to be tested in the platforms. These include not only the data fusion related algorithms described from chapters three and four, but also "standard" benchmarks such as Dhrystone and Linpack, and cold-chain specific algorithms such as calculation of shelf life as function of temperature deviation, and prediction of future temperature profiles.

6.5.1 Standard Benchmarks

In times when personal computers appeared and these were resource constrained compared with today's ones, "standard" benchmarks were designed; they fall into two categories:

1. Benchmarks specially designed to test performance in non numeric applications and string processing, for example word processors.
2. Benchmarks specially designed to test the speed of floating point operations. The performance was measured in Mflops (millions of point instruction per second)

We have selected one benchmark from each category to test the platforms: Dhrystone for non-numeric applications and Linpack for numeric applications.

6.5.1.1 *Dhrystone*

The main characteristics of Dhrystone benchmark are [91]:

- It contains no floating point operations
- A considerable percentage of time is spent in string operations
- It contains hardly any tight loops so in the case of very small caches the majority of instruction accesses will be missed
- Only a small amount of global data is manipulated

- There are two versions of the Dhrystone benchmark. We selected version 2.1 that is the latest one.

6.5.1.2 *Linpack*

The main characteristics of the Linpack benchmark are [91]:

- It has a large percentage of floating point operations (division is not used);
- It uses no mathematical functions
- There are no global variables; operations being carried out on local variables results are for single or double precision operations
- The benchmark relies heavily on the libraries being used

6.5.2 Cold-Chain specific algorithms

Through this section, it will be demonstrated that if the sensor data is processed locally, the radio communication between hop nodes can be drastically reduced, the costs related to satellite communication avoided and eventual quality losses due to air flow obstacles detected. But what is the relation between the environmental parameter surrounding the refrigerated perishable goods and the quality losses? We have to take into account that perishable goods, are subject to metabolic processes For example, bananas are "breathing": they ingest oxygen and exhale CO_2 and the plant hormone ethylene (C_2H_4) that generates additional heat, furthermore, the final quality of the product depends directly on the severity of the temperature deviations during transportation. Two cold-chain specific benchmarks were selected. The aim of their inclusion is to verify if it is possible to shift the decision making to the sensor node layer: temperature prediction and the estimation of bacterial growth as effect of the temperature.

6.5.2.1 *Temperature prediction*

The future temperature values inside a refrigerated container during transportation can be made through system identification techniques, that estimate the parameters of a modeled system. Specially fitted to resource constrained devices are the recursive representations of such algorithms due to their low memory and CPU requirements when compared with the offline counterparts.

In order to model the effect of the thermal energy generated by the ripening of bananas, the so-called Feedback-Hammerstein model [26] is used. As can be seen in

Figure 6.10, it uses a static pseudo-linear feedback to take the effect of organic heat into account. In the case of meat, the cargo does not produce organic heat and the linear feedback block of the model is removed, the system is considered to be linear.

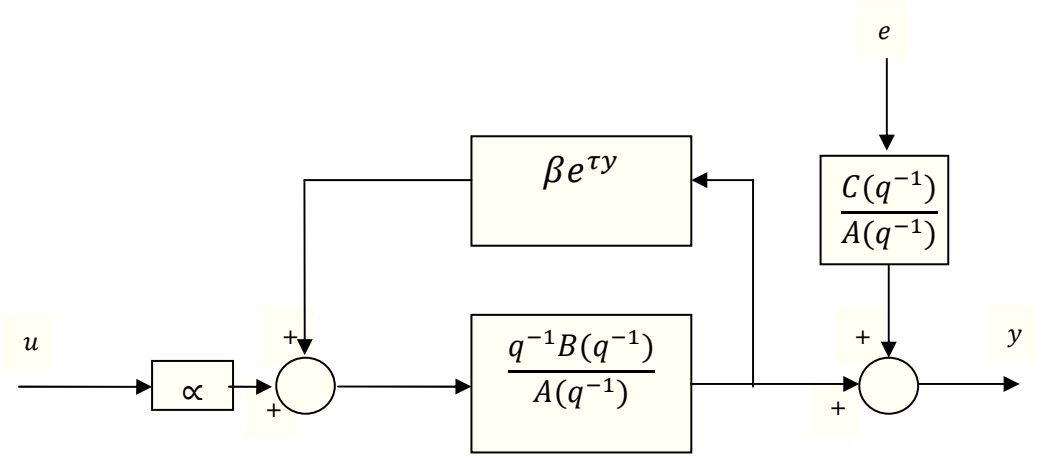

Figure 6.10 Model of the Feedback-Hammerstein-algorithm [26]

In the model τ is a key parameter that characterizes the heat production in Watts, is a constant, that is fixed for a certain type of fruit and ripening-state, β is a scaling factor, that depends on the amount of food and is given in kilograms, b_1 is the zero of the first-order linear system and a_1^* is the pole of an equivalent pseudo-linear system. In total, three parameters for the equivalent system are estimated (a_1^* , $b_1\alpha$ and $b_1\beta$) and are updated after each measurement. The model parameters of the FH and linear system have to be estimated by a parameter adaptation algorithm. The recursive form of this algorithm is given by the following equations:

$$\Theta(t+1)=\Theta(t)+\left(Q(t+1)\varphi(t)\right)^T\xi(t) \quad (6.1)$$

$$\xi(t) = y(t) - \Theta(t)^T\varphi(t-1) \quad (6.2)$$

$$Q(t+1) = \frac{Q(t)-Q(t)\varphi\varphi^T\left(\frac{Q(t)}{\varphi^T P\varphi+\lambda(t+1)}\right)}{\lambda(t+1)} \quad (6.3)$$

$$\delta(t+1) = \delta_o \cdot \lambda(t) + 1 - \delta_o \quad (6.4)$$

Where $\varphi(t)$ and $\Theta(t)$ are the so-called observation and parameter vector correspondingly. The arrangement of the elements depends on the considered model, as shown in Table 6.3.

The prediction error is described in equation 5.2, $Q(t+1)$ is an adaptation matrix to perform the minimization of using Recursive Least Squares method, and is the observation matrix that contains the input and the output data. As can be noted not any matrix inversion is needed.

Table 6.3 Arrangement of the elements in the algorithm matrices

System	Symbol	Arrangement of the elements into the matrices
Feedback Hammerstein	φ(t)	$[-y(t), u(t-1), (e^{\tau y(t)} - \tau y(t))]$
	$\Theta^T(t)$	$[a_1^*, b_1\alpha, \beta b_1]$
Linear Order 2	φ(t)	$[-y(t), -y(t-1), u(t-1)\ ]$
	$\Theta^T(t)$	$[a_1, a_2, b_1]$
Linear Order 1	φ(t)	$[-y(t), u(t-1)\ ]$
	$\Theta^T(t)$	$[a_1, b_1]$

6.5.2.2 *Estimation of bacterial growth*

The spoilage process of meat is caused by microbial growth, particularly by the accumulation of metabolic products [92]. An indicator for the quality of meat is the presence of bacteria on the sample. It is well known that the spoilage is only caused by a small fraction of the initial bacteria [93]. An unacceptable level of the bacterial accumulation is accompanied by discoloration, changes in texture as well as a specific smell and flavor.

The so-called shelf life models determine the speed of bacterial growth depend on temperature, because it is the main factor influencing it. The resulting remaining shelf life can be predicted accordingly to the temperature history. If the shelf life drops below a critical threshold a warning message can be sent either to the operator or to the logistics center.

In [94] is described a model that combines Gompertz- and Arrhenius-models. The Gompertz part contributes to model the effects of the temperature whereas the Arrhenius equation (5.5) gives a description of the relation between the speed of chemical reactions and temperature.

The reaction constant j can be calculated using the pre-exponential factor G, the activation energy E_a, the universal gas constant R and the temperature T.

A Gompertz function (equation 5.6) is a type of mathematical model for a time series, with slowest growth at the start and end of a time period. The function converges much slower to the future value asymptote than to the lower valued asymptote; ι is the upper asymptote, κ sets the x displacement and g sets the growth rate.

$$\boldsymbol{j = G \cdot e^{-\frac{E_a}{RT}}} \tag{6.5}$$

$$\boldsymbol{y(t) = \iota \cdot e^{\kappa \cdot e^{g \cdot t}}} \tag{6.6}$$

The combined model is given by equation 5.7

$$\boldsymbol{L(t_i) = L_0 + a \cdot e^{-e^{k_{T_i}(t - xc_i)}}} \tag{5.7}$$

The reversal point (inflection point of the curve) xc_i has to be adjusted to the new temperature, depending on the current microbial counts L0 according to equation 5.8.

$$\boldsymbol{xc_i = \frac{ln\left(-ln\left(\frac{L_{ti-1} - L_0}{\iota}\right)\right)}{k_{T_i}} + t} \tag{5. 8}$$

Where $L(t)$ represents the germ concentration at the time of t, L_0 is the initial germ concentration, ι is a temperature-independent variable and k_{T_i} is a temperature-dependent variable. If the temperature remains constant, only few mathematical operations have to be executed for each measurement interval.

6.6 Performance Measurements Results

It is hard to decide whether an *in-situ* implementation of the algorithms bring advantages over a centralized approach, based only in the timing results. It is hardly feasible to compare different algorithms because they have different objectives.

From the best of my knowledge, the developed *in-situ* data compression and recovery algorithms described in chapter 3 are the only ones suited for sensor nodes, therefore, a feasibility analysis is not necessary for them. The performance results are presented in three sections: standard benchmarks, cold-chain specific algorithms and statistical data-fusion related algorithms. Some of the results are reported in [95-97]; the standard benchmarks were tested by the first author of these publications whereas cold-chain specific and data-fusion algorithms were tested by the author of this thesis.

The standard benchmarks are tested for every mentioned hardware platform. The cold-chain specific algorithms were tested for every sensor node and for the VTC gateway. The data-fusion related algorithms were the most difficult to compare; matrix-inversion, that is required for OK and CK interpolation was tested for every platform except from DuraNav, cokriging interpolation and Goulard-Voltz fitting was only tested on VTC6100 because they are high resource and energy demanding and their implementation was only feasible to perform centralized. SunSPOT can perform floating point operations very fast and can perform CK interpolation, however it was not tested because its performance is already compared with the Matrix inversion.

Table 6.4 Algorithms tested for every hardware platform. The Goulard-Voltz algorithm[75] and CK interpolation required for fitting the linear model of coregionalization and perform cross-attribute fusion are only tested on the Gateway level.

		7 Standard benchmarks		8 Cold-chain specific		9 Data-fusion related		
		Dhrystone	Linpack	FH	Gompertz	Matrix Inversion	CK	Goulard-Voltz
Sensor node Level	Preon32	✓	✓	✓	✓	✓	Not feasible	Not feasible
	Sun SPOT	✓	✓	✓	✓	✓	Not tested.	Not feasible
	Imote2	✓	✓	✓	✓	✓	Not feasible	Not feasible
Gateway level	DuraNAV	✓	✓	×	×	×	Not feasible	Not feasible
	VTC6100	✓	✓	✓	✓	✓	✓	✓

9.1.1 Standard benchmarks

The VTC 6100 unit is the only hardware platform able to run each selected algorithm and is taken as reference point for the performance of the different platforms. Figure 6.11(a) shows the time required to run the Dhrystone algorithm, the VTC require only 523 ms. Figure 6.11(b) shows the performane in % to the refeence

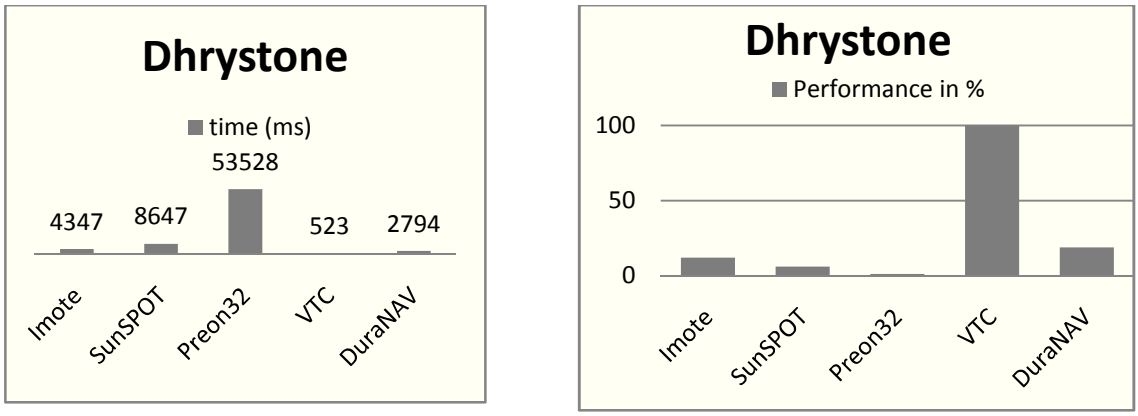

(a) (b)

Figure 6.11 Results of the Dhrystone 2.1 benchmark: (a) Time, (b) Performance in % to the reference

As can be seen, there is a positive correlation between the processing power and memory of the platform and the performance. Although the CPU clock-rate of DuraNav, Imote2 and SunSPOT are the same, the best performance is achieved by DuraNav that has twice and sixty-four times the memory of Imote2 and SunSPOT respectively.

Figure 6.12 shows the performance results for the LinPack benchmark. As expected VTC, that is the reference surpasses each other platform, it is able to execute more than fifty-four-thousand Mflops.

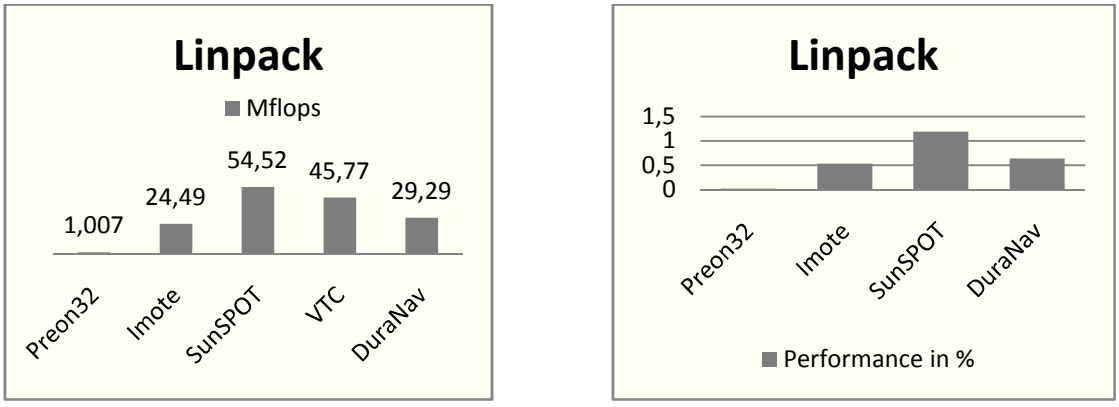

(a) (b)

Figure 6.12 Results of the Linpack benchmark: (a) Mflops, (b) Performance in % to the reference

In contrast to Dhrystone, Linpack seems to be less memory-demanding and depend more on the effectiveness of the language interpretation made by the installed Java virtual machine (JVM). Surprisingly, SunSPOT overcomes all hardware platforms including VTC, this could

be explained by the newer CPU architecture that has improved floating-point processing power and the lack of operating system.

9.1.2 Cold-chain specific algorithms

The results for temperature prediction are shown in Figure 6.13. VTC is taken as reference point for the performance of the different platforms. The parameter adaptation algorithms were run arranging the elements as described in Table 6.3. A dataset recorded within a cooperation project with Dole from Costa Rica to Antwerp in 2008 was used. The model parameters have to be iterated over three days at a measurement interval of one hour, equivalent to 72 cycles.

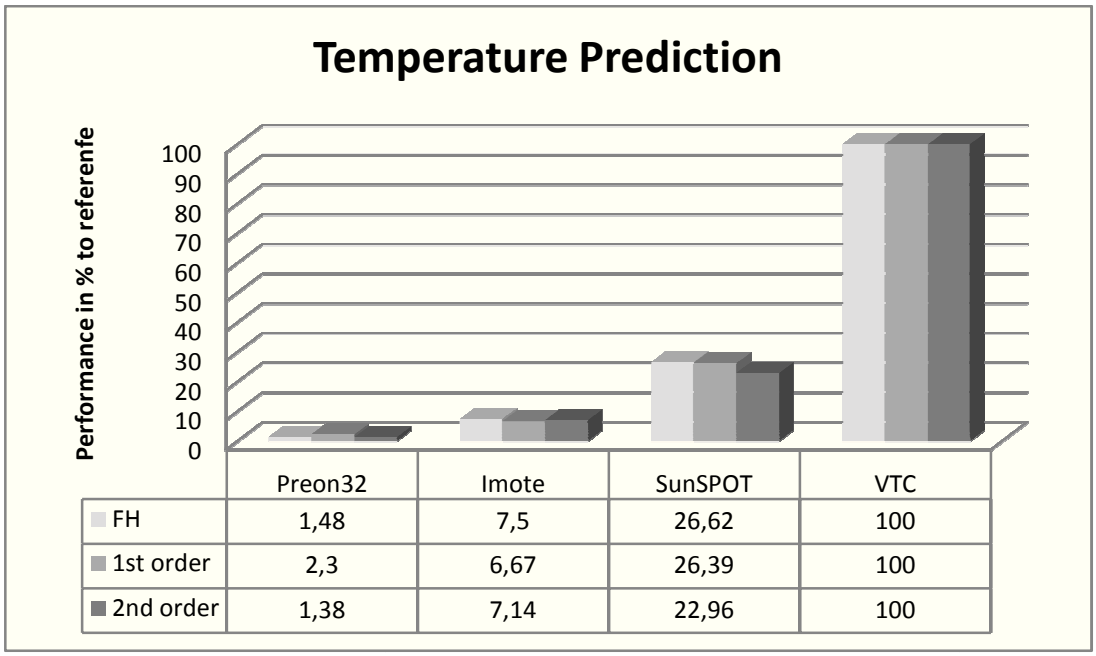

	Preon32	Imote	SunSPOT	VTC
FH	1,48	7,5	26,62	100
1st order	2,3	6,67	26,39	100
2nd order	1,38	7,14	22,96	100

Figure 6.13 Performance of Temperature prediction algorithms

The SunSPOT sensor performs the best. It is three times faster than IMote2. And takes only half of the time required by the powerful hardware architecture of VTC.

The performance results for the estimation of bacterial growth model by the Gompertz-algorithm are shown in Figure 6.14. The Imote2 takes about five times the time required by SunSPOT. Preon32 shows the poorest performance in both cases.

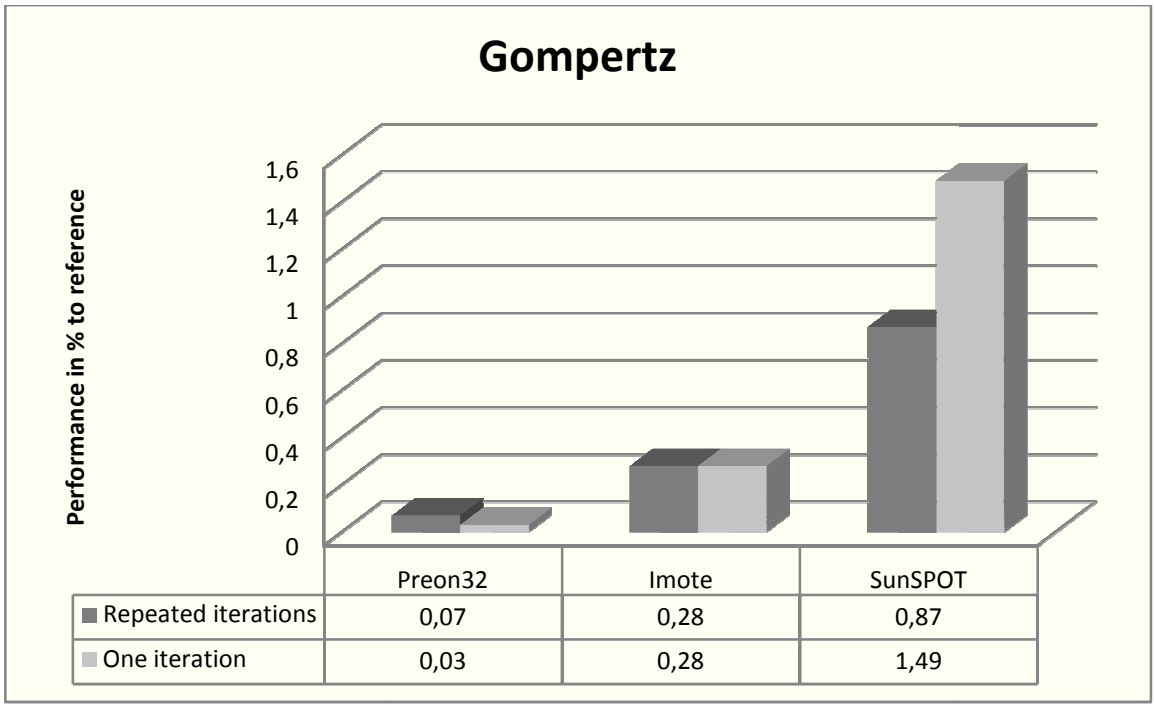

Figure 6.14 Performance of the Gompertz algorithm

The presented results are important considering energy consumption. For example, the time required to execute 72 FH iterations requires two seconds for the training of three days. Considering that overseas transport duration is about two weeks, the amount of measured and transferred data to the gateway may be reduced to a factor of five. The Gompertz algorithm requires about three to twelve seconds to estimate the bacterial growth depending of the temperature intervals that is fast in comparison with the sampling rate of the temperature that is in the order of minutes.

9.1.3 Statistical data fusion related algorithms

To solve the linear system of equations represented by equations 4.8 and 4.22, it is necessary to implement Matrix inversion. As mentioned before, the performance depends on the hardware restrictions but also the JVM being used and the Java libraries being used. The time required 20 by 20 matrix inversion in double precision was measured for the entire platform. The JAMA library [98] was used. As can be seen in Figure 6.15 Timing results for matrix inversion , the performance of the SunSPOT is eight time faster than the Imote2 at the same clock speed.

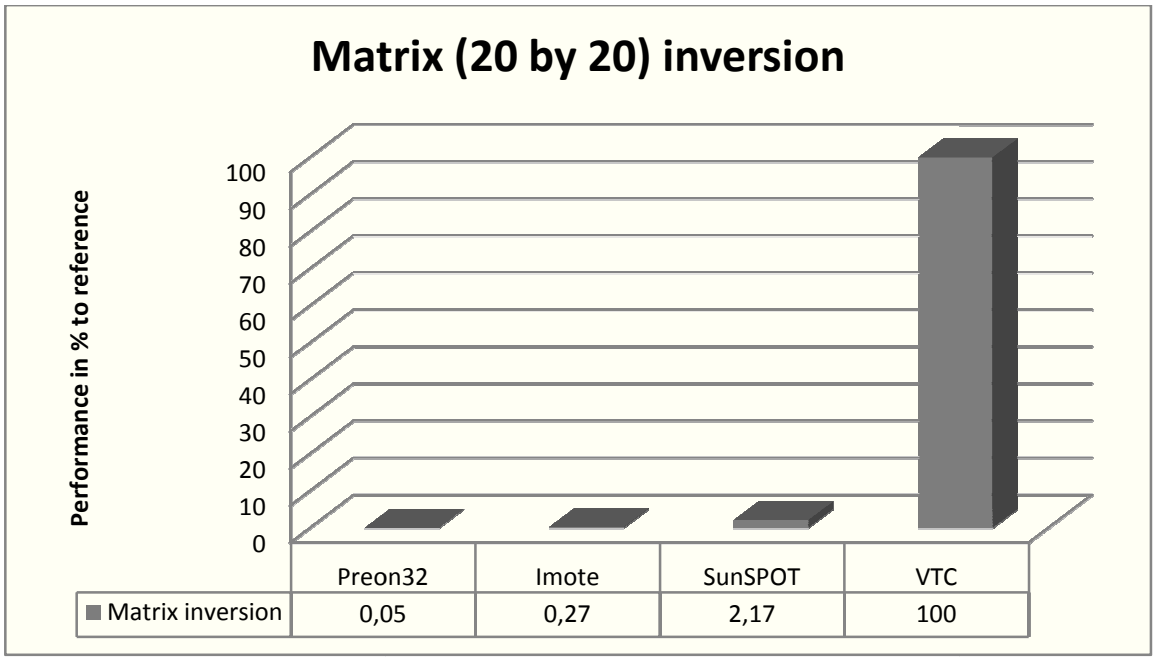

Figure 6.15 Timing results for matrix inversion

Finally, a centralized implementation of the required algorithms to perform fusion across attributes is made on a VTC 6100 gateway from Nexcom. The required CPU times for the OK and CK algorithms were compared on the telematic unit. The calculation time to solve the related matrix equations was compared under the condition that the algorithm achieves the accuracies given in Table 5.7. The tests were performed with the Prosyst OSGi implementation and the Jamaica Virtual Machine from Aicas.

Figure 6.16 shows a comparison of these measurements in milliseconds for CK and OK;

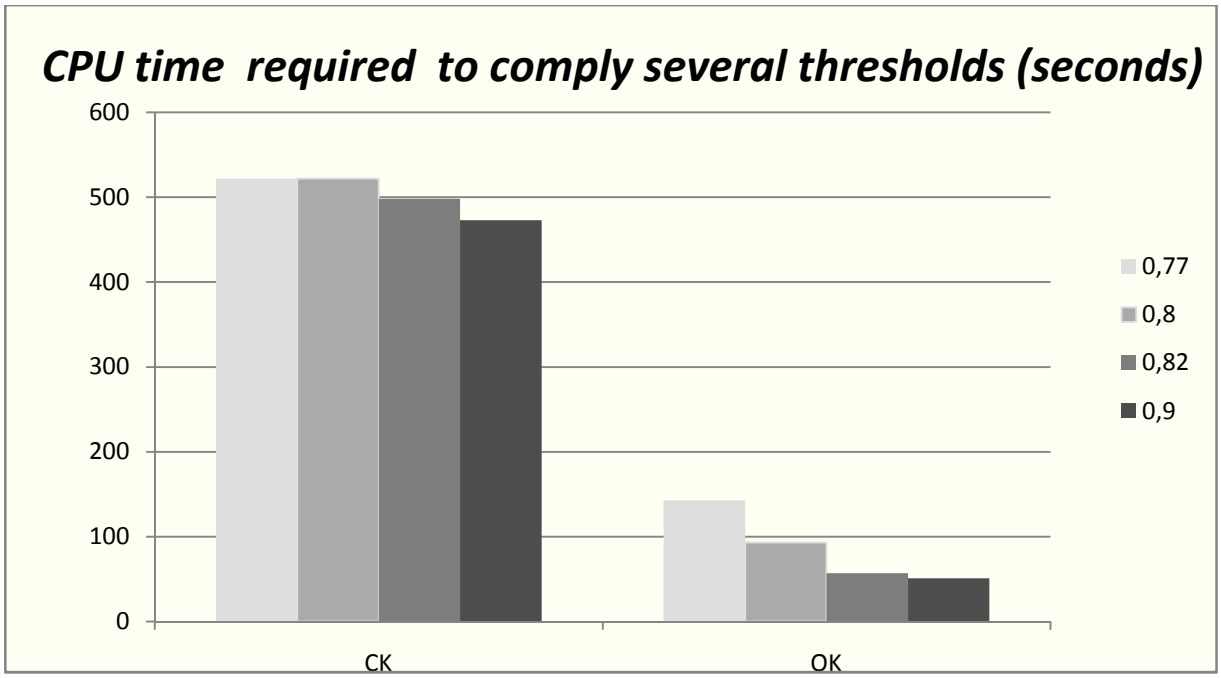

Figure 6.16 ***Comparison of required CPU time to comply with several thresholds***

Figure 6.17 shows the relation CK/OK for each one of the required accuracies. It can be seen that in all cases the timing required to perform CK is significantly greater than that required for the respective OK cases. However, the greater the accuracy required, the lower the relation CK/OK. For example to comply with a threshold of 0.77, eighteen humidity sensors will be required using ordinary Kriging, it can be done by using only seven humidity sensors with seventeen temperature measurements as support, however the time required for Cokriging interpolation is about 3.5 times.

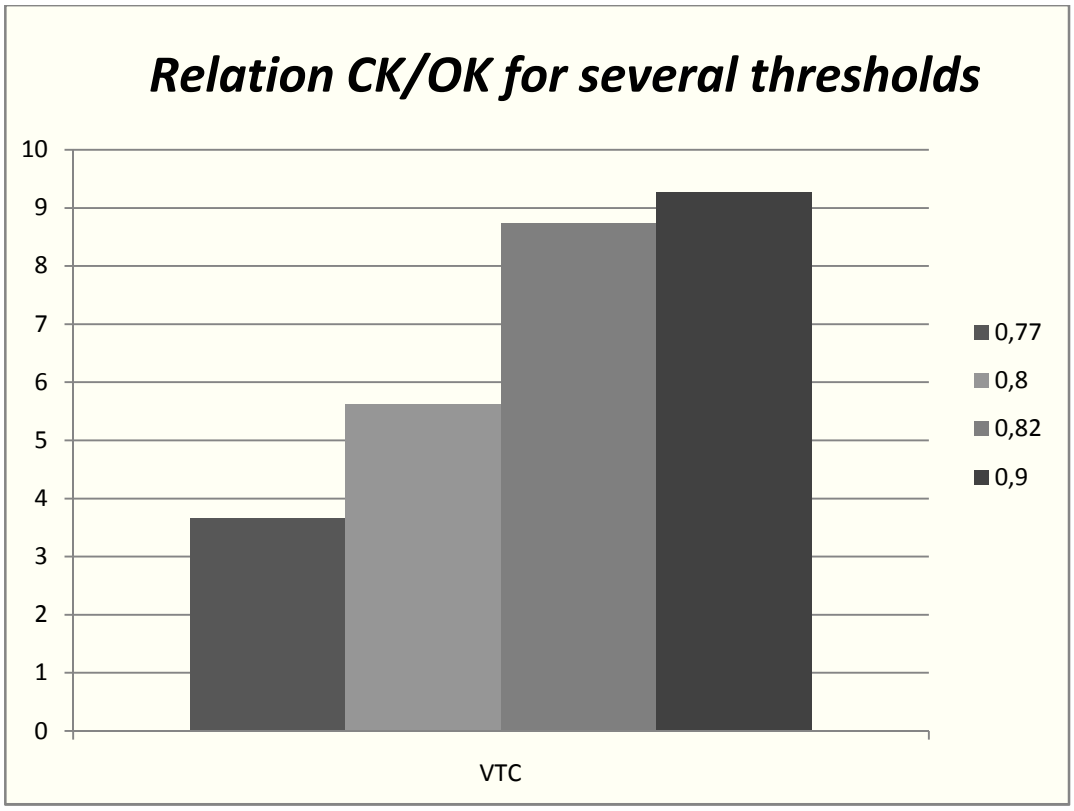

Figure 6.17 ***CK/OK Relation to comply with each threshold***

The timing to perform variogram-related algorithms is also measured in two cases: when only ten temperature and humidity measurements are applied and when we have the complete fifty collocated measurements.Figure 6.18 shows the results of the timing in seconds for building the EVs and to perform the GV algorithm. It can be seen that in both cases the timing can be reduced significantly without affecting the accuracy of the results.

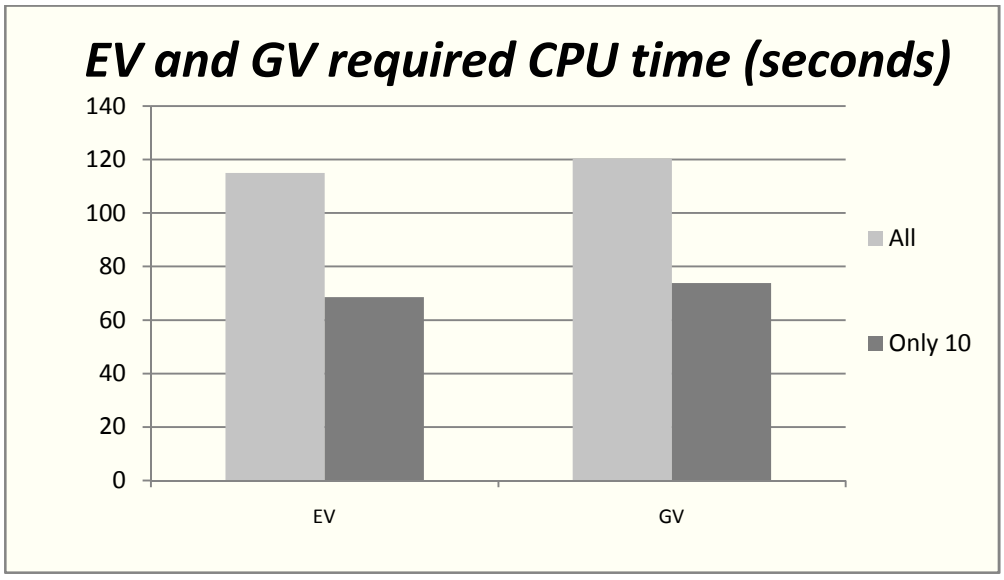

Figure 6.18 ***Required time for calculating EV's and GVz fitting algorithm***

9.2 Dynamic updates in OSGi-enabled devices

One of the most important figures of merit of OSGi is its ability to provide dynamic features to allow software updates or installation of new bundles during runtime without requiring to restart the system. Of special importance is how much overhead is created by using the OSGi framework to manage software updates. Direct execution times of Java class files and OSGi bundles of different algorithm was tested. Both standard benchmarks and the Feedback-Hammerstein algorithms were tested on the gateway devices and iMote2 for Equinox OSGi framework .

Figure 6.19 shows the results on the iMote2 and DuraNAV. The execution time of both standard benchmarks is in the order of eight percent slower when an OSGi bundle is executed instead of class file. The Feedback-Hammerstein OSGi bundle, however, was up to ten % faster than the corresponding Java class.

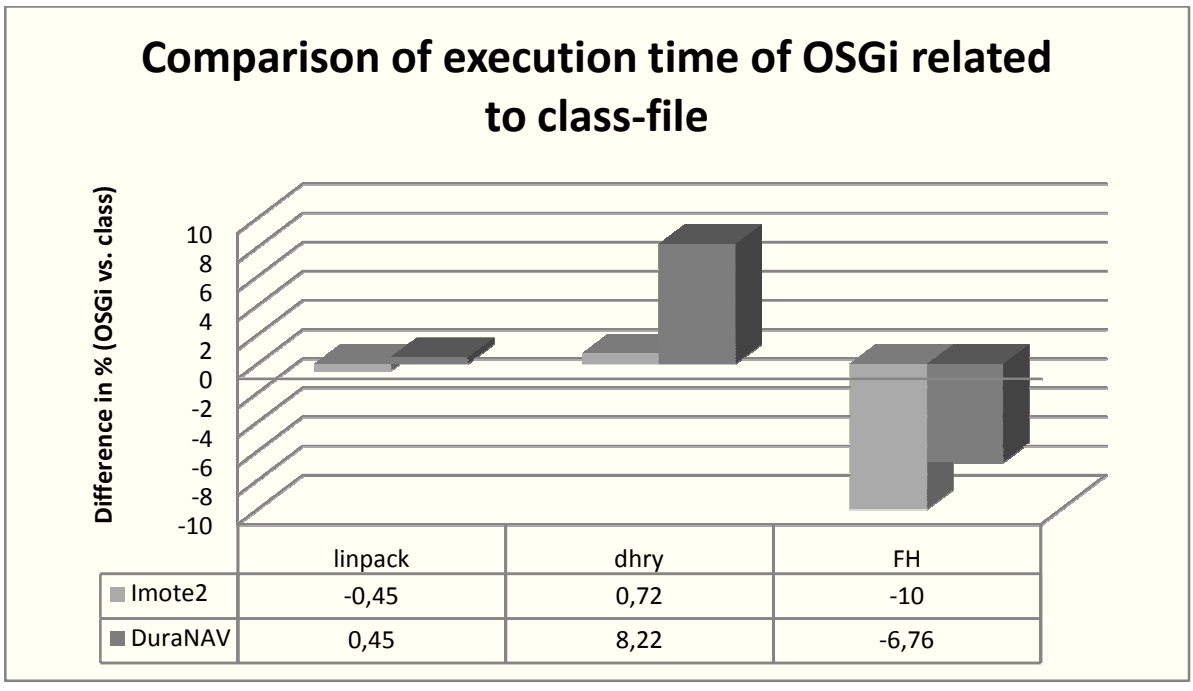

Figure 6.19 Diffrence in execution time in % between OSGi and class

The use of OSGi framework for the dynamic software updates of algorithms requiring few resources is possible with an increased execution speed when compared to Java class implementations.

9.3 Summary and conclusions chapter 5

This chapter has shown that Java is useful to manage hardware heterogeneity. Due to its high acceptance and maturity, portability of the code is possible. Sensor nodes that are the pillars of ubiquitous applications are their Achilles' heel as well. If the time required to interpret the instructions is too big, or if the memory required for the libraries is high, their implementation at the sensor level is unfeasible.

It was decided to test data fusion, standard benchmarks and cold-chain specific algorithms in selected Java-enabled sensor nodes and gateways. The best performance for algorithm requiring floating point operations are obtained with SunSPOT that uses JavaME, unfortunately, by using it modularity is limited to the use of Record Management System (RMS); furthermore neither, versioning nor dynamic programming is possible.

Versioning, dynamic programming and modularity in sensor nodes is possible even in sensor nodes by the installation of Java-based technologies such as OSGi. OSGi was installed on Imote2 sensor nodes, and DuraNAV and VTC telematic units. The time required to install OSGi bundles was measured. Only Imote2 has enough resources for making an OSGi-framework available on a sensor-platform. JavaME implementation of OSGi sounds promising, but it is not yet available.

In this chapter it is also demonstrated that data reduction techniques, that are a good approach to reduce energy consumption in the sensor nodes are energy-efficient and easy to implement on Java-enabled sensor nodes and therefore the transmission of high volumes of sensor data to the gateway is unnecessary.

The supervision of environmental parameters and quality state are also taken into consideration. The combined Gompertz model that calculates the bacterial growth in meat and the Feedback-Hammerstein that estimates the parameters of a non-linear model in fruit transport were selected, implemented and tested.

Statistical data fusion algorithms that are good approach to avoid dense deployment of sensors and to reduce communication if the measured data of many sensors is replaced by their estimations are only feasible to implement at the gateway level. The time required to achieve the same accuracy for OK by the use of CK interpolation is energy demanding, however, it is not important because it is performed in the gateway where there are no energy constraints.

10 Ubiquitous Cold-chain Monitoring Demonstrator Using Off-the-shelf devices

As mentioned by Iyengar [8], an ubiquitous application consists of three categories: sensor level, server level and client level. From the logistic point of view, they can be named sensors, gateways and decision makers. With the sensing, processing and data transmission of WSN is possible, for example to describe the current quality state of the product or predict future temperature profiles in specific locations of a refrigerated truck or container. The use of Internet-connected Gateways allow real-time monitoring and remote maintenance across the Internet [1]. Additionally, GSM-enabled gateways allow to send quality-related alarm messages via SMS; events can be detected early and directly at their point of origin during transportation [99]. Logistic applications can benefit from sensing, communication and processing heterogeneities of hardware devices. The decision maker can make use of existing global communication systems to take the proper management action based on alarm events and real-time monitoring; additionally remote software updates across the Internet is feasible. This chapter presents a demonstrator that shows how advances in Java-technologies on off-the-shelf hardware devices can be used to cope with these challenges; it makes use of the concept of Machine-to-Machine (M2M) communications that is a technology that allows communications-enabled remote devices to exchange information automatically without human interaction.

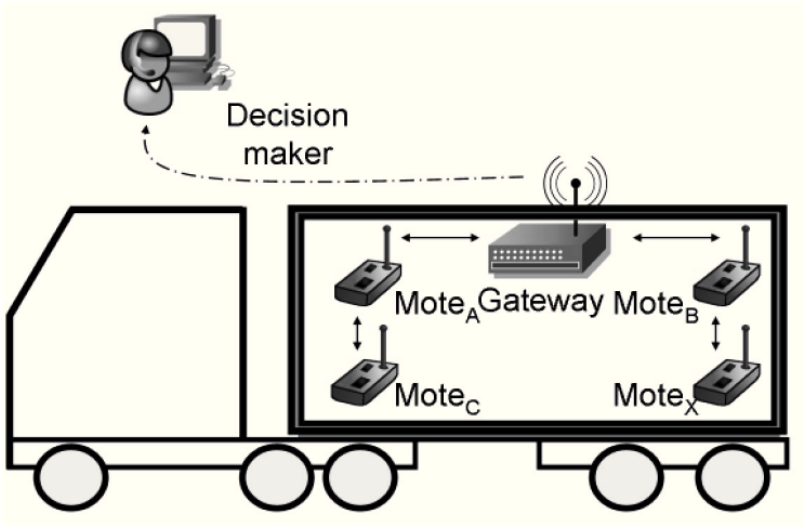

Figure 10.1 Connection via dedicated gateway in container [99]

10.1 The Overlap of WSN with M2M and other technologies

A differentiation between wireless M2M and WSN is not exact. According to Webb [100], the key requirements for M2M communications are:

- Support a large number of terminals
- Long battery life
- Mobility
- Low cost equipment
- Low cost service
- Global availability
- Ubiquity

The critical requirements for the design of M2M area networks are [101]:

- Low CPU processing power
- Limited memory
- Low data rate
- Battery operated
- Low cost
- Small size

Based on the previous descriptions, it can be said that both technologies can utilize sensors to perform remote monitoring and communicate with each other through wireless communication. Knowing the subtle differences will help to understand the implications of their combined use in logistics.

M2M are deployed when power consumption is not critical, the size/weight of the devices is not an important factor and a range of kilometres is required. Additional features may include for example bidirectional communication. Wireless M2M covers applications involving longer range and the node will typically be powered from the machine itself.

Wireless Sensor Networks (WSN) on the other hand is an emerging technology to monitor ambient conditions. They are commonly considered to be stand-alone; the sensor nodes communicate with other sensors and the gateway, but are in principle unable to communicate with the outside world; they have only short/medium range communication.

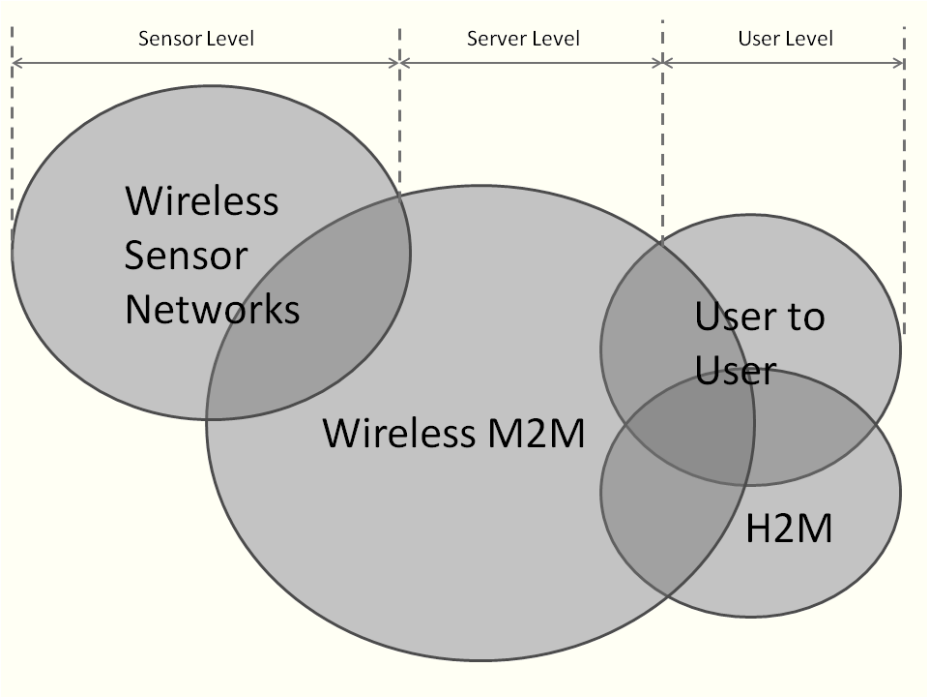

Figure 10.2 Wireless Sensor Networks compared to RFID and M2M(modified from [2])

Wireless M2M can be classified according to the communication technology it uses: It can be cellular (for example 3G or 4G), or short range technologies such as Zigbee [102] or Dash7 [103].

All of them have advantages and disadvantages: to bridge large distances 3G or 4G can be used, but they are expensive to maintain. Wireless sensor protocols such as Zigbee using 802.15.4 and Dash7 using ISO/IEC 18000-7 are cheap and Ad-hoc but they can only cover low distances and low data-rates (See Table 10.1Table 10.1)

Table 10.1 Wireless M2M technologies (modified from [104])

Criteria	3G	4G	ZigBee	Dash7
Architecture	Infra	Infra	Ad hoc	Ad hoc
Data Rates	High	Very High	Low	Low
Distance	High	High	Low	Low
Power Consumption	Medium	Medium	Low	Very Low
Cost	High	High	Low	Low
Nodes density	High	High	High	High
Maturity	High	Low	Medium	Low

10.2 Concept of the demonstrator

Figure 10.3 displays the concept of the demonstrator. It consists of sensor nodes, the gateway and a human decision maker that has either mobile phone or access to Internet through a

personal computer. All hardware platforms are Java-enabled, only open software is used. The M2M communications are represented by dashed lines.

The sensor nodes can be programmed as the conventional way: to perform a continuous monitoring of the goods; they would transfer the readings periodically to be visualized by the decision maker, the gateway processes the data and send and alarm when a temperature threshold is exceeded. However, the costs of such a solution is highly nonfeasible regarding service costs for the use of 3G or 4G infrastructure and on the current draw of the sensor nodes. Unnecessary data transmission must be avoided; the sensor must be able to process data in-situ and transmit only warning messages or summaries instead of full raw data.

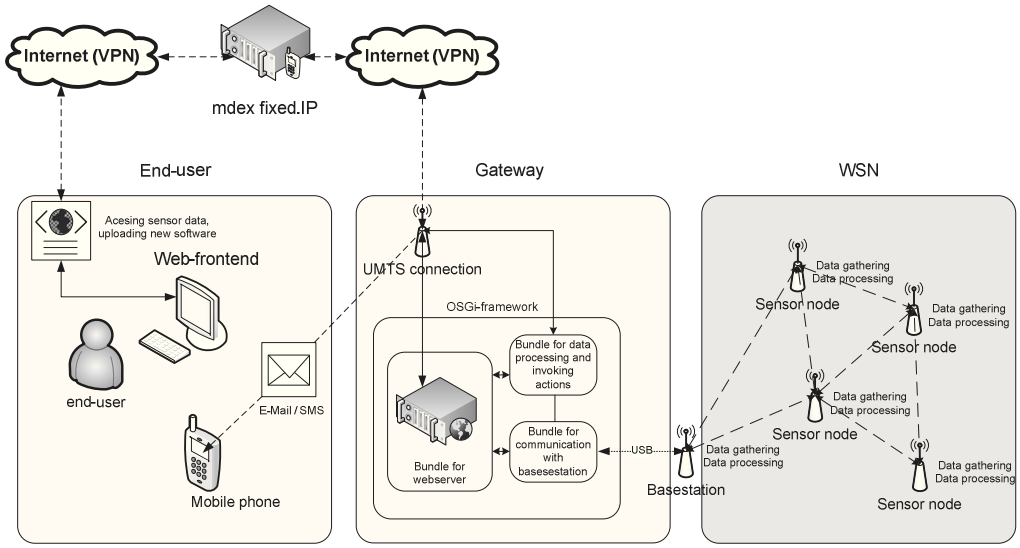

Figure 10.3 Concept of the demonstrator (M2M communications represented by dashed lines)

If the sensor data is processed locally, the radio communication between hop nodes can be drastically reduced, the costs related to the use of infrastructure avoided and eventual quality losses due to air flow obstacles detected.

Our implementation differs to that in running algorithms on the sensor boards to predict the temperature change. The task of the WSN is the gathering of environmental data – here temperature values – and local data-processing. The processed data is transferred wirelessly and can be received by the base station – the juncture between the WSN and the gateway. The gateway can for example send an e-mail or SMS to the decision maker.

The decision maker, can for example inform the logistic centre to perform a carefully inspection of the goods once arrival, but also require further information about the product

quality; the system must have the ability to deploy new software such as the Gompertz model to a chosen sensor node.

10.3 Demonstrator Implementation

The Feedback-Hammerstein algorithm for temperature prediction was selected to demonstrate the concept of the use of local processing of data to support decision making at affordable costs. Regarding hardware devices, VTC6100 and SunSPOTs are selected.

For the Gateway, the Equinox OSGi-framework is installed on top of the Linux OS, that enables a high degree of dynamics by allowing the installing or updating of software modules remotely during runtime.

The demonstrator integrates existing M2M and WSN with Information and communication technologies (ICT) for a logistic application, the goal is to demonstrate the use common infrastructure for multiple application domains using heterogeneous devices [105]. The concept was published in [106], the contribution of the author of this thesis is on the program of the sensor node, the communication of the resulting system parameters to the gateway and the prediction of temperature at the gateway level.

10.3.1 Sensor Level

As can be seen in Figure 10.3Figure 10.4, a SunSPOT sensor node is located near the cold-air-supply samples the local temperature periodically and broadcasts it to the rest of the sensors located inside the boxes. These sample the local temperature in the boxes every time a measurement from the air-supply sensor arrives. For demonstration purposes, the reading from the sensors is replaced by reading an array of floating values containing the resulting datasets from an experiment during a shipment of bananas from Costa Rica to Antwerp in May 2008

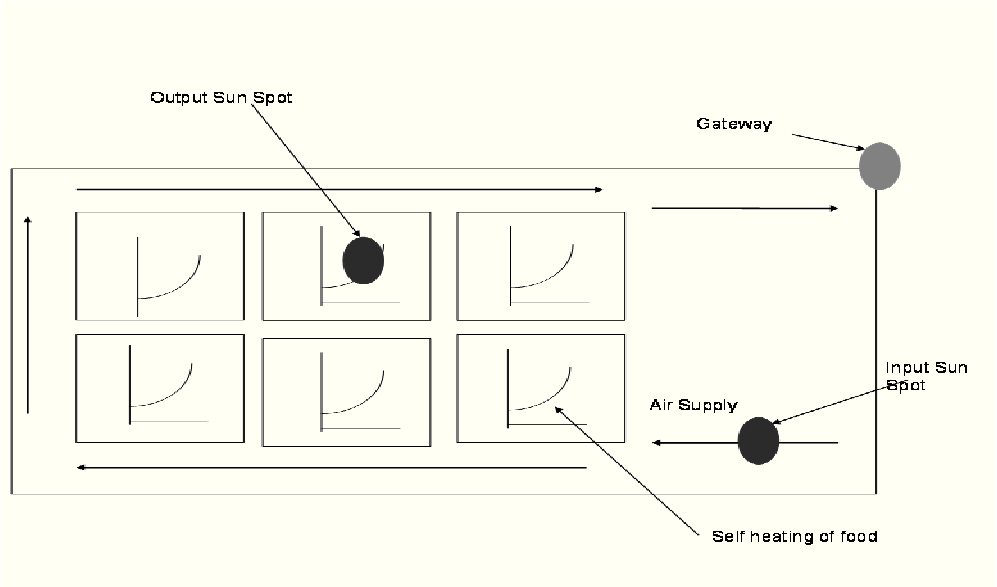

Figure 10.4 Implementation of the platforms in a refrigerated container

The parameters of the Feedback-Hammerstein model shown in Figure 5.10 are calculated by using system identification techniques. It provides a meaningful description of the factors involved in the physical system including the effect of transporting living goods such as fruits and vegetables. An online recursive method was chosen, as it requires much lower resources in terms of memory and CPU power than offline counterparts. In order to give an accurate prediction, the model parameters have to be iterated over three days at a measurement interval of one hour, equivalent to 72 cycles. After the data processing in each SunSPOT is performed, the three resulting model parameters and the last supply and output parameters are forwarded to the base station that is connected to the gateway.

10.3.2 Gateway Level

The gateway is OSGi-enabled. Different software modules are installed in this environment in the form of bundles. All OSGi programms were implemented by the second author in [106].

- One bundle receives data from the base station and also runs a prediction algorithm, that is able to calculate each point of the output temperature profile for the remaining transport duration – typically two weeks. Based on the calculations in correspondence with a defined threshold value, an event can be triggered in the OSGi-context.
- Other software bundle is added to the environment, it send notifications via SMS or e-mail when receiving an event. For sending these notifications, an uplink to a mobile service provider is necessary.
- Another bundle contains an application, that can be connected to the environment, is a web-interface for displaying data in form of a table or graph. It can also be used for

remote configuration, e.g. to change the threshold value for notifications. It contains a web-server and servlets for generating dynamic web-pages – this is for displaying data and altering of software on the sensors.

10.3.3 Client Level

Ubiquitous access to the container measurements is provided by existent infrastructure via a web-interface, to allow remote software updates, bidirectional communication needs to be established. Due to the fact that mobile service providers only assign IPs in the private network address range like 10.x.x.x, a connection to the gateway device can't be established. An extra service is needed to allow that. Here, we choose the gateway provider mdex, that represents the juncture between the two ends: Gateway and decision-maker. Both ends join a virtual private network at the service and are so able to communicate with each other.

10.3.4 Software updates over multi modal networks

To provide software updates from the decision-maker to the sensor nodes, a mechanism for the deployment is necessary. With the implementation of such mechanism, the WSN will be able to react to environment changes and failures that were unknown at the time of their initial deployment. Our solution consists of four steps.

1. Firstly, the new Java code has to be compiled and linked that results in a jar-archive, which is then used to create a MIDlet suite.
2. The MIDlet suite is transferred to the OSGi-enabled gateway device, which is connected to the base station. This can be done via an upload dialogue provided by the web-interface.
3. A deployment script which is accessible via the web-frontend has to be executed. The script contains information about an application descriptor and a provisioning server.
4. The SunSPOT sensor, which is a JavaME enabled device, can automatically download the application from the specified provisioning server. Since MIDP2, the Application Management Software (AMS) is also responsible for the downloading of applications; it is possible to perform over-the-air (OTA) provisioning. The term describes the ability to download and install content over a wireless network [107]. The OTA specification defines the expected device functionality, the OTA provisioning life-cycles, the installation process and the interactions between the AMS and the provisioning server.

10.4 Summary and conclusions chapter 6

This chapter has presented the use of off-the-shelf hardware devices and CIT technologies to enable ubiquitous monitoring of perishable goods. The approach is simple and affordable. It was implemented using only free software. Linux and the OSGi-framework Equinox, with the additional bundles needed in this context, were installed on the Gateway, and Java ME used for the SunSPOTs.

Ubiquitousness is achieved by exploiting the long range communication capabilities of the gateway which is the connection point to the outer world, M2M, WSN and communications and existing infrastructure.

Furthermore, a more intelligent cargo is possible. Environmental parameters are sensed, intelligent algorithms run on the sensor node using this acquired data and the result is transmitted wirelessly to a gateway. This leads to the ability to create autonomous decision making or supporting functionality or inform a (human) decision maker who can then deliver the products by the quality state or inform the logistic center for detailed inspections. The software needed to handle the dynamics of the application can be remotely installed or updated.

The dynamic updates are supported by JavaME on sensor nodes and OSGi in the gateway. JavaME on the sensor nodes is useful, because the communication volume for updating software bundles is lower than in the case of monolithic software. However, JavaME running on sensor nodes does not yet allow the communication between MIDlets therefore the modularity is limited due to missing communication between different modules. Furthermore, dynamic updating is not possible, old-versioned MIDlets must be first uninstalled. The first OSGi ME might be soon on the market, it would be interesting to see if it will keep core features of the OSGi technology and the Java ME CLDC compliances.

11 Conclusions

Wireless sensor networks are a technology that will have an impact in the future due to their broad range of applications. It is a technology that has not been benefited from Moore's Law; the processors have become more powerful, faster and smaller, but due to the fact that sensor nodes are operated by batteries, the hardware is designed to consume the less energy as possible. The challenges in hardware design are numerous, and they include low-power communication and low-power microcontrollers. MEMS-based sensors and actuators and energy-scavenging [108]. As Feherenbacher [109] mentioned :

"Yes, batteries will come down in price and become smaller, but at nowhere near the same speed — and with a lot less progress — as to be able to be compared to Moore's Law"

Regarding information technology, solutions designed for devices with no energy-constraints are not suitable for sensor nodes. For example, TinyOS [110] is a component-based operating system and platform designed specifically for wireless sensor networks and 6LoWPAN [111] is an Internet Protocol aimed to be applied to low-power devices with limited processing capabilities such as sensor nodes.

This thesis describes the research of various interdisciplinary methods to cope with the main technical, logistical and economical issues of applying WSN to ubiquitously monitor perishable goods during transportation, namely low-energy consumption, large area of coverage and flexibility. Throughout this thesis novel approaches to cope with these have been developed and tested.

To increase the life expectancy of the WSN, it was selected to compress data by reducing the data rates at the sensor level. Traditional information theory techniques have failed to the computational resources required to compress and uncompress the data. The information theories such as Slepian-Wolf [20] were developed in the seventies when every algorithm was a computational burden and their real-world implementation of them was not under research. With the increasing power of computers, it seems that every algorithm is feasible to be implemented; unfortunately WSN did not profit from this trend.

In chapter 3, it was demonstrated the drawbacks of DSC. The main problem lies in the model itself; the environment is modeled as a noisy channel when in reality it is a stochastic process. A novel method for distributed data compression was developed. It exploits the concepts of semivariance and pair correlation that belong to the field of spatial statistics. In situ compression and recovery are possible but requires knowledge of the mean value. We

believe that this approach constitutes a fundamentally different way of compressing correlated data that can have an enormous impact in environmental sensor networks and other related research fields.

A novel solution to increase coverage in environmental WSN by using single and cross-attribute information fusion is explained in chapter four. It surpasses existing techniques in the sense that it does not require mobility of the nodes and provides a measure of the uncertainty. It is a powerful and mature information fusion method that has been applied in geostatistics but not on WSN. The so-called Kriging and Co-kriging interpolation methods are Best Linear Unbiased Estimations (BLUE). The single attribute fusion brings advantages when it is compared with deterministic models; cross-attribute fusion reduces the number of sensors drastically in an accurate and robust way. The tested statistical fusion methods are not limited to the scenarios of refrigerated containers considered in this work, but they are applicable to other case scenarios.

Through feasibility tests and a demonstrator it is proposed the combination of features of diverse existing technologies that include M2M, WSN and UMTS to cope with the requirements of ubiquitous applications. The use of heterogeneous hardware platforms, comprising of devices with different computational capabilities can be managed by the use of Java technologies. The tests performed in this thesis show that today's Java solutions can scale to a wide range of devices. Software updates are possible thanks of the maturity of standardized Java and OSGi technologies; as an example, SunSPOT [87] sensor nodes already support Over-the-Air provisioning and IPv6 connections.

11.1.1 Summary of the results

Table 7.1 and figure 7.1 summarize the results. The desired figures of merit can be improved by shifting between different levels of the ubiquitous application. The energy consumption due to radio communication can now be reduced by compressing and decompressing the data at the sensor node; previously only the gateway had the computational capabilities to decode (decompress) the data.

The area of coverage can be increased by performing Kriging and Co-kriging interpolation at the gateway level. Previously, it was only possible by deploying additional nodes or by repositioning the existing ones. The profitability of the application can be increased if *in-situ* data processing is performed and only some model parameters are transmitted to the decision maker instead of the complete raw data. Finally, flexibility and maintenance is increased if the

maturity of Java technologies is exploited. The decisions regarding remote deployment of intelligent algorithms in the sensor nodes can be made by the decision maker if the sensor node was not programmed with the required algorithm at the time of deployment.

Table 11.1: Summary of the results

Improves	From	To	Replacing	By using	Exploiting	See Chapter
Energy	Gateway Level	Sensor Level	DSC	Data Compression	Spatial Correlation	Three
Coverage	Sensor Level	Gateway Level	Dense deployments Mobility	Kriging and Cokriging	Spatial Correlation and cross-correlation	Four
Profitability	Decision-maker	Sensor Level	Raw-data transmision	System identification	Local Processing	Six
Flexibility and Maintenance	Sensor Level	Decision maker	Fixed code	Java/OSGi	Infrastucture Java maturity	Five

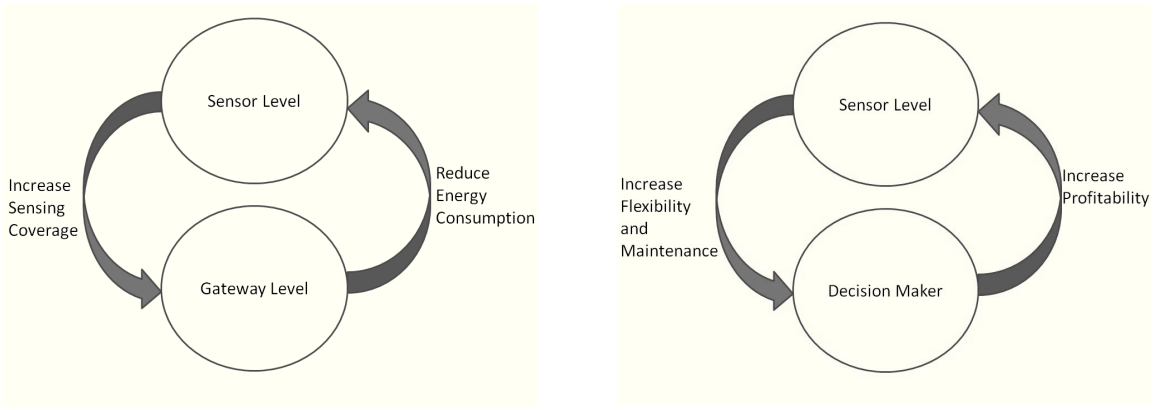

(a) (b)

Figure 11.1: Shifting of levels to improve the figures of merit

11.2 Future Work

There are many opportunities for future research, especially in the presented statistical data fusion methods. It is desirable to calculate the experimental variogram (EV) in a distributed and energy efficient way. Previous research work has been made to calculate the EV based on aggregation trees that recursively partitions the space into quadrants; the problem with this approach is that it requires broadcasting to create the trees that are complicated to implement and energy consuming, and the variogram is only calculated for one fixed distance.

It is also necessary for the development and implementation of a distributed method for the detection of statistical outliers. It can for example, to compare the amount of sent bits by the source node with the difference between the mean value and the side information at the sinking node. The robustness of the approach against dynamic changes in the environment is also required; the variances and the mean value might change in time. Therefore, the sensor network must be able to detect if the correlation model is valid at all times.

The presented compression methods must be compared with the existing approaches. The effect of the network size on its lifetime must also be estimated.

Regarding Java technologies, further research on the nodes energy consumption is required. It will be interesting to measure the energy and computational performance of the upcoming OSGi-ME implementations and to test the dynamic updates at the sensor level. Dedicated Java Virtual Machines and OSGi implementations will be required for more automated and efficient dynamic updates at the three levels of the ubiquitous applications.

List of Symbols

a,c	Cokriging weights for the primary variables
b,d	Cokriging weights for the secondary variable
$A(q^{-1})$	Polynomial containing zeros of a linear system
b_{ijs}	ij-th element of matrix Bs
B_u	Set of 2x2 real-valued coregionalization matrices
$B(q^{-1})$	Polynomial containing poles of linear system
C(h)	Centred covariance
$C(q^{-1})$	Polynomial describing a Moving Average process
g	Bacterial growth rate
E	Expectation
F	Relation between prediction error and standard deviation
G	Exponential factor in Gompertz Model
h	Lag separation vector
H	Parity matrix
H(u,v)	Mutual information
H(u)	Marginal entropy
H(u|v)	Uncertainty
i	i-th variogram model
j	reaction constant in Gompertz Model
k	Total number of lags
k_{T_i}	temperature-dependent variable.
K	Total number of source points for secondary variable
L	Germ concentration
M	Binary word size
n	Total number of source points for primary variable
N	Number of bits of compressed binary word
N_k	Number of samples
N_z	Number of destination points
p	Probability of bit flip
Q(t)	Adaptation gain at time t
r	Variogram range
R	Compression rate
s	Syndrome

S	Number of basic variogram models
U	Source information in real-valued domain
$\hat{U}_0$	Estimated primary variable at point 0
U_i	Measured primary variable at point i
$\hat{V}_0$	Estimated secondary variable at point 0
V_i	Measured secondary variable at point i
w_k	Weight at lag k
W	Weight Matrix
y	Predicted value of Feedback Hammerstein
z_i	Measured value for destination point i
$\hat{z_i}$	Predicted value for destination point i
α	Isolation loses in a container
β	Scaling factor that depends of the amount of food
$\gamma(h)$	Variogram
γ_0	Variogram nugget
γ_∞	Variogram sill
$\hat{\gamma}_{ij}(h_k)$	ij-th element of matrix Γ
$\gamma_{ij}(h_k)$	ij-th element of matrix $\hat{\Gamma}$
$\Gamma(h)$	2x2 matrix of simple and theoretical cross variograms
$\hat{\Gamma}(h)$	2x2 matrix of simple and experimental cross variograms
μ	Main value
Δ	Quantization step
ε_i	Interpolation error for destination point i
$\bar{\varepsilon}$	Average prediction error for all destination points
ξ	Prediction Error in Feedback Hammerstein
σ_i^2	Variance of variable i
σ_e^2	Noise variance of the noise in a binary channel
η	Additive noise in a binary channel
λ	Lagrange multiplier
Θ	Parameter vector
φ	Observation Vector
δ	Forgetting factor
τ	Constant that is fixed for a certain type of fruit
ι	Upper asymptote in Gompertz Model
κ	Displacement in Gompertz Model

List of Abbreviations

A/D	Analogue to Digital
BSC	Binary Source Channel
CI	Covariance Intersection
CK	Cokriging
DISCUS	Distributed Source Coding Using Syndromes
DSC	Distributed Source Coding
EV	Experimental Variogram
GPRS	General Packet radio Service
GV	Goulard-Voltz
IDW	Inverse Distance Weighing
IF	Information Fusion
KV	Kriging Variance
LAN	Local Area Network
LDPC	Low Density Parity Check Codes
LS	Linear Space
MI	Mutual Information
M2M	Machine to Machine
NaN	Not a Number
OK	Ordinary Kriging
OSGi	Open Services Gateway initiative
OTA	Over the Air
RH	Relative Humidity
ROI	Region of Interest

UMTS	Universal Mobile Telecommunication System
WSN	Wireless Sensor Network
WSS	Weighted Sum of Squares

List of Figures

List of Tables

References

[1] D. J. A. Bijwaard, *et al.*, "Industry: using dynamic WSNs in smart logistics for fruits and pharmacy," presented at the Proceedings of the 9th ACM Conference on Embedded Networked Sensor Systems, Seattle, Washington, 2011.

[2] C. Rhee, *et al.*, "USN applied to Smart Cold Chain based on the mesh wireless sensor network," presented at the CartaSense, 2011.

[3] AmbientSystems. (2008, February 14). *Ambient Systems' intelligent RFID reduces fruit and vegetables spoilage*. Available: http://coolchain.org/Websites/cca/Blog/1730299/PR%20-%20Ambient%20RFID.pdf

[4] R. Jedermann, *et al.*, "Demo Abstract: Wireless quality monitoring in the food chain," presented at the 6th European Conference on Wireless Sensor Networks, Cork, Ireland, 2009.

[5] D. Culler. (2003, February 12). *10 Emerging Technologies That Will Change the World*. Available: http://www2.technologyreview.com/featured-story/401775/10-emerging-technologies-that-will-change-the/2/

[6] M. Becker, *et al.*, "Challenges of Applying Wireless Sensor Networks in Logistics," presented at the CEWIT 2009. Wireless and IT driving Healthcare, Energy and Infrastructure Transformation, 2009.

[7] M. Weiser, "The computer for the 21st century," *SIGMOBILE Mob. Comput. Commun. Rev.,* vol. 3, pp. 3-11, 1999.

[8] S. S. Iyengar, *Fundamentals of sensor network programming: applications and technology*. Hoboken, NJ: Wiley 2011.

[9] Z. Tafa, "Ubiquitous Sensor Networks," in *Application and Multidisciplinary Aspects of Wireless Sensor Networks*, L. Gavrilovska, *et al.*, Eds., ed: Springer London, 2011, pp. 267-268.

[10] F. Schlachter, "No Moore's Law for batteries," *Proceedings of the National Academy of Sciences,* vol. 110, p. 5273, April 2, 2013 2013.

[11] G. Anastasi, *et al.*, "Energy conservation in wireless sensor networks: A survey," *Ad Hoc Netw.,* vol. 7, pp. 537-568, 2009.

[12] J. Li and P. Mohapatra, "Analytical modeling and mitigation techniques for the energy hole problem in sensor networks," *Pervasive Mob. Comput.,* vol. 3, pp. 233-254, 2007.

[13] Y. Liyang, *et al.*, "Deploying a Heterogeneous Wireless Sensor Network," in *Wireless Communications, Networking and Mobile Computing, 2007. WiCom 2007. International Conference on*, 2007, pp. 2588-2591.

[14] A. Reinhardt and D. Burgstahler, "Exploiting Platform Heterogeneity in Wireless Sensor Networks by Shifting Resource-Intensive Tasks to Dedicated Processing Nodes," in *Proceedings of the 14th International Symposium on a World of Wireless, Mobile and Multimedia Networks (WoWMoM)*, 2013.

[15] E. Fasolo, *et al.*, "In-network aggregation techniques for wireless sensor networks: a survey," *Wireless Communications, IEEE,* vol. 14, pp. 70-87, 2007.

[16] C. Intanagonwiwat, *et al.*, "Directed diffusion for wireless sensor networking," *IEEE/ACM Trans. Netw.,* vol. 11, pp. 2-16, 2003.

[17] N. Kimura and S. Latifi, "A survey on data compression in wireless sensor networks," in *Information Technology: Coding and Computing, 2005. ITCC 2005. International Conference on*, 2005, pp. 8-13 Vol. 2.

[18] D. Petrovic, *et al.*, "Data funneling: routing with aggregation and compression for wireless sensor networks," in *Sensor Network Protocols and Applications, 2003.*

Proceedings of the First IEEE. 2003 IEEE International Workshop on, 2003, pp. 156-162.

[19] T. Arici*, et al.*, "PINCO: a pipelined in-network compression scheme for data collection in wireless sensor networks," in *Computer Communications and Networks, 2003. ICCCN 2003. Proceedings. The 12th International Conference on*, 2003, pp. 539-544.

[20] D. Slepian and J. K. Wolf, "Noiseless coding of correlated information sources," *Information Theory, IEEE Transactions on,* vol. 19, pp. 471-480, 1973.

[21] F. Oldewurtel, "Exploiting spatial correlations for efficient communication and deployment optimisation in wireless sensor networks," PhD Thesis, RWTH, Achen, 2011.

[22] Z. Rezaei and S. Mobininejad, "Energy Saving in Wireless Sensor Networks," *International Journal of Computer Science & Engineering Survey (IJCSES)* vol. 3, p. 14, 2012.

[23] D. Chu*, et al.*, "Approximate Data Collection in Sensor Networks using Probabilistic Models," in *Data Engineering, 2006. ICDE '06. Proceedings of the 22nd International Conference on*, 2006, pp. 48-48.

[24] D. Tulone and S. Madden, "PAQ: Time Series Forecasting for Approximate Query Answering in Sensor Networks," in *Wireless Sensor Networks*. vol. 3868, K. Römer*, et al.*, Eds., ed: Springer Berlin Heidelberg, 2006, pp. 21-37.

[25] D. Tulone and S. Madden, "An energy-efficient querying framework in sensor networks for detecting node similarities," presented at the Proceedings of the 9th ACM international symposium on Modeling analysis and simulation of wireless and mobile systems, Terromolinos, Spain, 2006.

[26] J. Palafox-Albarrán*, et al.*, "Energy-Efficient Parameter Adaptation and Prediction Algorithms for the Estimation of Temperature Development Inside a Food Container," in *Lecture Notes in Electrical Engineering - Informatics in Control, Automation and Robotics*, A. J. Cetto*, et al.*, Eds., ed Berlin: Springer, 2011, pp. 77-90.

[27] G. Zito and I. D. Landau, *Digital control systems: design, identification and implementation*. London: Springer, 2006.

[28] F. Hu and Q. Hao, *Intelligent sensor networks: the integration of sensor networks, signal processing and machine learning*. Boca Raton, Fla.: CRC Press, 2013.

[29] N. Ahmed*, et al.*, "The holes problem in wireless sensor networks: a survey," *SIGMOBILE Mob. Comput. Commun. Rev.,* vol. 9, pp. 4-18, 2005.

[30] C.-F. Huang and Y.-C. Tseng, "The coverage problem in a wireless sensor network," presented at the Proceedings of the 2nd ACM international conference on Wireless sensor networks and applications, San Diego, CA, USA, 2003.

[31] S. Meguerdichian*, et al.*, "Coverage problems in wireless ad-hoc sensor networks," in *INFOCOM 2001. Twentieth Annual Joint Conference of the IEEE Computer and Communications Societies. Proceedings. IEEE*, 2001, pp. 1380-1387 vol.3.

[32] L. Lazos and R. Poovendran, "Stochastic coverage in heterogeneous sensor networks," *ACM Trans. Sen. Netw.,* vol. 2, pp. 325-358, 2006.

[33] L. Lazos and R. Poovendran, "Coverage In Heterogeneous Sensor Networks," in *Modeling and Optimization in Mobile, Ad Hoc and Wireless Networks, 2006 4th International Symposium on*, 2006, pp. 1-10.

[34] A. Ali*, et al.*, "Information Driven Approach for Sensor Positioning in Wireless Sensor Networks," presented at the INFORMATIK 2011 Informatik schafft Communities 4.–7. , Berlin, 2011.

[35] M. Umer*, et al.*, "Kriging for Localized Spatial Interpolation in Sensor Networks," presented at the Proceedings of the 20th international conference on Scientific and Statistical Database Management, Hong Kong, China, 2008.

[36] A. Krause and C. Guestrin, "Optimizing Sensing: From Water to the Web," *Computer,* vol. 42, pp. 38-45, 2009.
[37] A. Krause*, et al.*, "Robust submodular observation selection," *Journal of Machine Learning Research,* vol. 9, pp. 008) 2761-, 2008.
[38] F. Szidarovszky, "Multiobjective observation network design for regionalized variables," *International Journal of Mining Engineering,* vol. 1, pp. 331-342, 1983/12/01 1983.
[39] CrossBow. (2013, September 5 2013). *TelosB Datasheet*. Available: http://www.willow.co.uk/TelosB_Datasheet.pdf
[40] (TinyOS, September 5 2013). *TinyOS Web page*. Available: http://www.tinyos.net/
[41] I. Mahgoub and M. Ilyas, *Smart dust: sensor network applications, architecture, and design*. Boca Raton, Fla.: CRC, Taylor & Francis, 2006.
[42] H. B. Mitchell, *Data fusion: concepts and ideas*. Berlin Springer, 2012.
[43] R. Boudjemaa and A. B. Forbes, *Parameter Estimation Methods for Data Fusion*: National Physical Laboratory.Great Britain, Centre for Mathematics and Scientific Computing, 2004.
[44] E. F. Nakamura*, et al.*, "Information fusion for wireless sensor networks: Methods, models, and classifications," *ACM Comput. Surv.,* vol. 39, p. 9, 2007.
[45] R. Faragher, "Understanding the Basis of the Kalman Filter Via a Simple and Intuitive Derivation [Lecture Notes]," *Signal Processing Magazine, IEEE,* vol. 29, pp. 128-132, 2012.
[46] J. Bibby and H. Toutenburg, *Prediction and improved estimation in linear models*. Chichester Wiley, 1977.
[47] X. R. Li*, et al.*, "Optimal linear estimation fusion .I. Unified fusion rules," *Information Theory, IEEE Transactions on,* vol. 49, pp. 2192-2208, 2003.
[48] M. Kanevski and M. Maignan, *Analysis and modelling of spatial environmental data* Lausanne: EPFL Press, 2004.
[49] R. Jedermann and W. Lang, "The Minimum Number of Sensors --- Interpolation of Spatial Temperature Profiles in Chilled Transports," presented at the Proceedings of the 6th European Conference on Wireless Sensor Networks, Cork, Ireland, 2009.
[50] R. Jedermann*, et al.*, "Interpolation of spatial temperature profiles by sensor networks," in *Sensors, 2011 IEEE*, 2011, pp. 778-781.
[51] A. R. Murugan*, et al.*, "Correlated sources over wireless channels: cooperative source-channel coding," *Selected Areas in Communications, IEEE Journal on,* vol. 22, pp. 988-998, 2004.
[52] (2012, February 12). *ASN Inc*. Available: http://www.asn-inc.co.kr/
[53] (2012, February 12). *Datasheet SHT20*. Available: http://www.sensirion.com/fileadmin/user_upload/customers/sensirion/Dokumente/Humidity/Sensirion_Humidity_SHT20_Datasheet.pdf
[54] J. Chou*, et al.*, "A distributed and adaptive signal processing approach to reducing energy consumption in sensor networks," in *INFOCOM 2003. Twenty-Second Annual Joint Conference of the IEEE Computer and Communications. IEEE Societies*, 2003, pp. 1054-1062 vol.2.
[55] J. Chou*, et al.*, "Tracking and exploiting correlations in dense sensor networks," in *Signals, Systems and Computers, 2002. Conference Record of the Thirty-Sixth Asilomar Conference on*, 2002, pp. 39-43 vol.1.
[56] M. Vaezi and F. Labeau, "Improved modeling of the correlation between continuous-valued sources in LDPC-based DSC," in *Signals, Systems and Computers (ASILOMAR), 2012 Conference Record of the Forty Sixth Asilomar Conference on*, 2012, pp. 1659-1663.

[57] S. S. Pradhan and K. Ramchandran, "Distributed source coding using syndromes (DISCUS): design and construction," in *Data Compression Conference, 1999. Proceedings. DCC '99*, 1999, pp. 158-167.
[58] E. Berlekamp*, et al.*, "On the inherent intractability of certain coding problems (Corresp.)," *Information Theory, IEEE Transactions on,* vol. 24, pp. 384-386, 1978.
[59] J. G. Proakis and M. Salehi, *Digital communications*, 5. ed., internat. ed. ed. Boston 2008: McGraw-Hill.
[60] J. M. Walsh and P. A. Regalia, "On the Relationship Between Belief Propagation Decoding and Joint Maximum Likelihood Detection," *Communications, IEEE Transactions on,* vol. 58, pp. 2753-2758, 2010.
[61] V. Stankovic*, et al.*, "On code design for the Slepian-Wolf problem and lossless multiterminal networks," *Information Theory, IEEE Transactions on,* vol. 52, pp. 1495-1507, 2006.
[62] W. Schwanghart. (2009, *Description of the 'variogramfit' function*. Available: http://www.mathworks.com/matlabcentral/fileexchange/25948-variogramfit
[63] J. A. Nelder and R. Mead, *A simplex method for function minimization*, 1964.
[64] N. Cressie, "Fitting variogram models by weighted least squares," *Journal of the International Association for Mathematical Geology,* vol. 17, pp. 563-586, 1985/07/01 1985.
[65] A. B. McBratney and R. Webster, "Choosing functions for semi-variograms of soil properties and fitting them to sampling estimates," *Journal of Soil Science,* vol. 37, pp. 617-639, 1986.
[66] S. J. Julier and J. K. Uhlmann, "A non-divergent estimation algorithm in the presence of unknown correlations," in *American Control Conference, 1997. Proceedings of the 1997*, 1997, pp. 2369-2373 vol.4.
[67] M. B. Hurley, "An information theoretic justification for covariance intersection and its generalization," in *Information Fusion, 2002. Proceedings of the Fifth International Conference on*, 2002, pp. 505-511 vol.1.
[68] V. Popovich, *Information fusion and geographic information systems: towards the digital ocean*. Berlin Springer, 2011.
[69] H. Wackernagel, *Multivariate geostatistics: an introduction with applications* 3ed. Berlin Springer, 2003.
[70] R. Jedermann*, et al.*, "Modelling and interpolation of spatial temperature during food transportation and storage by the Variogram," in *The 10th International Conference on Modeling and Applied Simulation (MAS 2011)*, Rome, Italy, 2011, pp. 195-201.
[71] J. Chiles and P. Delfiner, *Geostatistics: Modeling Spatial Uncertainty*, second ed. New Jersey: Wiley, 2012.
[72] J. Rodríguez-Bermejo*, et al.*, "Thermal study of a transport container," *Journal of Food Engineering,* vol. 80, pp. 517-527, 2007.
[73] SealedAir. (2013, September 30). *TurboTag® System*. Available: http://www.sealedairspecialtymaterials.com/eu/de/products/turbotag.aspx
[74] Maxim. (2013, September 30). *Button Devices*. Available: http://www.maximintegrated.com/products/ibutton/
[75] M. Goulard and M. Voltz, "Linear coregionalization model: Tools for estimation and choice of cross-variogram matrix," *Mathematical Geology,* vol. 24, pp. 269-286, 1992/04/01 1992.
[76] J. Chiles and P. Delfiner, *Geostatistics: Modeling Spatial Uncertainty*, first ed. New Jersey: Wiley, 1999.
[77] X. Emery, "Iterative algorithms for fitting a linear model of coregionalization," *Computers & Geosciences,* vol. 36, pp. 1150-1160, 2010.

[78] M. Yarvis, *et al.*, "Exploiting heterogeneity in sensor networks," in *INFOCOM 2005. 24th Annual Joint Conference of the IEEE Computer and Communications Societies. Proceedings IEEE*, 2005, pp. 878-890 vol. 2.
[79] R. B. Hayun and S. Mason, *Java ME on Symbian OS: [inside the Smartphone model]*. Chichester: Wiley, 2009.
[80] R. Teodorescu and R. Pandey, "Using JIT Compilation and Configurable Runtime Systems for Efficient Deployment of Java Programs on Ubiquitous Devices," in *Ubicomp 2001: Ubiquitous Computing*. vol. 2201, G. Abowd, *et al.*, Eds., ed: Springer Berlin Heidelberg, 2001, pp. 76-95.
[81] IBM. (2013, Oktober 7). *J2ME record management store*. Available: http://www.ibm.com/developerworks/library/wi-rms/
[82] O. Alliance. (2013, September 5 2013). *OSGi Alliance*. Available: http://www.osgi.org/Main/HomePage
[83] G. Wütherich, *et al.*, *Die OSGi-Service-Platform: eine Einführung mit Eclipse Equinox*, 1 ed. Heidelberg: dpunkt.verl., 2008.
[84] F. Böse and K. Windt, "Catalogue of Criteria for Autonomous Control in Logistics," in *Understanding Autonomous Cooperation and Control in Logistics*, M. Hülsmann and K. Windt, Eds., ed: Springer Berlin Heidelberg, 2007, pp. 57-72.
[85] Eurotech. (2013, February 12). *Duranav 1000*. Available: http://www.eurotech.com/en/products/DuraNAV
[86] Nexcom. (2013, February 12). *VTC 6100*. Available: http://www.nexcom.com/Products/mobile-computing-solutions/in-vehicle-pc/in-vehicle-pc/car-pc-vtc-6100
[87] Oracle. (2013, *SunSPOT*. Available: http://www.sunspotworld.com/
[88] Virtenio. (2013, July 2013). *Preon32*. Available: http://www.virtenio.com/en/products/radio-module.html
[89] Aicas. (2013, November 14). *JamaicaVM*. Available: https://www.aicas.com/cms/en/JamaicaVM
[90] CrossBow. (2013, *Imote2*. Available: http://www.xbow.jp/Imote2.Builder_kit.pdf
[91] R. P. Weicker, "An overview of common benchmarks," *Computer,* vol. 23, pp. 65-75, 1990.
[92] G. J. E. Nychas, *et al.*, "Meat, poultry and seafood," ed Washington: ASM Press, 2007, pp. 105-140.
[93] E. Borch, *et al.*, "Bacterial spoilage of meat and cured meat products," *International Journal of Food Microbiology,* vol. 33, pp. 103-120, 1996.
[94] J. Kreyenschmidt, *et al.*, "Determination of the shelf life of sliced cooked ham based on the growth of lactic acid bacteria in different steps of the chain," *Journal of applied microbiology,* vol. 108, pp. 510-520, 2010.
[95] A. Dannies, *et al.*, "Feasibility of shifting decision support tools for quality estimation in food logistics to the sensor node level," presented at the 6th International Conference on Software Knowledge Information Management and Applications (SKIMA), Chengdu University, 2012.
[96] A. Dannies, *et al.*, "Dynamic Java Components in Pervasive Systems - A Review of the Feasibility of Dynamic Data Processing on Wireless Platforms," in *PECCS 2012 - International Conference on Pervasive and Embedded Computing and Communication Systems*, Rome, Italy, 2012, pp. 58-66.
[97] A. Dannies, *et al.*, "Smart dynamic software components enabling decision support in Machine-to-machine networks," *JCSI International Journal of Computer Science Issues, Vol. 10, Issue 1, No 3, www.IJCSI.org,* vol. 10, pp. 540-550, January 2013 2013.

[98] NIST. September 2013). *JAMA: A Java Matrix Package*. Available: math.nist.gov/javanumerics/jama
[99] S. Zöller*, et al.* (2010, *Deployment oft Wireless Sensor Networks in Logistics-Potential, Requirements and a Testbed*.
[100] W. Webb, *Understanding Weightless: [technology, equipment, and network deployment for M2M communications in white space]*. Cambridge Cambridge Univ. Press, 2012.
[101] D. Boswarthick*, et al.*, *M2M communications: a systems approach*. Chichester: Wiley, 2012.
[102] Zigbee. (2013, October 16). *Zigbee Alliance*. Available: http://www.zigbee.org/
[103] Dash7. (2013, October 16). *Dash7 Alliance*. Available: http://www.dash7.org/
[104] P. Antonio*, et al.*, "Architecture and Methods for Innovative Heterogeneous Wireless Sensor Network Applications," *Remote Sensing,* vol. 4, pp. 1146-1161, 2012.
[105] H. Stütgen. *The M2M Cloud Evolution*. Available: http://www.nec.com/en/event/mwc/pdf/18.pdf
[106] J. Palafox-Albarrán*, et al.*, "Combining Machine-to-Machine Communications with Intelligent Objects in Logistics," in *ImViReLL'12 The Impact of Virtual, Remote and Real Logistics Labs*, Bremen, Germany, 2012, pp. 102-112.
[107] E. Ortiz. (2002, September 5 2013). *Introduction to OTA Application Provisioning*. Available: http://www.oracle.com/technetwork/systems/ota-156595.html
[108] D. Puccinelli and M. Haenggi, "Wireless sensor networks: applications and challenges of ubiquitous sensing," *Circuits and Systems Magazine, IEEE,* vol. 5, pp. 19-31, 2005.
[109] K. Fehrenbacher. (2010, November 18th). *Dear Friedman: There Is No Moore's Law for Batteries*. Available: http://gigaom.com/2010/09/27/dear-friedman-there-is-no-moores-law-for-batteries/
[110] TinyOS. (2013, September 5 2013). *TinyOS Web page*. Available: http://www.tinyos.net/
[111] Z. Shelby and C. Bormann, *6LoWPAN: the wireless embedded internet*. Chichester: Wiley, 2009.

Appendix: List of publications

Book Chapters

J. Palafox-Albarrán, R. Jedermann, W. Lang, Energy-Efficient Parameter Adaptation and Prediction Algorithms for the Estimation of Temperature Development Inside a Food Container, in: A.J. Cetto, J.-L. Ferrier, J. Filipe (Eds.) Lecture Notes in Electrical Engineering - Informatics in Control, Automation and Robotics, Springer, Berlin, 2011, pp. 77-90.

R. Jedermann, J. Palafox-Albarrán, A. Jabbari, W. Lang, Embedded intelligent objects in food logistics - Technical limits of local decision making, in: M. Hülsmann, B. Scholz-Reiter, K. Windt (Eds.) Autonomous Cooperation and Control in Logistics, Springer, Berlin, 2011, pp. 207-228.

Journals (accepted)

A. Dannies, J. Palafox-Albarrán, W. Lang, R. Jedermann, Smart dynamic software components enabling decision support in Machine-to-machine networks, JCSI International Journal of Computer Science Issues, Vol. 10, Issue 1, No 3, www.IJCSI.org, 10 (2013) 540-550.

Journals (under review)

J. Palafox-Albarran, R. Jedermann,B. Hong, W. Lang, Cokriging for cross-attribute fusion in sensor networks. Under second review. Submitted to Elsevier's Information Fusion Journal **Impact Factor: 2.262. 5-Year Impact Factor:2.838**

J. Palafox-Albarran, B. Hong, W. Lang, R. Jedermann, A statistical method for Data Compression and Recovery Between Continuous-Valued Sources in WSN. Being Submitted to International Journal of Sensor Networks (IJSNet) **Impact Factor: 1.386**

Conferences

J. Palafox-Albarrán, R. Jedermann, W. Lang, Prediction of temperature inside a refrigerated container in the presence of perishable goods, in: 7th International Conference on Informatics in Control, Automation and

Robotics (ICINCO), Funchal, Portugal, 2010.

R. Jedermann, J. Palafox-Albarrán, J. Barreiro, L. Ruiz-Garcia, J.I. Robla, P.D.-I.W. Lang, Modelling and interpolation of spatial temperature during food transportation and storage by the Variogram, in: The 10th International Conference on Modeling and Applied Simulation (MAS 2011), Bruzzone, A.; et. al.,(eds.), Rome, Italy, 2011, pp. 195-201.

R. Jedermann, J. Palafox-Albarrán, J.I. Robla, J. Barreiro, L. Ruiz-Garcia, P.D.-I.W. Lang, Interpolation of Spatial Temperature Profiles by Sensor Networks, in: 2011 IEEE SENSORS Proceedings, IEEE, Limerick, Ireland, 2011, pp. 778-781.

J. Palafox-Albarrán, A. Dannies, B.K. Sanjeeva, W. Lang, R. Jedermann, Combining Machine-to-Machine Communications with Intelligent Objects in Logistics, in: D. Uckelmann, B. Scholz-Reiter, I. Rügge, B. Hong, A. Rizzi (Eds.) ImViReLL'12 The Impact of Virtual, Remote and Real Logistics Labs, Springer, Bremen, Germany, 2012, pp. 102-112

A. Dannies, J. Palafox-Albarrán, R. Jedermann, W. Lang, Feasibility of shifting decision support tools for quality estimation in food logistics to the sensor node level, in: 6th International Conference on Software Knowledge Information Management and Applications (SKIMA), Chengdu University, 2012, pp. 5.

Dannies, J. Palafox-Albarrán, W. Lang, R. Jedermann, Dynamic Java Components in Pervasive Systems - A Review of the Feasibility of Dynamic Data Processing on Wireless Platforms, in: C. Benavente-Peces, F. Ali, J. Filipe (Eds.) PECCS 2012 - International Conference on

Pervasive and Embedded Computing and Communication Systems, 2012 SciTePress – Science and Technology Publications, Rome, Italy, 2012, pp. 58-66.

H. Zhang, N. El-Berishy, D. Zastrau, S.N.K. Marwat, Y. Tan, J. Palafox-Albarrán, I. Rügge, Interdisciplinary perspective on knowledge management in logistics, in: LogistikManagement 2013, Bremen, Germany, 2013.

Magazines/Research Reports

J. Palafox-Albarran, DASH7 applications, First issue of the Dash7 University Working Group (UWG)Magazine., (2012) 20-23.

J. Palafox-Albarran, A. Dannies, B.K. Sanjeeva, W. Lang, R. Jedermann, Machine-to-Machine Communications and Intelligent Objects in refrigerated containers Research Report 2012/13 International Graduate School for Dynamics in Logistics, (2013).

J. Palafox-Albarran, R. Jedermann, W. Lang, Temperature Prediction Inside a Refrigerated Food Container, Research Report 2010/11 International Graduate School for Dynamics in Logistics, (2011) 41-50.